FOIA Number: 2012-0769-F

FOIA MARKER

This is not a textual record. This is used as an administrative marker by the William J. Clinton Presidential Library Staff.

Collection/Record Group: Clinton Presidential Records

Subgroup/Office of Origin: Council on Environmental Quality

Series/Staff Member: Kathleen (Katie) McGinty

Subseries:

OA/ID Number: 2901

FolderID:

Folder Title:
Cuddapah/Spencer-Christy

Stack:	Row:	Section:	Shelf:	Position:
S	61	6	1	3

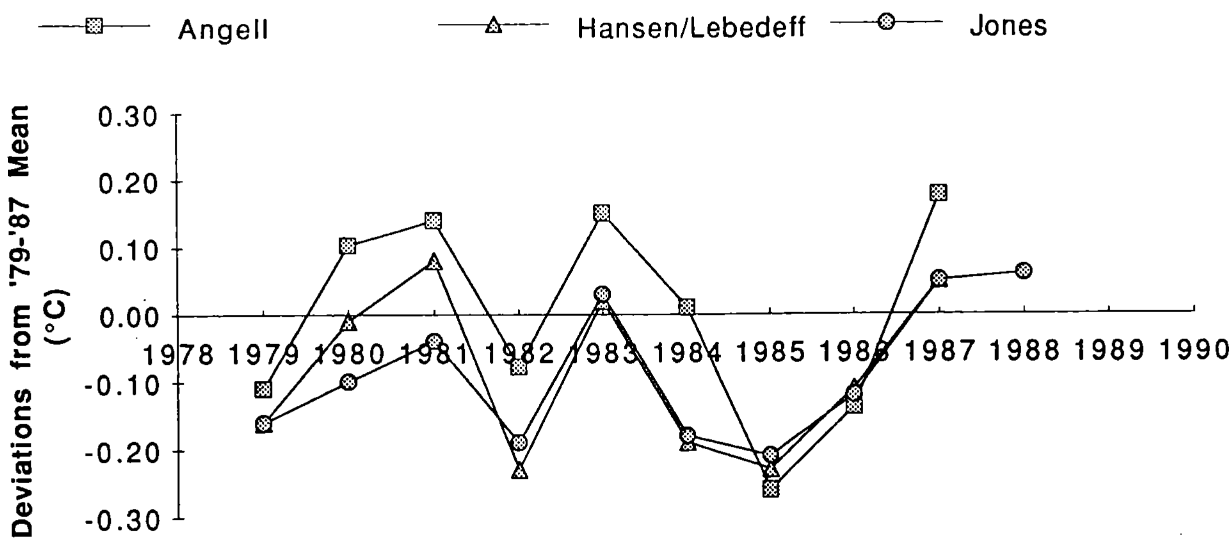

Dr. TOM BELL / NASA - Goddard

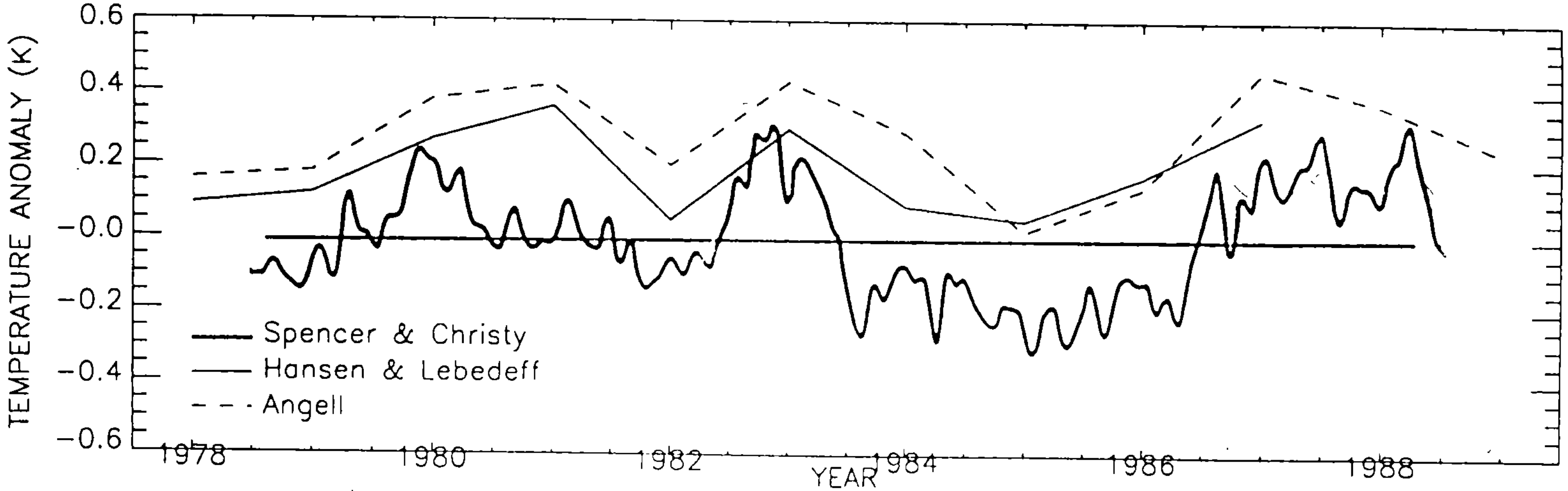

Dr. ALBERT ARKING.

ALBERT GORE, JR.
TENNESSEE

393 RUSSELL SENATE OFFICE BUILDING
PHONE: 202-224-4944

United States Senate
WASHINGTON, DC 20510-4202

Date: July 27, 1991

To: Albert Gore Jr.   S, Anthony Socci

From: Katie McGinty

spencer and christy cont'd

c&a correct s&c's data by looking also at the satellite's channel 1 data that IS sensitive to the surface. their conclusion in the paper they submitted for publication -- "Therefore a global index derived from MSU Ch 2 data should be scrutinized carefully before firm conclusions about global warming could be drawn." -- In conversations, they assure me that the result of this scrutiny will be to bring s&c more in line w/ hansen. they are currently working to quantify the inaccuracy that is inherent in s&c's data.

HOWEVER---c&a submitted their paper to the same journal (journal of climate) that s&c will publish in in sept or oct. they have been REJECTED. they tell me this is because spencer was one of the two reviewers.

THEREFORE, we will not have c&a's publication as an immediate counter to s&c's. BUT, my read of s&c's paper is that it will not be it will not be interpreted as the damning evidence against hansen as their first paper was. meanwhile c&a are working to get pub'd elsewhere.

on another matter -- arking tells me that shelby tilford publicly castigated him for having made a comment supportive of a small satellite system -- continuing to try and enforce a gag rule on the eos question. tilford apparantly is loosing out, however. at a meeting last week in california called to discuss reconfiguration of eos, hansen and others tell me that the small satellite idea is receiving a much warmer reception.

7/26/91 Arking, Cuddapah, Bell.
Mtg

18 Jan 1991 Sci. vol. 251 p. 274

much TOP definitely going up.

1980 - 1990 → Hansen ~~Hurd~~ = 1°/century
Angel = 0.5°/century
Spencer & Christy 0

Can't exclude a few tenths of a percent Δ in solar output but not enough to explain this.

Thermal inertia -- probably won't see pinatubo [illegible] affect for a yr.

Paul Handler - says the big El Niño of 82-3 linked to El Chichon. ↗ UPLA.
Not many believe this
[illegible] stratospheric circulation.

now expecting an El Niño → if [illegible] models of [illegible] out to be big → need to look again at big - need to look @ Handler again!

* Pinatubo is great test of models -- an a [illegible] - now will tell if have a [illegible] models [illegible]

Bug is over the tropics — there is proportional [illegible] cause S&C agree their data [illegible] agree w/ others except for over tropics → then explanation is that Hansen data had → Cuddapah — explanation equally c'ld be that "bug in S&C data.

Need LIDAR system — will go to MARS — need to have here to analyze clouds.

25 kg. *C'ld go on a B2*

~10 mill.

Tells abt cirrus clouds
bulk of info re: clouds has to be thru passive radiometers.

C'ld be ready in 2 or 3 yrs.
super ~~AVRR~~ ~~AVHR~~

Kind of GISS — Kleinbeck responsive / likes small satellite.

Shelby Telford — EOS! castigated ARKIN for talking abt anything else.

Global Warming: What Do Satellite Microwave Measurements Show?

C.Prabhakara and Albert Arking

NASA/Goddard Space Flight Center, Greenbelt, MD 20771

Jung-Moon Yoo

Applied Research Corporation, Landover, MD 20785

May 15, 1991

Submitted to Journal of Climate

ABSTRACT

In a recent study Spencer and Christy (1990) suggested that passive microwave brightness temperature measurements made by Microwave Sounding Unit (MSU) on board NOAA operational satellites at 53.74 GHz in channel 2 (Ch 2) have a potential to monitor global warming on a long-term basis. Spencer and Christy demonstrated that the long-term anomalies of the surface air temperature over the continental United States are reflected by the Ch 2 anomalies with high correlation of about 0.9. However, their study also shows that the anomalies of surface air temperature over the tropical oceans are only poorly reflected by this channel. In this note an attempt is made to explain the good correlation on land versus the poor correlation on tropical oceans. The primary reason for the poor correlation is the contamination introduced by hydrometeors in Ch 2 data. This contamination is estimated and we find it can change from year to year following events such as El Niño. Therefore caution has to be exercised in interpreting the Ch 2 anomalies as indicators of global temperature change.

agree w/ Hansen et al except over Tropics.

1. Introduction

The most commonly used measure of the climatic state is surface air temperature (Hansen and Lebedeff, 1987, 1988; Jones et al., 1986a, 1986b, 1988) probably because it is widely available, with historical records going back hundreds of years, and because it measures that part of the climate system which has the most direct impact on man and his habitat. Surface air temperature, which is measured in the conventional network, also serves as a reasonably good indicator of the bulk energy of the ocean-atmosphere system, because of the strong coupling between the surface and atmosphere.

Passive satellite observations, because of their poor vertical resolution, are not well suited for measuring surface air temperature. Satellite observations on the other hand can give the radiative temperature of a thick layer of air extending to a height of several kilometers above the surface. However, unlike the surface air temperature, the satellite data cover the globe uniformly. For this reason Spencer and Christy (1990), and Spencer et al. (1990, hereinafter referred as SCG) explored the usefulness of the microwave channel, around 53.74 GHz in the oxygen band, for the purpose of monitoring global temperature. This channel has been part of the Microwave Sounding Unit (MSU) on NOAA operational satellites since 1978. In this channel the emission from the land or ocean surface is $\lesssim 8$ %, and contamination due to precipitation, clouds, and water vapor in the atmosphere is less than it is in other channels that sense deeper into the atmosphere. From their examination of the 53.74 GHz measurements SCG hypothesize that these data are measuring the mid-tropospheric temperature from about 800 to 400 mb and the above contaminations are not significant. They conducted a ten-year analysis of 53.74 GHz data (1978-1988) and found there was no global trend in temperature during that period. They propose that these data be used in the future as a global index for monitoring climate, in addition to or as an alternative to an index based on surface air temperature. The objective of this note is to show that the 53.74 GHz data are significantly contaminated by the hydrometeors and this contamination in the data can not be filtered out satisfactorily.

In this note we examine the sensitivity of the MSU channel at 53.74 GHz to varying surface conditions and varying atmospheric constituents--such as precipitation, clouds, and water vapor. We do this by comparing it to the MSU channel at 50.30 GHz, which senses primarily the surface, but which is also affected by precipitation, clouds, and water vapor. This comparison, coupled with a theoretical analysis, indicates that the measurements in the 53.74 GHz channel are significantly affected by the above-mentioned factors. Therefore caution is required in deducing global temperature changes with the help of the anomalies in the 53.74 GHz microwave measurements.

2. Sensitivity of the MSU data

In Figs. 1a and b the transmission and the weighting functions due to atmospheric oxygen (O_2) in Ch 1 and Ch 2 of the MSU are shown to illustrate the difference in the information sensed in these channels. Ch 1 (50.30 GHz) is sensitive mostly to emission from the surface, while Ch 2 (53.74 GHz) responds to the mid-troposphere, with about half of the radiance coming from the 400-800 mb layer. Only a small fraction, about 8 %, of the radiance in Ch 2 is coming from surface on land where the surface emissivity is close to 1. On the ocean, since the surface emissivity is much smaller, ~0.5, the surface contribution in Ch 2 is even smaller.

In addition to oxygen absorption there is absorption due to water vapor, and liquid water in clouds and rain, and there is scattering due to precipitation-size ice particles or water drops. The absorption due to water vapor is relatively small (SCG), and is neglected in the computation below. Liquid water effects can be substantial. For simplicity scattering effects are neglected. Instead, we illustrate the effects of clouds and liquid water through their absorption. Typically absorption by a cloud 1 km thick, with 1 g/m^3 liquid content, is ~0.4 in these channels, which is substantially stronger than that due to oxygen in an atmospheric layer of the same thickness (see Figs. 1a and b). The effect of the cloud is such that it suppresses emission from the surface and oxygen in the warm layers below the cloud. The oxygen emission above cloud is unaffected.

To illustrate the relative responses of the two channels, we calculate the changes in brightness temperature due to changes in (1) surface temperature (T_S), (2) surface emissivity (ε_s), (3) air temperature (T^*), and (4) liquid water (ℓ). The results are shown in Table 1, separately for land and ocean.

A tropical atmosphere with the surface temperature equal to 300 K and a lapse rate of 6.5 K/km is used in the above calculations. To perturb the air temperature T^* by 1 K the physical temperature of the air, between surface and 200 mb, is uniformly changed by 1 K. The surface emissivity over the land is taken as 1, and 0.5 on ocean. In these calculations to assess sensitivity to liquid a cloud with water drops amounting to 2 g/m^3 is introduced in the atmosphere between 2.5 and 4.5 km. Based on the following arguments, this cloud is assumed to represent the hydrometeors.

In comparison to the wavelength ~.56 cm (at 53.74 GHz) of the microwave channel the rain drop size is not very small and so the absorption in Ch 2 follows the Mie regime (Van de Hulst, 1957). On the other hand the cloud drops are very small compared to this wavelength and their absorption follows the Rayleigh regime. Because of this nature typically for the same liquid content (g/m^3) volume absorption coefficient (km^{-1}) for rain in Ch 1 and

Ch 2 is about two times the volume absorption coefficient of the cloud. Furthermore the ratio Ch 2 / Ch 1 shown in Table 1 will be similar to that due to clouds, provided the scattering is negligible.

In the absence of hydrometeors theoretical calculations show T_1 is sensitive to surface temperature and emissivity, while T_2 is sensitive to oxygen emission in the atmosphere. When hydrometeors are present, these sensitivities are modified substantially. In Ch 1 the absorption due to cloud decreases brightness T_1 on land but it increases T_1 on oceans. This is a consequence of the surface emissivity that changes from ~1 on land to ~0.5 on ocean. In Ch 2 the surface emission is not important and as a result T_2 decreases both on land and ocean due to cloud effect.

In order to demonstrate the effects of liquid water we compare simultaneous Ch 1 and Ch 2 observations. We separately examine data from the equatorial regions and from the midlatitudes of the two hemispheres during one month, March 1982.

a) Equatiorial region

In Figs. 2a-d MSU measurements at nadir in Ch 1 and Ch 2 over four land areas of 2° lat X 3° long size close to the equator, are compared and correlated against one another. The correlations are positive and large, ranging from 0.74 to 0.89. The night and day observations are identified by different symbols, and they appear to be separately correlated.

A similar comparison at four equatorial oceanic areas is shown in Figs. 3a-d. One notices that Ch 1 and Ch 2 are now negatively correlated. The magnitudes of the correlation are high over the equatorial rainy areas of the Indian ocean and western Pacific ocean, with a correlation coefficient of about -0.7. Over the equatorial eastern Pacific, where it is relatively dry, the correlation is poor ~-0.1 to -0.4. Again, the negative correlation can be perceived separately in the night and day observations.

The observations shown in Figs. 2 and 3 indicate that although Ch 2 data undergo a relatively small variation of a few degrees in brightness, it is correlated with Ch 1 data at several locations. The strong positive correlation over land and not so strong negative correlation over rainy areas of the oceans may be explained with the help of the sensitivity calculations shown in Table 1.

The mean slope of the lines of regression between T_2 and T_1 is approximately +1/3 over land and -1/5 over the oceans, which is in accord with the sensitivity to hydrometeors (see Table 1).

In order to demonstrate more vividly the nature of the precipitation contamination in the MSU Ch 2 observations, we have selected the equatorial western Pacific ocean between 5°N-5°S and

150°E-170°E. The data from one orbital swath over this area (at 7:30 p.m. on March 30, 1982) are shown in Figs. 4a and b. The observations along the subsatellite track are shown by the symbol 'X' and the cross track scan data are identified by the symbol 'O'. The cross track scan data correspond approximately to 11, 22, 33, 44 and 55 view angle on either side of the subsatellite track.

The Ch 1 data shown in Fig. 4a are contoured at 5 K intervals between 245 K and 260 K. These contours show brightness maxima of about 260 K with a relatively small spatial scale of the order of 100 km. This scale corresponds to the size of the Mesoscale Convective Systems (MCS) (see Houze and Hobbs, 1982). The limb darkening effect in this channel is not conspicuous as the oxygen absorption is weak.

In Fig. 4b the Ch 2 data together with the 260 K contour from Fig. 4a are presented. The MCS features are identified as A, B, C, D and E. The limb darkening effect is clearly noticed in Ch 2 data. Superimposed on the limb darkening effect, one can notice the decreased Ch 2 brightness at the MCS locations (A to E). This means at the MCS locations Ch 1 and Ch 2 brightness data show a negative correlation as described earlier.

Spencer and Christy (1990) recognized the potential for contamination by rain clouds and adopted a scheme for filtering out such effects. If we apply their filter, the scan line containing A, B, and D is eliminated while the scan line with C and E is not. (Spencer and Christy's procedure excludes "any scan lines that had individual footprint measurements that deviated more than 1.5°C from their average relationship to both neighboring footprint measurement".) Hence, despite the filtering scheme, contamination remains. To show that the filtering scheme has little effect, we re-plot in Fig. 5 the points of Fig. 3b after removing the points that would have been removed by Spencer and Christy's filter. The correlation is still large and negative (-0.80). (The infrared observation made by HIRS, near 11 μm, that are simultaneous with MSU observation clearly show cold cloud top temperatures ~210 K where the MCS are indicated in Fig. 4b).

The magnitude of the contamination due to hydrometeors in Ch 2 over the tropical ocean can be estimated in a conservative way with the help of Ch 1 data as follows;

$$\Delta T_2 = \Delta T_1 \; r^2 \; S$$

where $\Delta T_1 = \overline{T}_1 - T_{1\,min}$ is a measure of the hydrometeor contamination in Ch 1. Here $\overline{T}_1$ is the mean value of Ch 1 in a grid box of 2° X 3° lat X long in one month. $T_{1\,min}$ is the minimum temperature in Ch 1 measured in this grid box during the month, which represents clear sky brightness temperature background. ΔT_2 is a measure of the hydrometeor contamination in Ch 2. r is the correlation coefficient between Ch 1 and Ch 2. Hence r^2 is the explained variance. S = -1/6 is the slope factor (the ratio of Ch 2 / Ch 1 shown in Table 1) for ℓ the hydrometeor contamination. For example during March 1982 from the 2° X 3° grid box over the rainy region close to Indonesia shown in Fig. 5, we obtain $\Delta T_1 = 15^\circ K$, r = 0.8 and S = -1/6 which gives $\Delta T_2 = -1.6$ K. This is a conservative estimate of the hydrometeor contamination in Ch 2.

This hydrometeor contamination in Ch 2 can vary in space and time depending upon interannual events such as El Niño. Such events can drastically change the rainfall patterns. In fact the same geographic box during March 1983 gives $\Delta T_2 = -0.2$ K. Thus, 83-82 anomaly in this grid box due to hydrometeors is 1.4 K. We find such anomalies over vast regions of the tropical oceans. Zonal average of such anomalies range from -0.3 K to 0.3 K in the tropical oceans. The magnitude and sign of these hydrometeor induced Ch 2 anomalies are comparable to the Ch 2 anomalies shown by Spencer and Christy (1990; Science, p. 1559, Fig. 3).

From the discussion presented above in the equatorial regions and most of the tropics, where deep and strong convective activity prevails, the MSU Ch 2 measurements reveal the contamination or the 'noise' in this channel due to the hydrometeors. This can degrade the correlation between the anomalies in the surface air temperature and Ch 2 over tropical oceans. Since a large number of Ch 2 observations are showing the effect of atmospheric contamination, it will not be possible to filter out objectively such effects in the data.

b) Midlatitudes

In Figs. 6a-d the MSU Ch 1 and Ch 2 data at nadir obtained from some land areas of 2° lat X 3° long size, over the midlatitudes around 40°N and 40°S, during the month March 1982 are compared. As expected on land, the correlation between the data of the two channels is positive and the correlation coefficient is quite strong, ~0.5 to 0.9. A similar comparison of the MSU Ch 1 and Ch 2 data over the midlatitude oceans is shown in Figs. 7a-d. The Ch 1 and Ch 2 data over the midlatitude oceans also shows a positive correlation; however, the correlation coefficients are somewhat weaker, ~0.1 to 0.7. The behavior of the MSU observations over the midlatitude oceans contrasts with that of the tropical oceans. This is believed to be due to the shallow and somewhat weak nature of the convective phenomena in the midlatitudes. In addition, in the latitudinal regime beyond the tropics, the effect of the strong baroclinic waves, which influence the bulk of troposphere including surface air, leads to a positive correlation between Ch 1 and Ch 2 both over land and oceans.

Based on the analysis of the MSU data over midlatitudes, one infers that Ch 2 data can correlate well with surface air temperature both on land and oceans.

Conclusions

Observations of the relationship between Ch 1 and Ch 2 of the MSU, combined with a theoretical analysis, have provided some insight into the sensitivity of these channels to various atmospheric parameters, and lead us to some general conclusions on the ability of Ch 2 to monitor atmospheric temperature anomalies.

First, one notes that the sensitivity to surface emission is an order of magnitude smaller for Ch 2 than for Ch 1. Hence, any correlation between the two channels is most likely due to: (1) a physical correlation between surface temperatures and atmospheric temperatures in the lower to middle troposphere, and/or (2) the common effects of liquid water variations in the atmosphere.

Over land areas, where surface emissivity is close to one, variations in surface and atmospheric temperatures, which are generally correlated, as well as variations in liquid water, will lead to a positive correlation between Ch 1 and Ch 2. The stronger the physical correlation between surface and atmospheric temperatures, the stronger the correlation between the two channels. This result is substantiated by significant positive correlations observed over equatorial and mid-latitude regions.

Over oceanic areas, the surface and air temperature variations will contribute to a positive correlation between Ch 1 and Ch 2, but liquid water variations will contribute to a negative correlation. The reason why the two effects go in different directions is the low emissivity of the sea surface, causing hydrometeors (rain and clouds) to increase total emission in Ch 1, which is sensitive to the surface, and to decrease total emission in Ch 2, which is insensitive to the surface. The result is substantiated by negative correlations observed over equatorial oceanic regions, where temperature variations are small but where deep convection gives rise to substantial variations in rain clouds and hydrometeors.

Over mid-latitude oceans, the two processes--atmospheric temperature and liquid water variations--compete with each other, yielding relatively low correlations between Ch 1 and Ch 2.

These results demonstrated that both channels 1 and 2 of the MSU are substantially affected by liquid water in the form of rain clouds and hydrometeors. In particular, Ch 2 anomalies do not exclusively represent the effects of air temperature variations.

The conclusions drawn here are consistent with the results of correlation studies made by SCG between MSU Ch 2 and surface temperature. The good agreement they find over the U.S. is due to large temperature variations that occur over land at mid-latitudes, which correlate well with land surface temperature. The effects of hydrometeors, which lower the Ch 2 brightness temperature, would also correlate with surface temperatures, which are generally cooled under the effects of rain clouds. The poor agreement when averaged over an entire hemisphere-- especially the Southern Hemisphere--reflects the response over the oceans, where atmospheric liquid water variations are not correlated with surface temperature.

Satellite data cover the globe uniformly and can be potentially valuable in assessing global changes over extended periods of time. Studies of the global temperature change from 1979-88 made by SCG, and Spencer and Christy with the help of MSU Ch 2 data are very useful from this point of view. However we find that the MSU Ch 2 data are not free from contaminations. One significant contamination is that introduced by hydrometeors. This hydrometeor induced contamination for a given month can change from one year to another producing an interannual anomaly. The size of such anomalies is comparable to that of the anomalies shown by Spencer and Christy (1990). Therefore a global index derived from MSU Ch 2 data should be scrutinized carefully before firm conclusions about global warming could be drawn.

Acknowledgments

We are grateful to Drs. Dennis Chester and David Kratz for their helpful comments.

Reference:

Hansen, J., and S. Lebedeff, 1987: Global trends of measured surface air temperature. J. Geophys. Res., 92, 13345-13372.

Houze, R.A., and P.V. Hobbs, 1982: Organization and structure of precipitating cloud systems. Advances in Geophysics, 24, 225-315.

Jones, P.D., 1988: Hemispheric surface air temperature variations: Recent trends and an update to 1987. J. Climate, 1, 654-659.

___________, S.C.B. Raper and T.M.L. Wigley, 1986b: Southern Hemisphere surface air temperature variations: 1851-1984. J. Climate Appl. Meteor., 25, 1213-1230.

___________, R.S. Bradley, H.F. Diaz, P.M. Kelly and T.M.L. Wigley, 1986a: Northern Hemisphere surface air temperature variations: 1851-1984. J. Climate Appl. Meteor., 25, 161-179.

Spencer, R.W., and J.C. Christy, 1990: Precise monitoring of global temperature trends from satellites. Science, 247, 1558-1562.

___________, J.C. Christy and N.C. Grody, 1990: Global Atmospheric temperature monitoring with satellite microwave measurements: method and results 1979-84. J. Climate, 3, 1111-1128.

Van de Hulst, H.C., 1957: Light scattering by small particles. John Wiley and Sons, New York, N.Y., Chapman and Hall, London, 470 pp.

Table 1. Theoretically derived sensitivity of MSU Ch 1 and Ch 2 brightness temperature to various perturbations.

Perturbation	Land Ch 1	Land Ch 2	Land Ratio (Ch2/Ch1)	Ocean Ch 1	Ocean Ch 2	Ocean Ratio (Ch2/Ch1)
$\delta T_s = 1^\circ C$	$0.75^\circ C$	$0.08^\circ C$	1/10	$0.37^\circ C$	$0.04^\circ C$	1/10
$\delta \varepsilon_s = .1$	$17.4^\circ C$	$0.4^\circ C$	1/44	$17.4^\circ C$	$0.4^\circ C$	1/44
$\delta \ell = .4 g/cm^2$	$-6^\circ C$	$-2^\circ C$	1/3	$31^\circ C$	$-5^\circ C$	-1/6
$\delta T^* = 1^\circ C$	$0.26^\circ C$	$0.92^\circ C$	3/1	$0.34^\circ C$	$0.96^\circ C$	3/1

Figure Captions:

Fig.1 a. Atmospheric oxygen transmission τ_{O_2} for the MSU Ch 1 and Ch 2.

b. Weighting function $\frac{\Delta \tau_{O_2}}{\Delta z}$ for Ch 1 and Ch 2.

Fig.2 a-d. Comparison of MSU Ch 1 vs Ch 2 nadir observations over equatorial land areas. Observations made close to 07:30 a.m. are shown by 'X' and close to 07:30 p.m. by 'O'.

Fig.3 a-d. As in Fig. 2 except for equatorial oceanic areas.

Fig.4 a. MSU Ch 1 (50.30 GHz) measured brightness temperature along the orbital swath of the descending node (local 7:30 p.m.) on March 30, 1982 over the western equatorial Pacific. Observation points along the subsatellite track of the orbit are indicated by the symbol 'X'.

Cross track scan points are shown by the symbol 'O'.

Contours with dashes indicate isolines of Ch 1 brightness temperature.

b. As in Fig. 4a except for MSU Ch 2 (53.74 GHz). Contours with dashes labeled A, B, C, D and E indicate the 260 K contour of Ch 1 superposed on Ch 2 data.

Fig.5. Display of data in Fig. 3b after they are filtered by Spencer et al's method.

Fig.6 a-d. As in Fig. 2 except for midlatitude land areas.

Fig.7 a-d. As in Fig. 2 except for midlatitude oceanic areas.

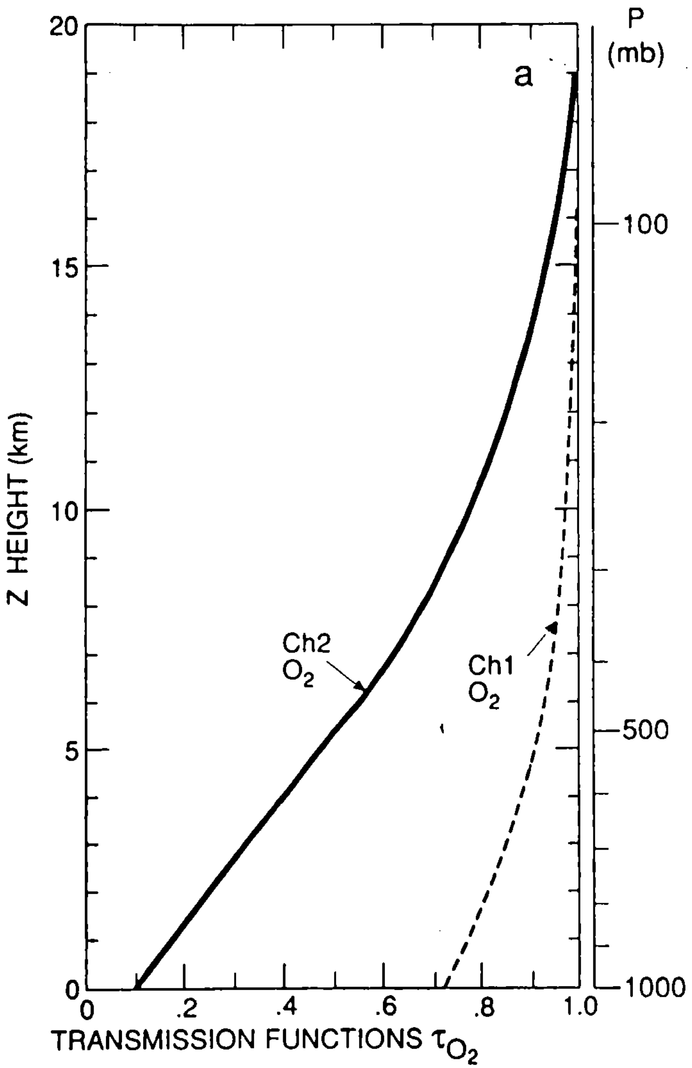

a
Z HEIGHT (km)
P (mb)
100
500
1000
Ch2 O2
Ch1 O2
0
.2
.4
.6
.8
1.0
20
15
10
5
0
TRANSMISSION FUNCTIONS τO2

Fig. 1a

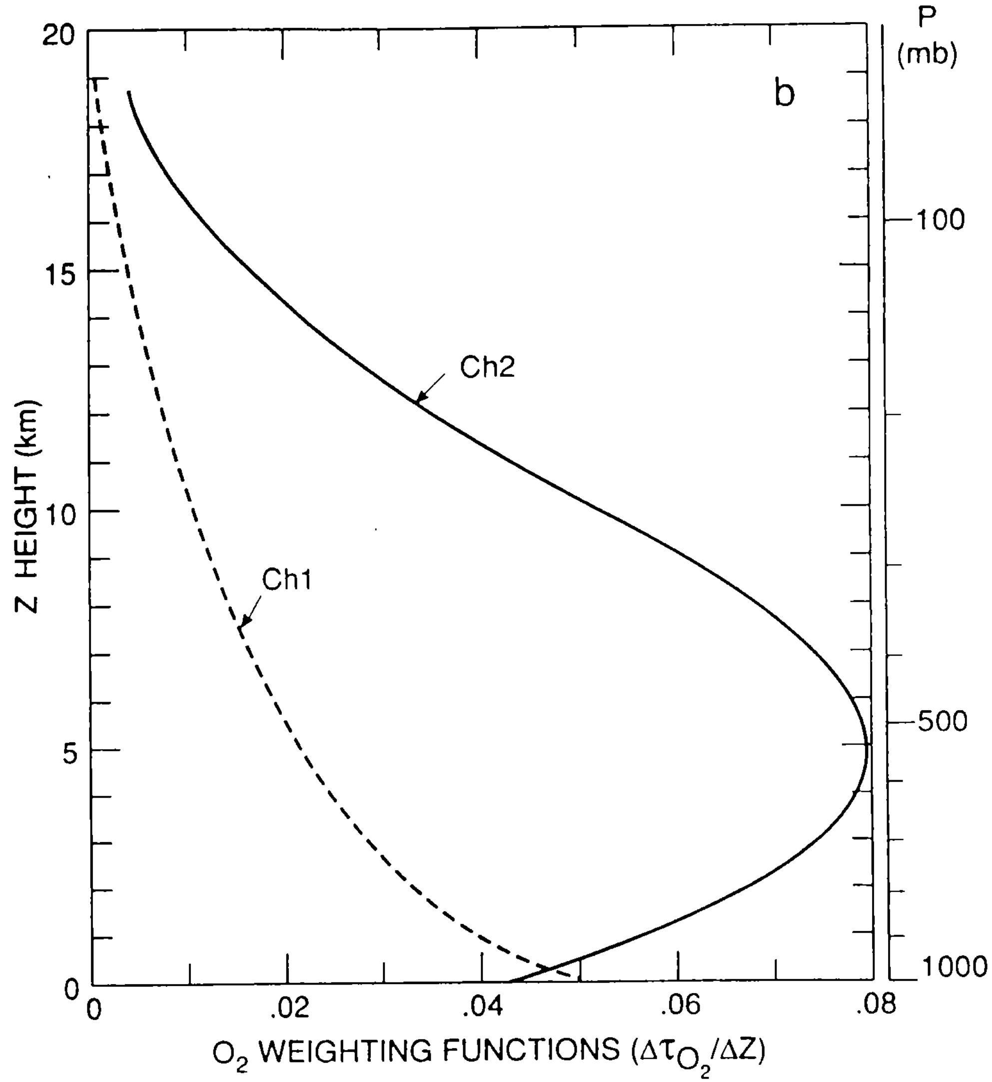

b
Z HEIGHT (km)
P (mb)
100
500
1000
Ch2
Ch1
0
.02
.04
.06
.08
20
15
10
5
0
O2 WEIGHTING FUNCTIONS (ΔτO2/ΔZ)

Fig. 1b

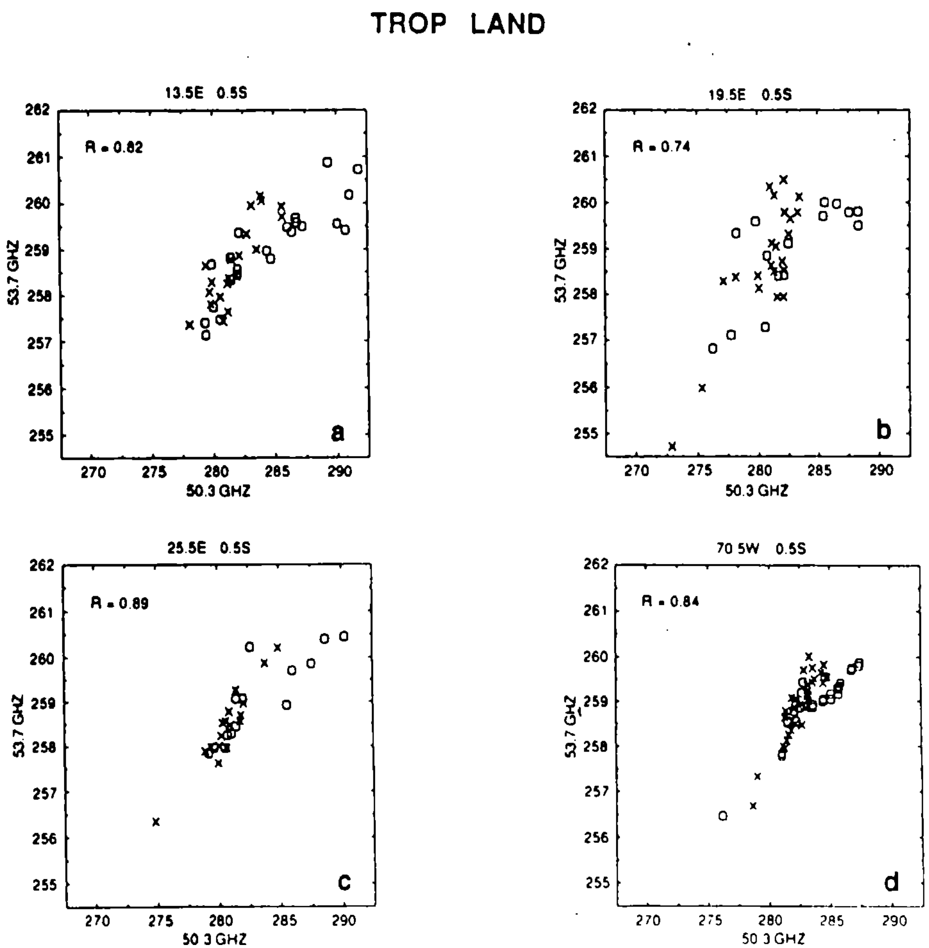
TROP LAND
13.5E 0.5S
R = 0.82
a
19.5E 0.5S
R = 0.74
b
25.5E 0.5S
R = 0.89
c
70 5W 0.5S
R = 0.84
d
53.7 GHZ
50.3 GHZ

Fig. 2

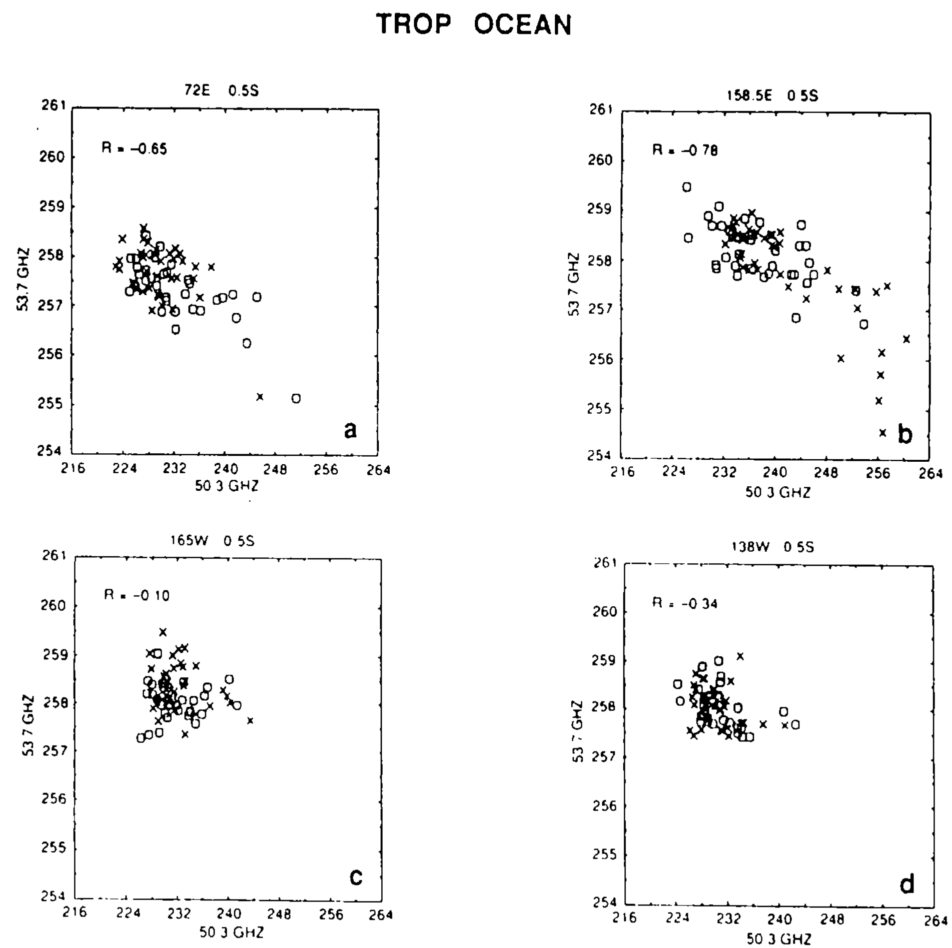
TROP OCEAN
72E 0.5S
R = -0.65
a
158.5E 0.5S
R = -0.78
b
165W 0.5S
R = -0.10
c
138W 0.5S
R = -0.34
d
53.7 GHZ
50.3 GHZ

Fig. 3

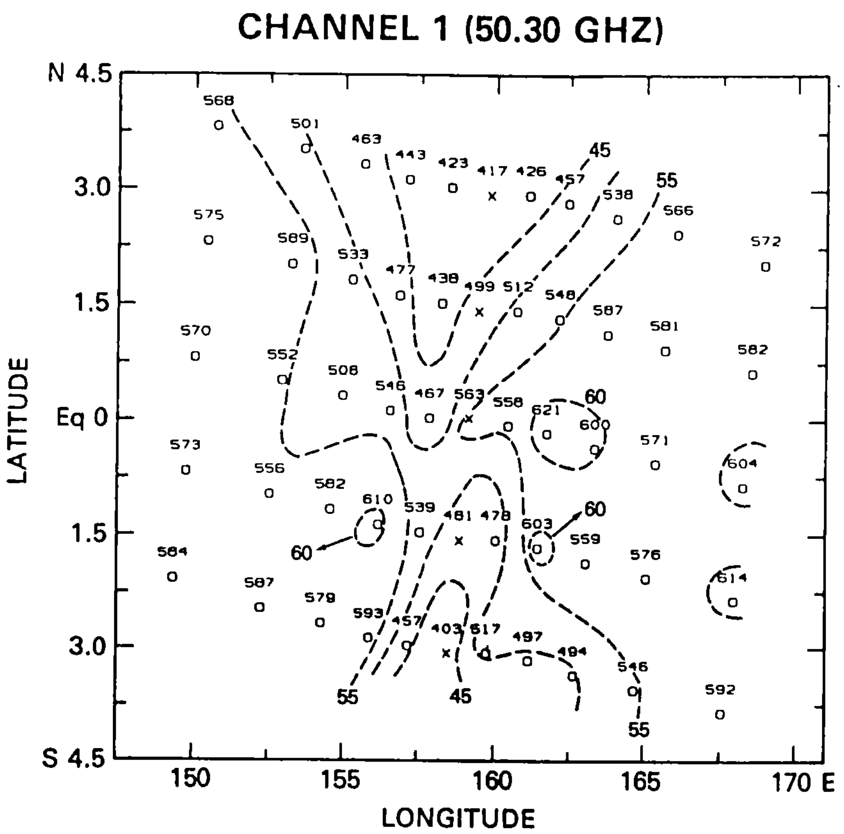

CHANNEL 1 (50.30 GHZ)
LATITUDE
N 4.5
3.0
1.5
Eq 0
1.5
3.0
S 4.5
LONGITUDE
150
155
160
165
170 E
45
55
60

Fig. 4a

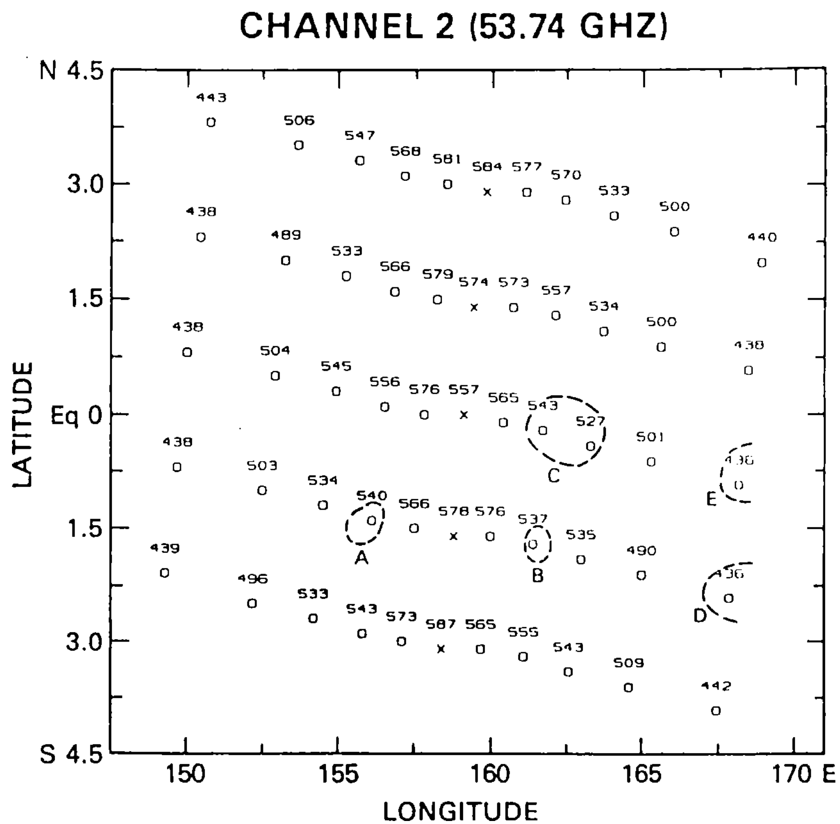

CHANNEL 2 (53.74 GHZ)
LATITUDE
N 4.5
3.0
1.5
Eq 0
1.5
3.0
S 4.5
LONGITUDE
150
155
160
165
170 E
A
B
C
D
E

Fig. 4b

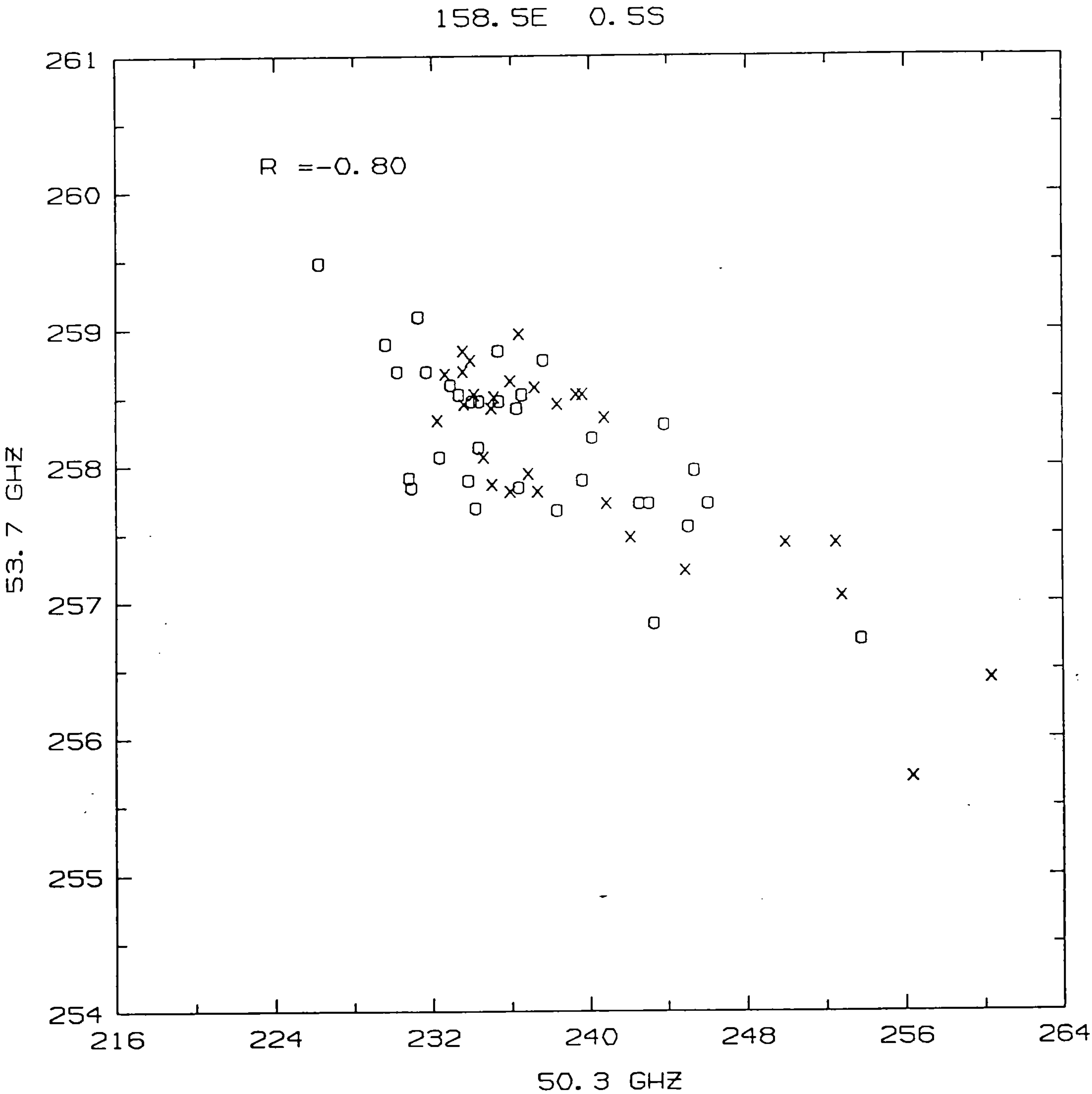

158.5E 0.5S
R =-0.80
261
260
259
258
257
256
255
254
216
224
232
240
248
256
264
53.7 GHZ
50.3 GHZ

Fig. 5

MID LAT LAND

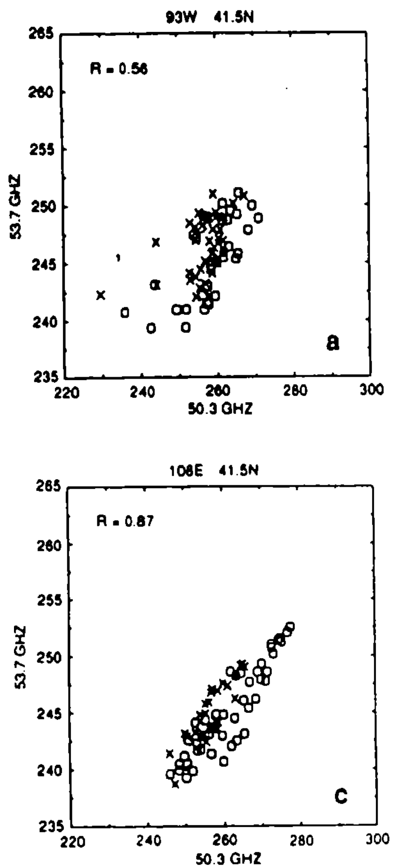

Fig. 6

MID LAT OCEAN

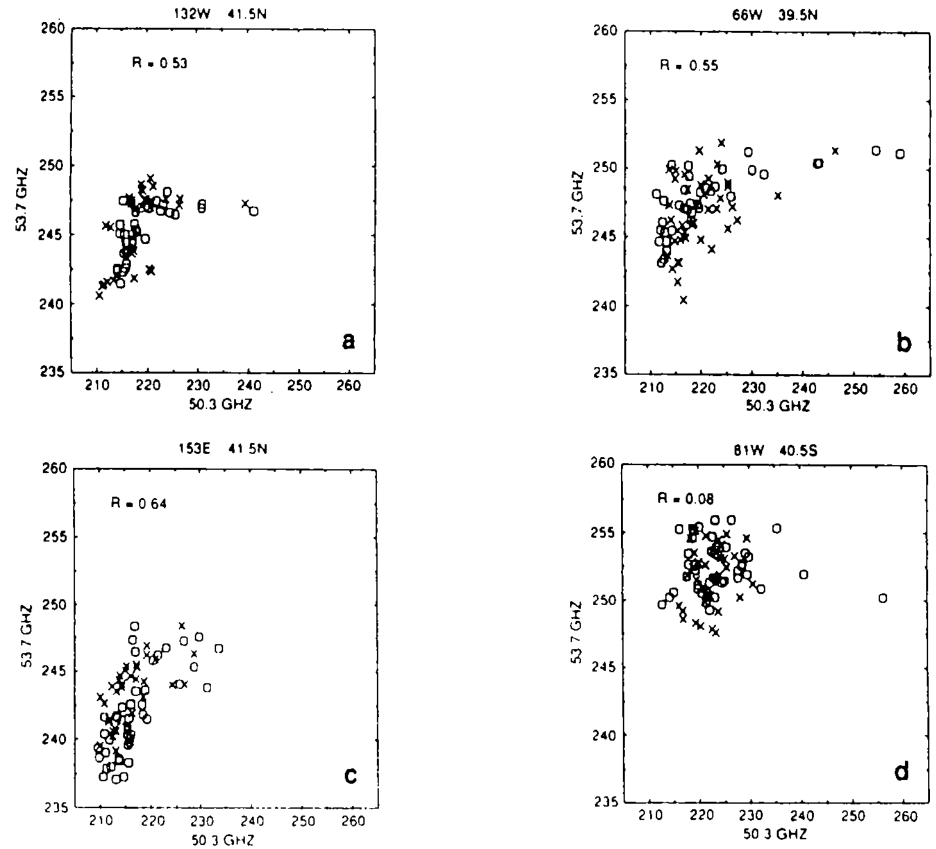

Fig. 7

Precision and Radiosonde Validation of Satellite Gridpoint Temperature Anomalies, Part II: A Tropospheric Retrieval and Trends during 1979-90

by

Roy W. Spencer

ES43 Earth Science and Applications Division

NASA Marshall Space Flight Center

Alabama 35812

John R. Christy

Johnson Research Center

University of Alabama in Huntsville

Huntsville, Alabama 35899

submitted to

Journal of Climate

April 1991

ABSTRACT

TIROS-N satellite Microwave Sounding Unit (MSU) channel 2 data from different view angles across the MSU scan swath are combined to remove the influence of the lower stratosphere and much of the upper troposphere on the measured brightness temperatures. The retrieval provides a sharper averaging kernel than the raw channel 2 weighting function, with a peak lowered from 50 kPa to 70 kPa and with only slightly more surface influence than raw channel 2. Monthly 2.5^{o} gridpoint anomalies of this tropospheric retrieval compared between simultaneously operating satellites indicates close agreement. The agreement is not as close as with raw channel 2 anomalies because synoptic scale temperature gradients across the 2000 km swath of the MSU are averaged out in the retrieval procedure, and because the retrieval involves the magnification of a small difference between two large numbers. Single gridpoint monthly anomaly correlations between the satellite measurements and the radiosonde calculations range from around 0.95 at high latitudes to below 0.8 in the tropical west Pacific, with standard errors of estimate of 0.16^{o}C at Guam to around 0.50^{o}C at high latitude continental stations. Calculation of radiosonde temperatures with a static weighting function instead of the radiative transfer equation degrades the standard errors by an average of less than 0.04^{o}C. Of various standard tropospheric layers, the channel 2 retrieval anomalies correlate best with radiosonde 100-50 or 100-40 kPa thickness anomalies. A comparison between global and hemispheric anomalies computed for raw channel 2 data versus the tropospheric retrieval show a correction in the 1979-1990 time series for the stratospheric warming of 1982-83, which was independently observed by MSU channel 4. This correction leads to a slightly greater tropospheric warming trend in the twelve year time series (1979-1990) for the tropospheric retrieval (+0.048^{o}C/decade) than for channel 2 alone (+0.015^{o} C/decade).

1. Background

In Part I we showed the excellent agreement between separate TIROS-N satellites when independently measuring monthly anomalies of MSU channel 2 T_b at the 2.5° gridpoint level. The average gridpoint agreement between satellites was better than 0.1°C over the tropical oceans, and better than 0.2°C virtually everywhere else on the Earth. This level of agreement was shown to be at least as good as adjacent tropical oceanic radiosonde stations provide. When the satellite measurements were compared to radiosonde measurements of ten years of monthly anomalies, nearly as good agreement was found with many correlations over 0.95 and standard errors of estimate of 0.15°C in the tropics to 0.25°C at high latitudes. In terms of conventionally measured atmospheric layers, the channel 2 anomalies correlated best with 100-15 kPa thickness anomalies. Decadal trends in both the satellite and radiosonde time series showed no significant trend in their difference, indicating stability of MSU channel 2 long-term monitoring.

However, the possibility of cooling in the lower stratosphere coupled with significant energy being received from above this level by MSU channel 2 (Fig. 1), suggests that MSU channel 2 trends and anomalies might not accurately reflect temperature trends in the lower and middle troposphere. Examination of ten year radiosonde temperature trends for different layers of the atmosphere (Table 1) reveals that different trends can be experienced depending upon the layer in question, even within the troposphere. Most of these regions, with the exception of the tropical Pacific, experienced considerable difference in trends above versus below the 30 kPa level. Note also that these ten-year trends are quite variable from region to region, making the lack of radiosonde data in remote regions a significant source of uncertainty in monitoring "global" temperature trends with radiosonde data. These differences suggest the need to remove as much of the upper troposphere and lower stratosphere as possible from the satellite measurements if maximum utility of the satellite is to be made for monitoring a single layer which is expected to behave more uniformly (e.g. the lower and middle troposphere).

We can examine the global temperature variability in the lower stratosphere during the period 1979-90 by applying the same procedures outlined in Part I of this study to MSU channel 4. All inter-satellite statistics on monthly agreement and long-term stability of MSU channel 4 (not shown) are even better than those reported for channel 2 in Part I, making channel 4 a superb resource for monitoring global lower stratospheric temperature trends. When we compute the channel 4 temperature anomalies for the period 1979-90 (Fig. 2) we find a relatively intense warm event during 1982-83. This appears to be superimposed upon an average cooling trend, although this cooling appears to have leveled off since 1985. The 1982-83 warming is generally attributed to solar heating of volcanic dust injected into the stratosphere by El Chichon volcano in early 1982 and by an equatorial African volcano in December 1981. This warm event happened to occur during the tropospheric El Nino Southern Oscillation (ENSO) warm event as seen by MSU channel 2 (also in Fig. 2). Since MSU channel 2 was viewing the tropospheric warmth "through" the stratospheric warmth, to the extent that the MSU channel 2 and 4 weighting functions in Fig. 1 overlap, the channel 2 warming might be partially due to the stratospheric event. We say "might be" because it is not proven that the warming seen by either channel 2 or 4 was contributed to by the overlap region of the weighting functions (although this would seem unlikely). Correction for any stratospheric influence would be increasingly important at high latitudes where the base of the stratosphere is much lower than in the tropics.

Fortunately, it is possible to combine MSU channel 2 data from various view angles in such a way as to cancel out any stratospheric contribution, and achieve a vertical weighting distribution which is sharper than a single channel can offer. Here we describe a method for removing most of the stratospheric influence on channel 2 based upon the differencing of MSU channel 2 near-nadir and limb measurements through the "averaging kernel" concept. This concept was originally described in the context of atmospheric temperature retrievals by Conrath (1972), where weighting functions can be linearly combined to achieve different vertical distributions of weighting. This is the fundamental basis for any satellite temperature retrieval procedures, and is in effect a deconvolution of overlapping weighting functions. This technique was discussed more recently by Grody (1980). Also, updated tropospheric time series of both channel 2 and the tropospheric retrieval are presented for the period 1979-90.

2. Multi-Angular retrievals of deep-layer temperature

a. retrieval philosophy

Retrieval of temperature information from the MSU (or other satellite sounding radiometers) is usually performed for specific pressure levels through various retrieval procedures which in effect deconvolve overlapping weighting functions into a sharper averaging kernel. The retrieval of specific pressure level information has provided conformity with traditional radiosonde measurements, and with numerical weather prediction models which have been tailored to accept radiosonde data. Unfortunately (as discussed in Part I) even though deconvolution of these weighting functions can achieve an averaging kernel which is sharper than the original weighting functions, it is not possible to compress the depth of the deconvolved layer beyond certain limits imposed by the finite number of channels and the existence of noise in those channels. Thus, a retrieval for a specific pressure level will always use information gathered from a relatively deep atmospheric layer. These attempts to retrieve a temperature for a specific pressure level exploit average statistical relationships which naturally exist between temperatures in different atmospheric layers. Because of their assumed time-invariant nature, these average statistical relationships have little use in climate monitoring.

Therefore, we assume at the outset that we wish to retrieve a deep-layer temperature measurement from the satellite (since it is not possible to reduce the thickness of the satellite measured layer beyond certain limits anyway). For climate monitoring this seems preferable since it would be unlikely that different climate trends would exist in adjacent, very thin layers of the troposphere. The individual channel weighting functions can in principle be used by themselves (as we saw in Part I), provided that their vertical weighting distribution is considered useful.

Removal of the stratospheric influence on MSU channel 2 might be accomplished through some deconvolution from MSU channel 3, which has information from the layer whose influence we wish to remove (Fig. 1). Unfortunately, our analysis of twelve years (1979-90) of MSU channel 3 data reveals that one or more MSUs show some sizeable calibration drifts in channel 3, evidenced by a trend in their difference (Fig. 3). While this drift is actually the difference in drifts between the two sensors, we have seen evidence to suggest that it is the NOAA-6 channel 3 which is drifting, which over the period represented in Fig. 3 would amount to 0.3°C. (The step function character of the drift in channel 3 is a result of the removal of a one year annual cycle (1982) which was not detrended. The drift by itself seems to be continuous and linear in time.) This amount of instrumental drift is too large to accept for climate monitoring purposes. Channel 3 drift problems were found for at least one other satellite. We have been unsuccessful in quantifying these drifts either through radiosonde comparisons or satellite intercomparisons. As a consequence of these drift problems, use of MSU channel 3 for any type of long-term climate monitoring should be done with extreme caution.

b. the tropospheric retrieval and its global precision

Fortunately, it turns out that if the goal is the removal of the stratospheric influence on MSU channel 2, then a combination of channel 2 data from different view angles provides better stratospheric canceling than any combination of channels 2 and 3. This is shown in Fig. 4, where the view angles corresponding to

MSU scan positions (#1,2,10,11) and (#3,4,8,9) can be combined with appropriate weighting to yield a new weighting function which removes most of the stratospheric influence, lowers and sharpens the peak of the averaging kernel, and results in only slightly more sensitivity to the surface than even the channel 2 nadir scan position (#6) provides. (SCG addressed the contaminating non-thermometric influence of surface processes on MSU channel 2). The use of eight scan positions was chosen to minimize measurement retrieval noise, which is greater than raw channel 2 noise because the retrieval involves the magnification of small differences between two large numbers. Separate retrievals for the two halves of the swath were attempted, but showed poor results.

This lower tropospheric retrieval (which for brevity we will call channel 2R) wipes out any horizontal temperature gradients across the 2000 km wide MSU swath. This gradient information had been retained in our channel 2 study (Part I) through the limb correction procedure. Thus, we can not expect channel 2R to provide very useful synoptic scale temperature information on short time scales. For our simple linear retrieval, after a ratio of weights is chosen which provides stratospheric canceling of the individual scan angle weighting functions in Fig. 4, the weights can then be adjusted so that their sum equals 1. This results in the retrieval being a brightness temperature, accurate for the averaging kernel distribution of weighting. The small amount of negative area under the channel 2R averaging kernel in Fig. 4, although probably insignificant in comparison to uncertainties in the oxygen absorption theory, would lead to a miniscule warming in the channel 2R T_b if stratospheric cooling occurs, and vice versa.

The same procedures for gridpoint assignment, satellite intercalibration, and anomaly calculation at both the 2.5^o gridpoint and zonal levels were used as described for raw channel 2 data in Part I. However, since the full swath of data is required for the retrieval, no limb corrections are applied to the individual MSU scan positions. The channel 2R T_b were assigned to only the middle three MSU scan position locations. From this point onward all daily gridpoint assignment and interpolation to empty gridsquares, monthly averaging, satellite intercalibration, and annual cycle removal follow the same procedures as were described in Part I for channel 2.

3. Gridpoint Channel 2R Validation

a. satellite intercomparisons

Despite the expected poorer performance of channel 2R for gridpoint comparisons, hemispheric and global averaging of the data again reveals excellent agreement between concurrently operating satellites during overlap periods (Table 2). It can be seen through comparison of this table with Table A1 of Part I that the monthly global signal to noise is is not as good for the tropospheric retrieval anomalies as it is for raw channel 2 anomalies. The standard deviation of the difference between satellites for single-satellite monthly global anomalies is often closer to $0.02^{o}C$ compared to $0.01^{o}C$ for channel 2 anomalies. This is, however, sufficiently good for the multi-month overlap periods to allow accurate intercalibration between satellites for long-term monitoring on at least a global basis. It should be emphasized that when two satellites are operating our final anomaly fields are an average of the two satellites fields, thus further reducing the noise by $2^{0.5}$.

As we did in Part I for channel 2 anomalies, we present a simple example of the precision of the monthly gridpoint retrieval anomalies by computing a difference between February 1983 and February 1982 channel 2R T_b fields (Fig. 5). Again we see that these monthly anomaly patterns measured separately by NOAA-6 and NOAA-7 are very similar, although the similarity is not quite as striking as the channel 2 anomaly fields. Any difference between the two satellites for channel 2R is almost always one of anomaly magnitude, and not of sign. The retrieval anomalies are larger at high latitudes than are the channel 2 anomalies from Fig. 3 of Part I. This is due to both removal of the stratospheric influence (which is usually negatively correlated with tropospheric temperature variations) and to the greater variability of temperature variations at lower tropospheric levels. The tropical retrieval anomaly magnitudes are not, however, greater than the channel 2 anomalies. This is due to both the tropical stratosphere being much higher, and the fact that tropical oceanic temperature anomalies are often slightly weaker in the lower troposphere than they are in the middle troposphere.

A notable exception to the lower troposphere/stronger anomaly rule at high latitudes is seen in the cold anomaly over Western Europe in Fig. 5. Comparison with the corresponding channel 2 cold pattern (Fig. 2 in Part I) reveals that, if anything, the retrieval anomaly is actually weaker than the channel 2 anomaly. The reason for this is seen in an image of the MSU channel 4 (lower stratosphere) difference fields for the February 1983-82 periods (Fig. 5c). Here we find that the channel 2 cold anomaly over Europe was contributed to by a very cold anomaly in the lower stratosphere. The retrieval removed this stratospheric influence, which by itself would have resulted in a weaker channel 2R cold anomaly, but combined with the typically stronger cold anomaly in the lower troposphere, the channel 2R anomaly ended up being not much different from the channel 2 anomaly. This gives empirical evidence that stratospheric effects are indeed being removed by the retrieval.

b. single-station radiosonde comparisons

The monthly gridpoint channel 2R anomalies were compared to radiosonde data with the same three methods used for the channel 2 anomalies in Part I. Radiosonde computations of channel 2R were performed with (1) the radiative transfer equation, and (2) a constant (standard atmosphere) weighting profile (Fig. 4) in combination with Eq. 2 from Part I. A third method involved comparisons to standard pressure level thicknesses. As in Part I, we computed thickness anomalies for all combinations of layers having bases at either 100 or 85 kPa, and tops ranging from 70 to 10 kPa. Consistent with Part I, we present comparisons between channel 2R and the radiosonde channel 2R and thickness temperature anomalies at Cold Bay, Alaska (Fig. 6); St. Cloud, Minnesota (Fig. 7); Oakland, California (Fig. 8); Lihue, Hawaii (Fig. 9); San Juan, Puerto Rico (Fig. 10); and Guam (Fig. 11).

At Cold Bay (Fig. 6), we find a monthly correlation of 0.94 and SE=0.50°C between the MSU measured anomalies and the radiosonde anomalies calculated with the radiative transfer equation. When the static weighting method is applied to the radiosonde temperature profile, the SE degrades by only 0.02°C to 0.52°C. When compared to the standard layers measured by radiosondes, the layers starting at 100 kPa, rather than 85 kPa, had the best correlations with the MSU. This is to be expected from the weighting profile shown in Fig. 4. For Cold Bay, as well as all other stations, we find that the best correlations to the retrieval exist with either the 100-50 kPa or 100-40 kPa layers.

At St. Cloud, Minnesota (Fig. 7) R=0.97 and SE=0.48°C, results which are similar to Cold Bay, Alaska. The static weighting method resulted in only 0.01°C degradation in the standard error. The 100-40 kPa layer had the best correlation of all conventionally measured radiosonde layers, with R=0.95 and SE=0.54°C.

At Oakland, California (Fig. 8) R=0.91 and SE=0.54°C. Use of the static weighting function method leads to SE=0.58°C. Highest correlation with a standard layer is the 100-50 kPa layer with R=0.91 and SE=0.70°C.

In Lihue, Hawaii (Fig. 9) R=0.89 and SE=0.25°C. Use of the static weighting function yields SE=0.32°C. Highest correlation with a standard radiosonde layer is 0.88 and SE=0.31°C.

At San Juan, Puerto Rico (Fig. 10) R=0.84 and SE=0.29°C. Slight degradation to SE=0.33°C is seen when the standard atmosphere weighting function is applied to the radiosonde temperature profile. Correlation to the 100-40 kPa thickness anomalies is 0.84 also, with SE=0.35°C.

The worst correlations are seen for Guam (Fig. 11, R=0.74), but as was the case for the channel 2 comparisons, this is because the monthly anomaly signal is so small that it approaches the noise of the radiosonde and satellite systems. In fact, the correlation with the satellite is about the same as between adjacent tropical radiosonde stations for the 100-40 kPa layer (0.76), while the standard error of estimate the satellite provides (0.16°C) is at the limit of the radiosondes ability to measure monthly anomalies anyway, as discussed in Part I. Use of the static weighting function method gives SE=0.20°C. The layer of highest correlation is 100-40 kPa with R=0.66 and SE=0.21°C.

c. composite station radiosonde comparisons

As was done for channel 2 in Part I, we computed statistics for radiosonde station grouping from several regions (Table 2). We find that these station grouping improve the levels of agreement considerably, with standard errors ranging from 0.11° over the tropical west Pacific to around 0.35°C at high latitudes and correlations sometimes exceeding 0.95 at high latitudes. These results suggest that, while individual gridpoint satellite data are good, the full 10,000 gridpoint dataset should allow low-noise estimates of global temperature anomalies even on a monthly time scale.

4. Retrieved Tropospheric Trends 1979-90

The good quality of the channel 2R gridpoint anomalies, combined with the small (0.02°C) monthly disagreement between simultaneously operating satellites (Table 1) suggests that hemispheric and global temperature trends in the lower half of the tropospheric can be monitored with this retrieval. The tropospheric retrieval temperature anomalies for 1979-90 are shown in Fig. 12 superimposed upon the channel 2 anomalies. The largest difference between channels 2 and 2R is seen in 1982-83, where the stratospheric warm event's influence has now been removed. Other differences can also be seen throughout the time series which, since apparently not stratospheric adjustments, probably indicate variations in globally-averaged tropospheric stability. That most of these differences between channel 2 and 2R are real is supported by their large magnitude (0.1°C - 0.2°C) relative to the monthly level of channel 2R disagreement between simultaneously operating satellites in Table 1 (0.01° to 0.02°C).

Of some importance is the finding that the long-term trend of the data is somewhat warmer for the retrieval time series (+0.032°C) than it is for the raw channel 2 time series (+0.015°C). This was a combination of a Northern Hemisphere trend of +0.058.°C, and a Southern Hemisphere trend of -0.026°C. The removal of the stratospheric influence on MSU channel 2 during 1982-83 is probably the major reason for the difference in long-term trends between channel 2 and 2R since it occurred in the first half of the twelve year record.

5. Conclusions

A procedure for removal of the stratospheric influence on MSU channel 2 for more useful long-term tropospheric temperature monitoring has been applied to MSU channel 2 data from 1979-90, and tested with radiosonde data during 1979-88. Single gridpoint comparisons with individual radiosonde stations give correlations ranging from 0.97 (SE=0.48°C) at St. Cloud, Minnesota where the monthly tropospheric temperature anomaly signal is strong, to 0.74 (SE=0.16°C) at Guam where the signal is very weak compared to the limiting accuracy of both the radiosonde and satellite systems. Groupings of stations improve the standard errors to 0.11°C over the west Pacific to SE=0.35°C at high latitudes, with correlations ranging from 0.83 to 0.98, respectively. As was the case for the channel 2 results in Part I, the tropical standard errors reach the levels of agreement displayed by adjacent radiosonde stations. Best agreement with standard layers which radiosondes traditionally measure is with either 100-50 or 100-40 kPa layer anomalies.

For tropospheric temperature trends, the tropospheric retrieval shows some differences with raw channel 2 data, particularly during 1982-83 when stratospheric warming exaggerated the MSU channel 2 warm signal of the 1982-83 ENSO event. Other differences between channel 2 and 2R variations are probably related to variations in tropospheric stability. The satellite record trends for the retrieval differ from the channel 2 trends by only 0.01°C, with a tropospheric retrieval trend of +0.032°/decade and a channel 2 trend of +0.015°C/decade for the period 1979-90.

6. References

Conrath, B.J., 1972: Vertical resolution of temperature profiles obtained from remote radiation measurements. *J. Atmos. Sci.*, **29**, 1262-1271.

Grody, N.C., 1980: Analysis of satellite-based microwave retrievals of temperature and thermal winds: Effects of channel selection and a-priori mean on retrieval accuracy. *Remote Sensing of the Atmosphere and Oceans*, A. Deepak, Ed., Academic Press, 381-410.

Spencer, R.W. and J.R. Christy, 1990: Precise monitoring of global temperature trends from satellites. *Science*, **247**, 1558-1562.

Spencer, R.W., J.R. Christy, and N.C. Grody, 1990: Global atmospheric temperature monitoring with satellite microwave measurements: Method and results, 1979-84. *J. Climate.*, **3**, 1111-1128.

Acknowledgments

We thank Norman Grody (NOAA/NESDIS) for helpful advice during this study.

List of Figures

from the radiosonde data, and the dashed line shows the satellite-measured agreement with the radiosonde thickness temperature anomalies.

Figure 7. As in Fig. 6, except St. Cloud, Minnesota.

Figure 8. As in Fig. 6, except Oakland, California.

Figure 9. As in Fig. 6, except Lihue, Hawaii.

Figure 10. As in Fig. 6, except San Juan, Puerto Rico.

Figure 11. As in Fig. 6, except Guam.

Figure 12. MSU channel 2 (thin line) and tropospheric retrieval (thick line) T_b time series for the globe, Northern Hemisphere, and Southern Hemisphere during 1979-90. Series have been low pass filtered.

Table 1. Composited radiosonde layer average temperature trends for the ten year period 1979-88 for different regions.

Layer	Florida[1]	NW U.S.[2]	NE U.S.[3]	Great Lakes[4]	Caribbean[5]	West Pacific[6]
30-15 kPa	-0.48°	-1.28°	-0.53°	-0.92°	-0.29°	+0.14°
50-30 kPa	-0.06°	+1.34°	+0.85°	+1.14°	-0.02°	+0.10°
70-50 kPa	-0.05°	+1.37°	+0.80°	+1.31°	+0.04°	+0.07°
85-70 kPa	0.00°	+1.37°	+0.84°	+1.67°	+0.19°	+0.25°

[1]Apalachicola, Tampa, Miami, Key West
[2]Salem, Oregon; Quillayute, Washington
[3]Caribou, Maine; Chatham, Massachusetts; Buffalo, New York; Albany, New York; Portland, Maine
[4]Flint, Michigan; Peoria, Illinois; Green Bay, Wisconsin; International Falls, Minnesota; St. Cloud, Minnesota; Huron, South Dakota
[5]Christ Church, Barbados; Santo Domingo, Dominican Republic; Piarco, Trinidad; San Juan, Puerto Rico; Curacao, Netherland Antilles
[6]Yap Island; Koror Island; Ponape Island; Truk Island; Majuro Island; Guam; Wake Island

Table 2. Global statistics of all overlaps between MSUs for the channel 2 tropospheric temperature retrieval.

Satellite route to NOAA-6		Overlap Dates	#days	daily error (1 sat/2 sat)	daily S/N	30-day error (1 sat/2 sat)	30-day S/N
TIROS-N	to NOAA-6	7/1/79-1/19/80	156	$.093^{o}/.066^{o}$	7.0	$.024^{o}/.017^{o}$	20.4
NOAA-6	BASE						
NOAA-7	to NOAA-6	6/26/81-4/16/83	566	$.087^{o}/.061^{o}$	8.4	$.015^{o}/.011^{o}$	124.8
NOAA-9	to NOAA-6	10/30/85-11/4/86	228	$.087^{o}/.061^{o}$	17.7	$.015^{o}/.011^{o}$	74.1
NOAA-10	thru NOAA-9	11/26/86-3/7/87	96	$.092^{o}/.065^{o}$	11.9	$.013^{o}/.009^{o}$	300.5
NOAA-11	thru NOAA-10	10/23/88-12/31/90	678	$.088^{o}/.062^{o}$	8.3	$.029^{o}/.020^{o}$	40.7

Table 3. Station composite correlations and standard errors of satellite versus radiosonde monthly anomalies in channel 2R. Numbers in parentheses are the corresponding single-station values from the stations represented in Figs. 5-10.

Region	R	SE
Alaska(15)	.97(.94)	$.31^{o}(.50^{o})$
Great Lakes(6)	.98(.97)	$.37^{o}(.48^{o})$
West Coast(4)	.95(.91)	$.35^{o}(.54^{o})$
Caribbean(6)	.91(.84)	$.16^{o}(.29^{o})$
West Pacific(7)	.83(.74)	$.11^{o}(.16^{o})$

Alaska:(15) Anette, Yakutat, Kodiak, King Salmon, Cold Bay, Adak, St. Paul Island, Anchorage, Fairbanks, McGrath, Bethel, Kotzebue, Nome, Barter Island, Barrow. **Great Lakes:**(6) Sault Ste. Marie, MI; International Falls, MN; Green Bay, WI; St. Cloud, MN, Huron, SD. **U.S. West Coast:**(4) Quillayute, WA; Salem, OR; Oakland, CA; San Diego, CA. **Tropical West Pacific:**(7) Koror, Yap, Majuro, Wake, Guam, Truk, Ponape. **Caribbean:**(6) Christ Church, Barbados; Santo Domingo, Dominican Republic; Piarco, Trinidad; San Juan, Puerto Rico; Curacao, Netherland Antilles; Roberts, Cayman Islands

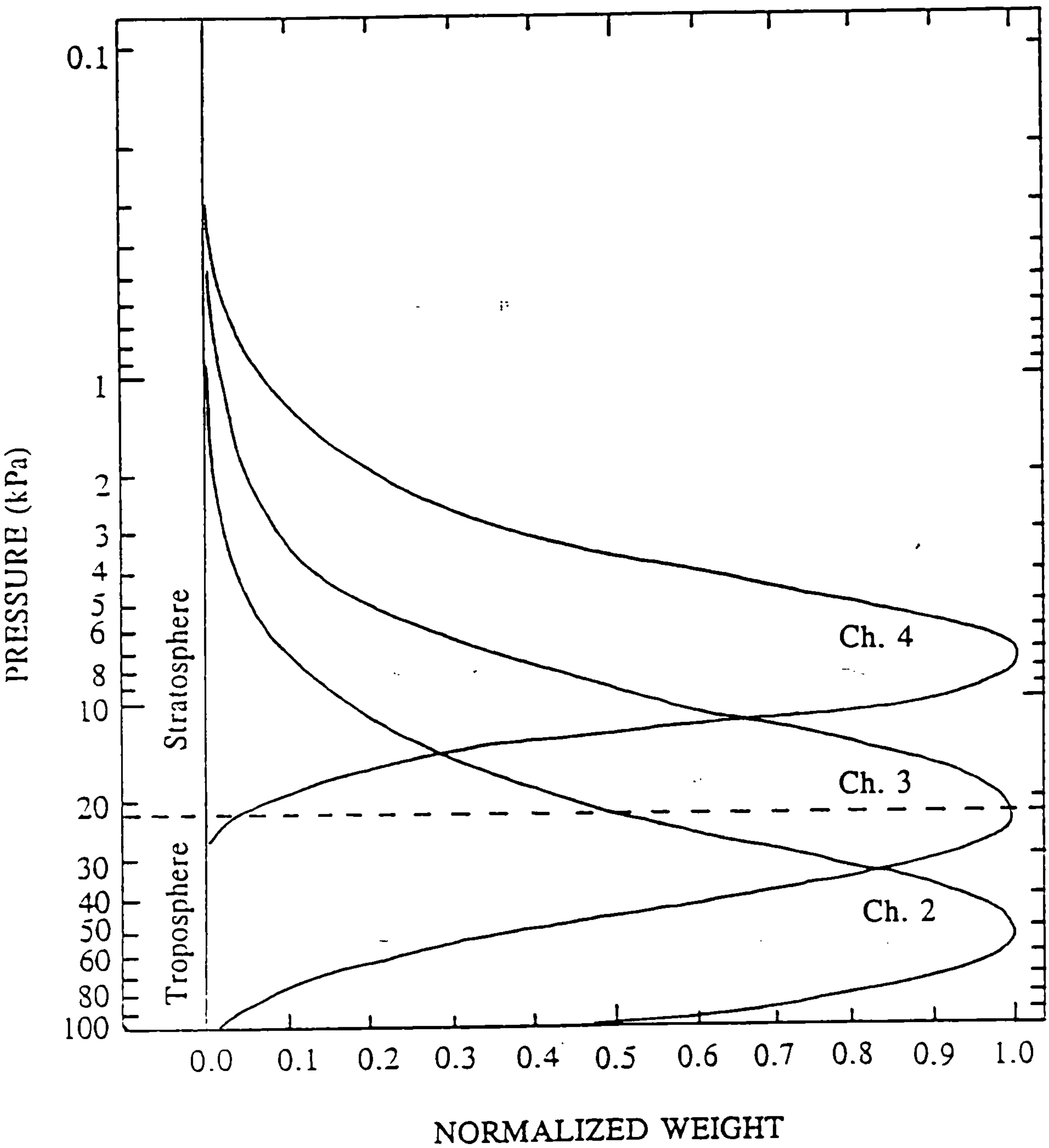
PRESSURE (kPa)
0.1
1
2
3
4
5
6
8
10
20
30
40
50
60
80
100
Stratosphere
Troposphere
Ch. 4
Ch. 3
Ch. 2
0.0
0.1
0.2
0.3
0.4
0.5
0.6
0.7
0.8
0.9
1.0
NORMALIZED WEIGHT

Fig. 1

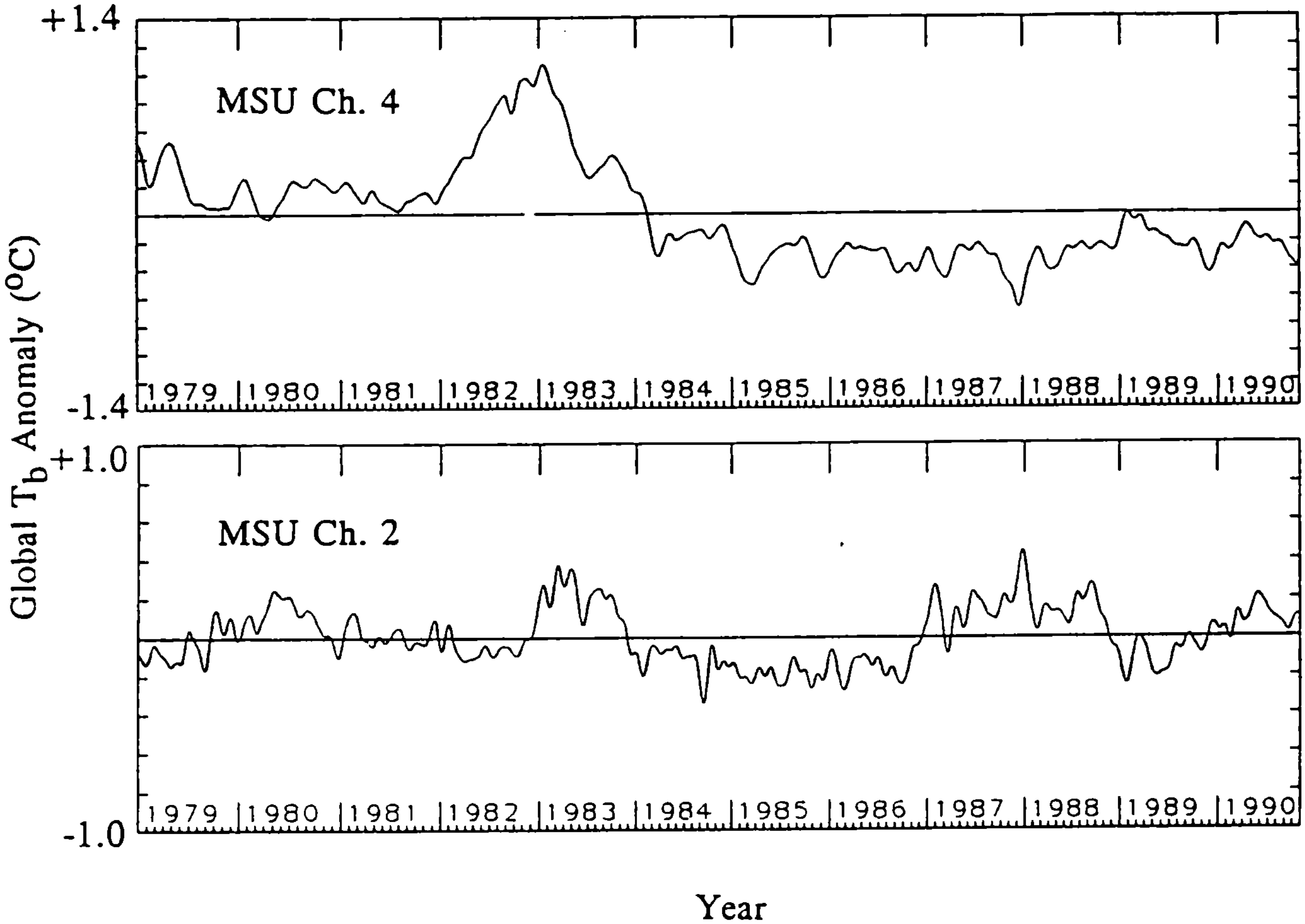
+1.4
MSU Ch. 4
-1.4
+1.0
MSU Ch. 2
-1.0
Global T_b Anomaly (^oC)
1979
1980
1981
1982
1983
1984
1985
1986
1987
1988
1989
1990
Year

Fig. 2

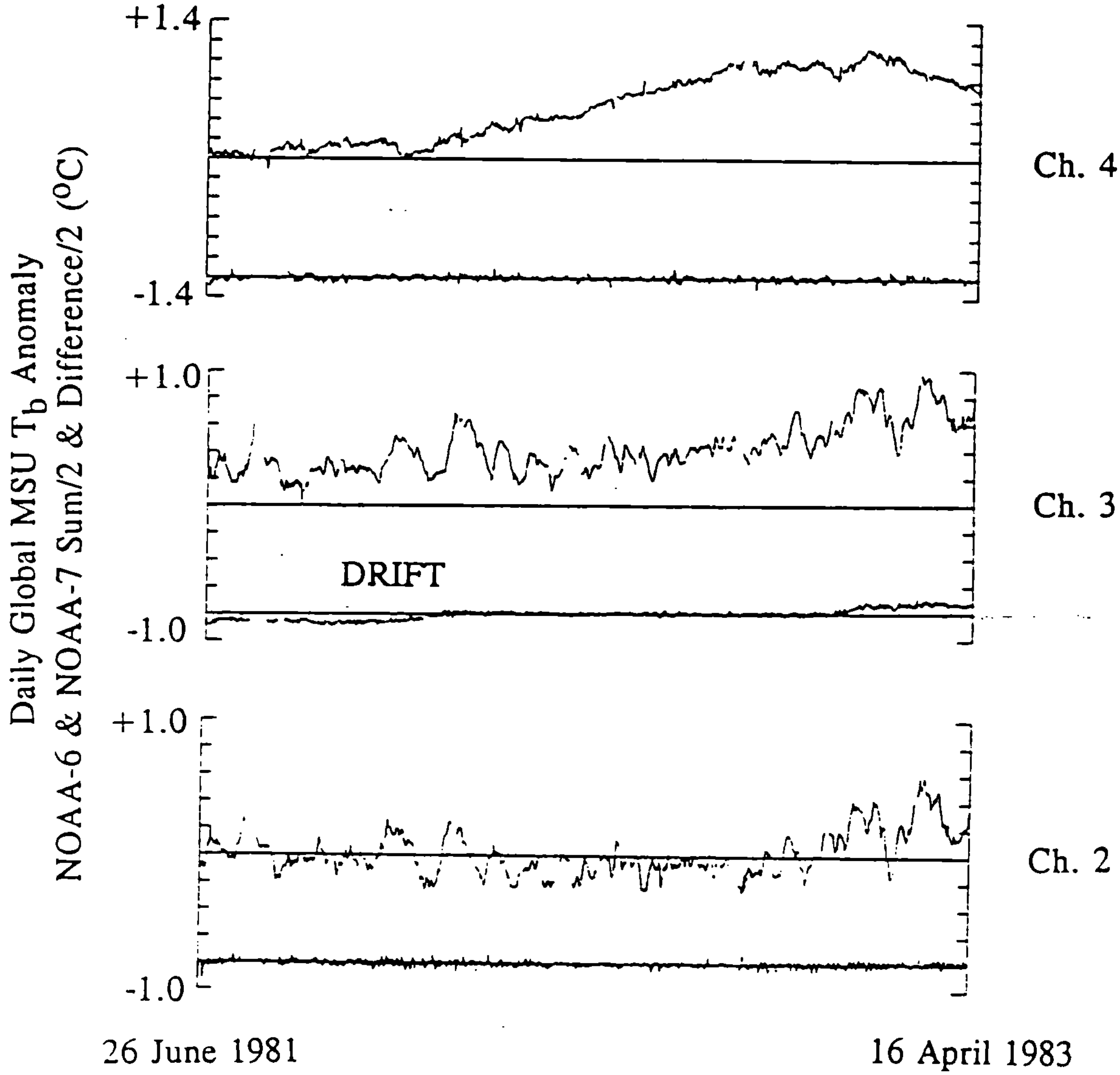

Daily Global MSU T_b Anomaly
NOAA-6 & NOAA-7 Sum/2 & Difference/2 (^oC)
+1.4
-1.4
Ch. 4
+1.0
-1.0
DRIFT
Ch. 3
+1.0
-1.0
Ch. 2
26 June 1981
16 April 1983

Fig. 3

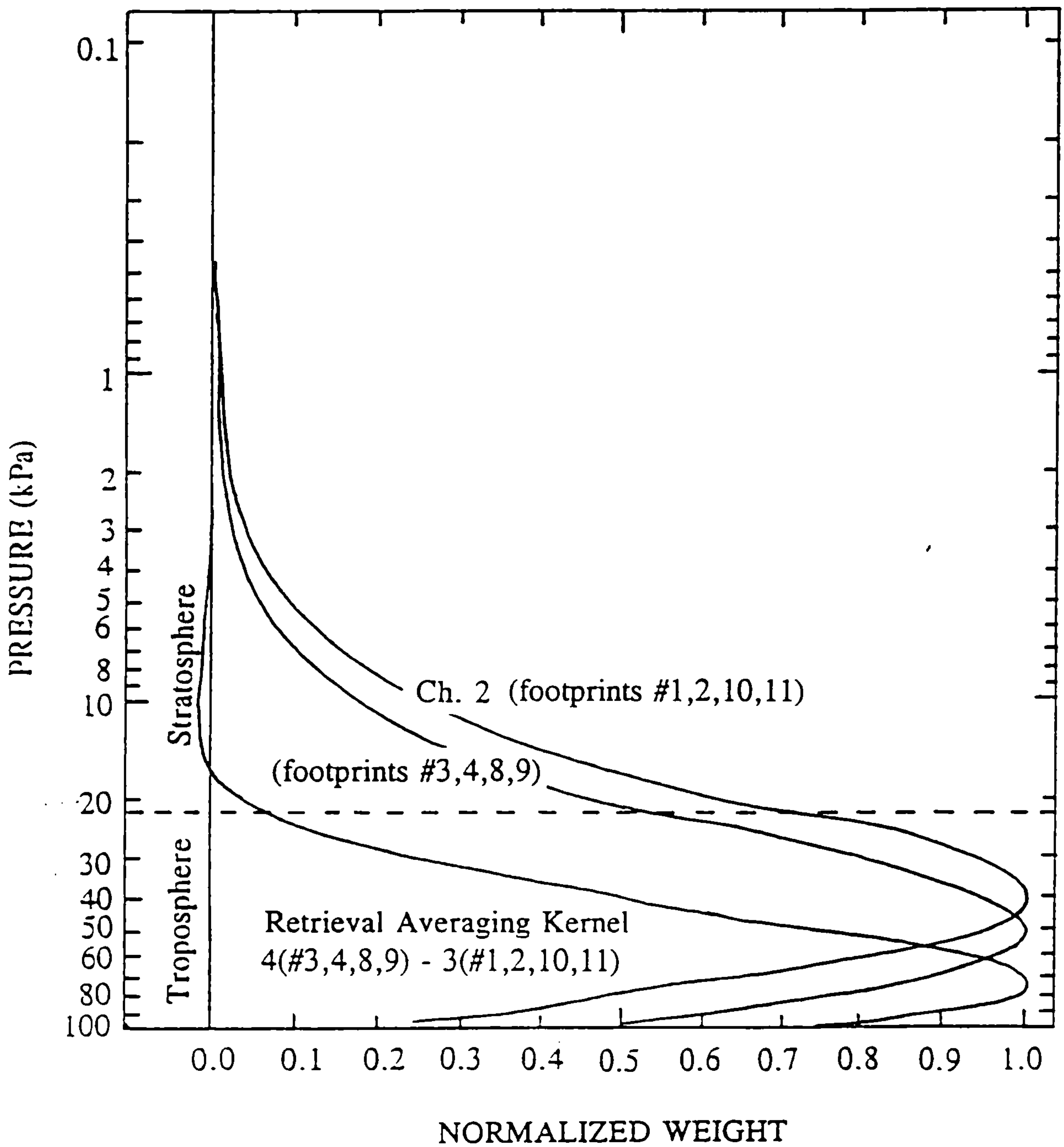

0.1
1
2
3
4
5
6
8
10
20
30
40
50
60
80
100
PRESSURE (kPa)
Stratosphere
Troposphere
Ch. 2 (footprints #1,2,10,11)
(footprints #3,4,8,9)
Retrieval Averaging Kernel
4(#3,4,8,9) - 3(#1,2,10,11)
0.0
0.1
0.2
0.3
0.4
0.5
0.6
0.7
0.8
0.9
1.0
NORMALIZED WEIGHT

Fig. 4

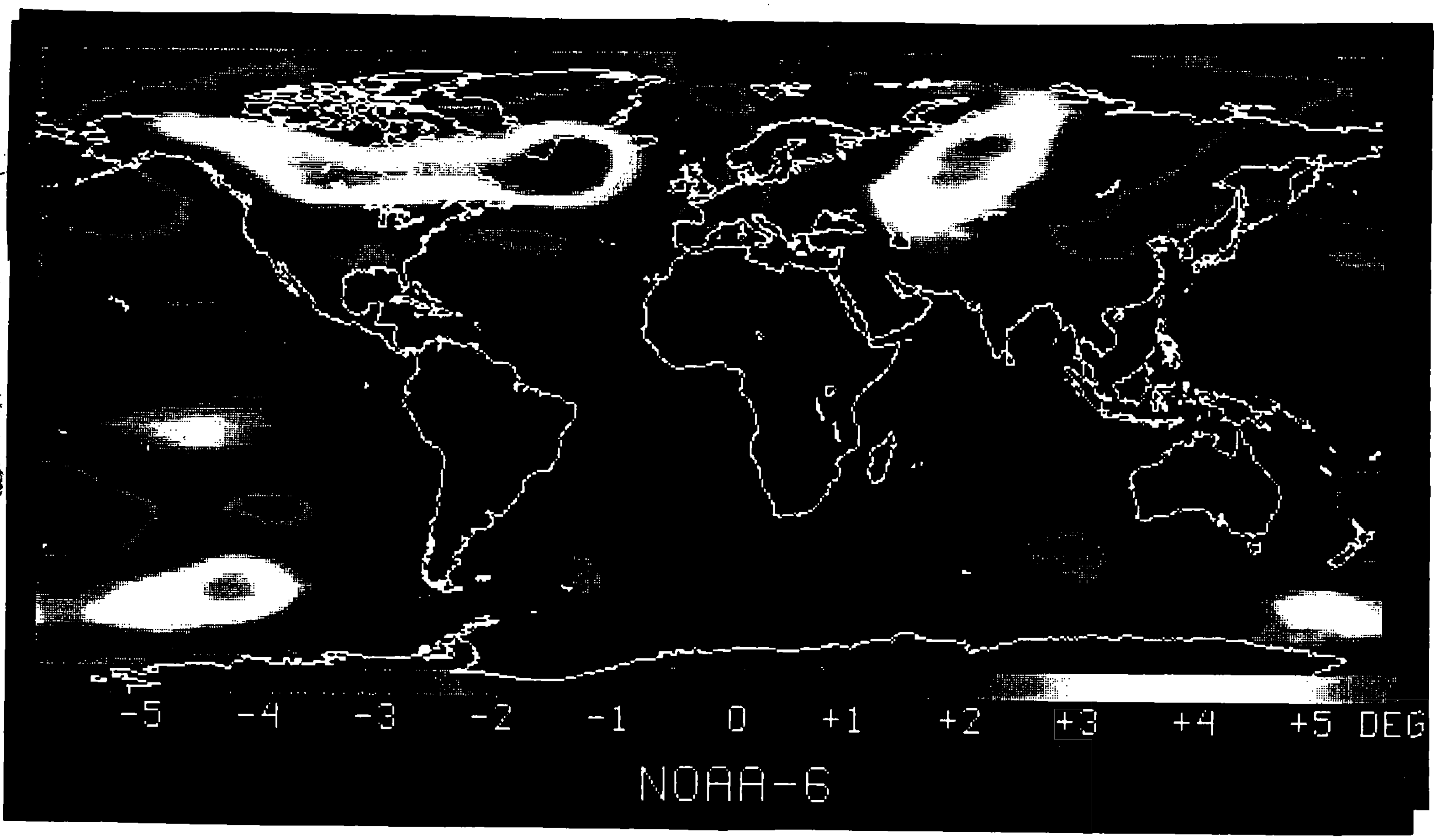

Ch 2
1983 Feb – 1982 Feb

Fig. 5 a,b,c (overlay)

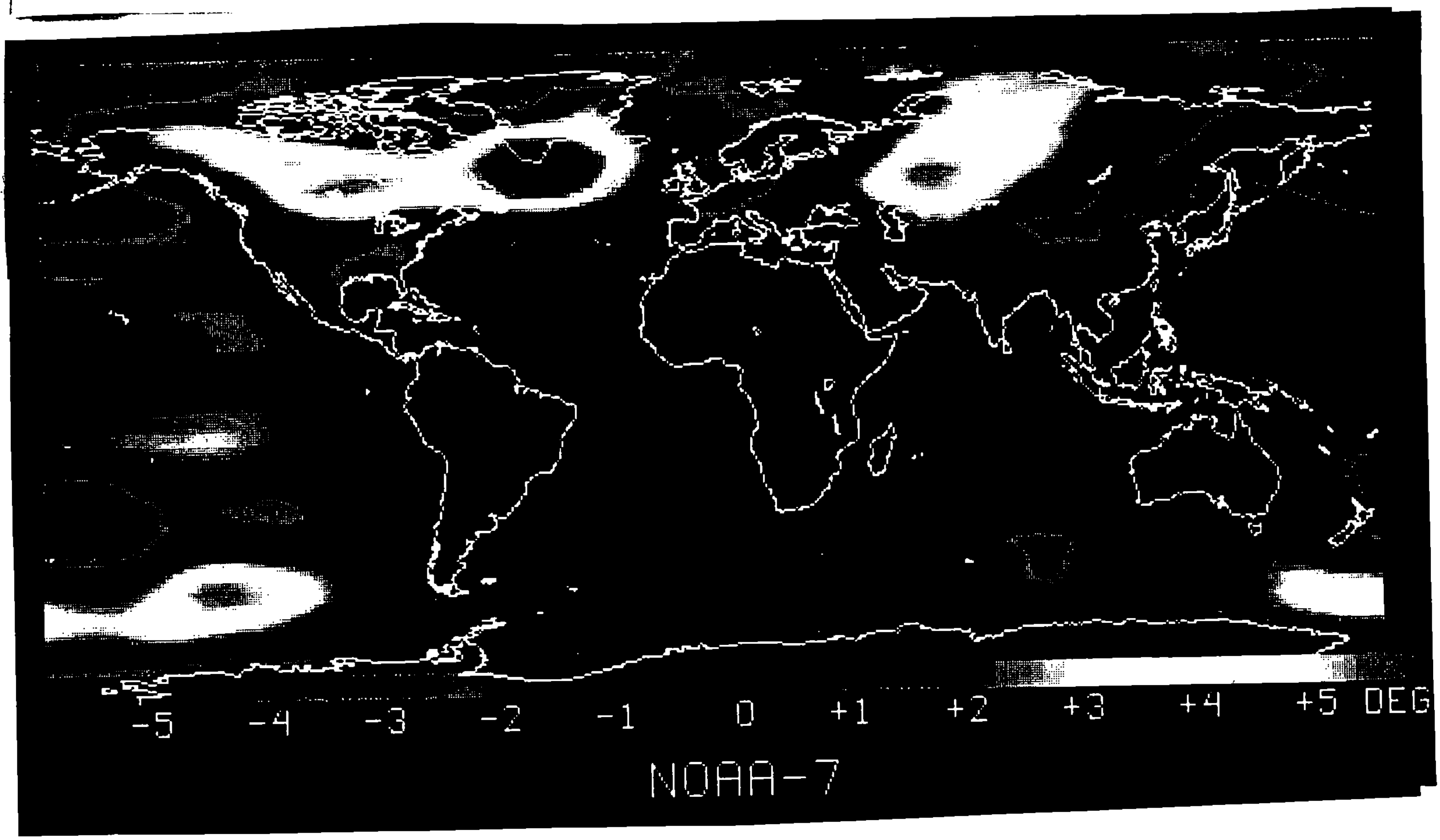

ch 2
1983 Feb - 1982 Feb

Fig. 5 a,b,c (overlay)

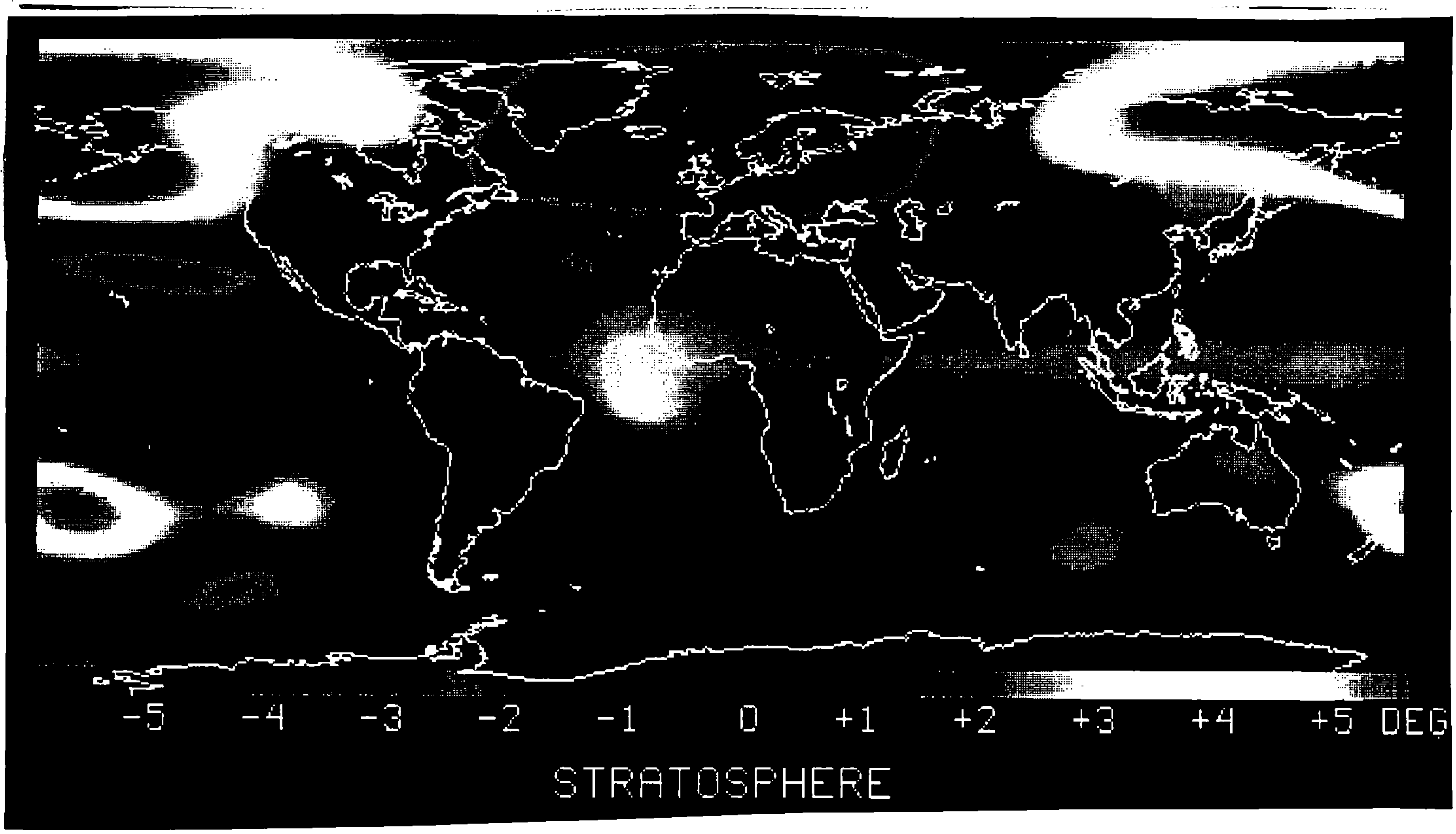

ch 2
1983 Feb – 1982 Feb

Fig. 5 a,b,c (overlay)

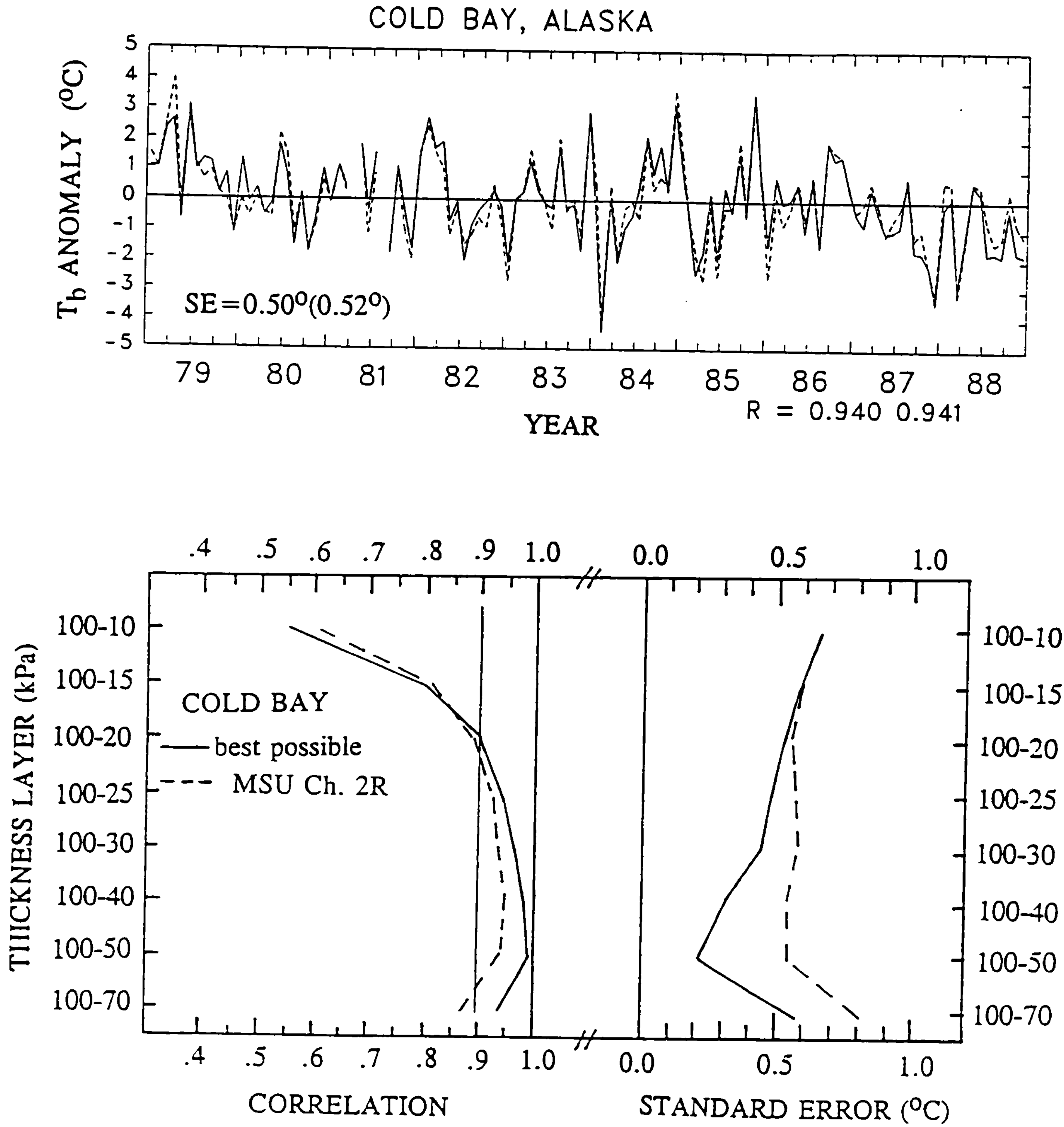

COLD BAY, ALASKA
T_b ANOMALY (^oC)
5
4
3
2
1
0
-1
-2
-3
-4
-5
SE=0.50°(0.52°)
79
80
81
82
83
84
85
86
87
88
YEAR
R = 0.940 0.941
.4
.5
.6
.7
.8
.9
1.0
0.0
0.5
1.0
THICKNESS LAYER (kPa)
100-10
100-15
100-20
100-25
100-30
100-40
100-50
100-70
COLD BAY
best possible
MSU Ch. 2R
CORRELATION
STANDARD ERROR (°C)

Fig. 6

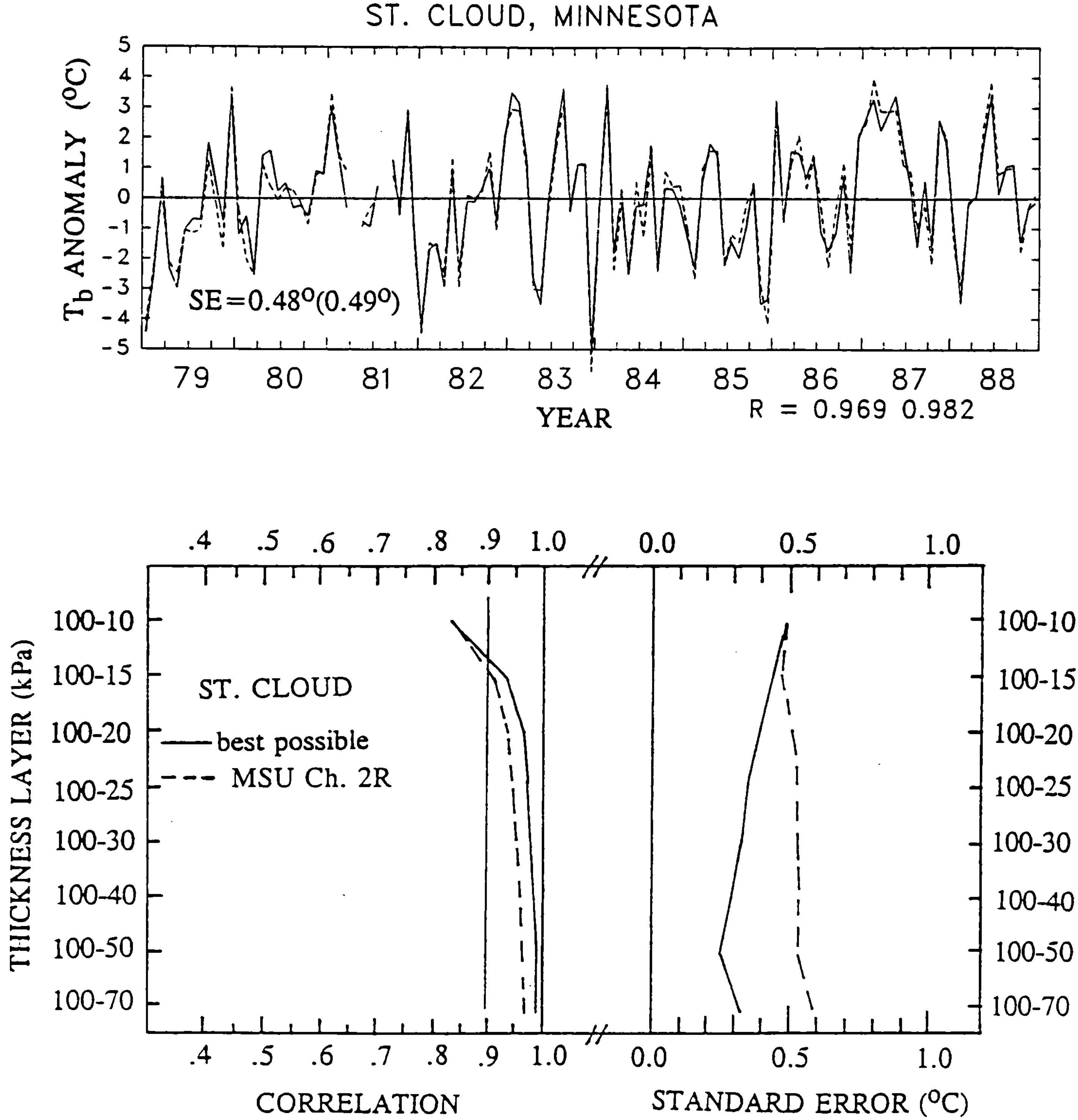

ST. CLOUD, MINNESOTA
Tb ANOMALY (°C)
SE=0.48°(0.49°)
79 80 81 82 83 84 85 86 87 88
YEAR
R = 0.969 0.982
ST. CLOUD
best possible
MSU Ch. 2R
THICKNESS LAYER (kPa)
100-10
100-15
100-20
100-25
100-30
100-40
100-50
100-70
.4 .5 .6 .7 .8 .9 1.0
0.0 0.5 1.0
CORRELATION
STANDARD ERROR (°C)

Fig. 7

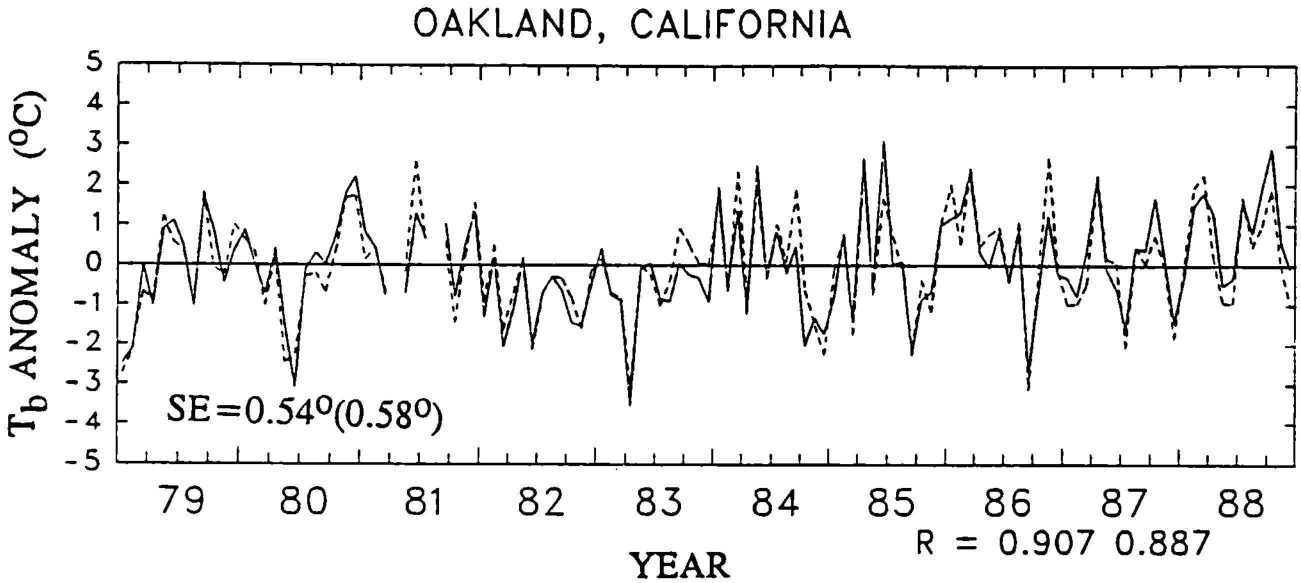
OAKLAND, CALIFORNIA
T_b ANOMALY (^oC)
SE=0.54°(0.58°)
79 80 81 82 83 84 85 86 87 88
R = 0.907 0.887
YEAR

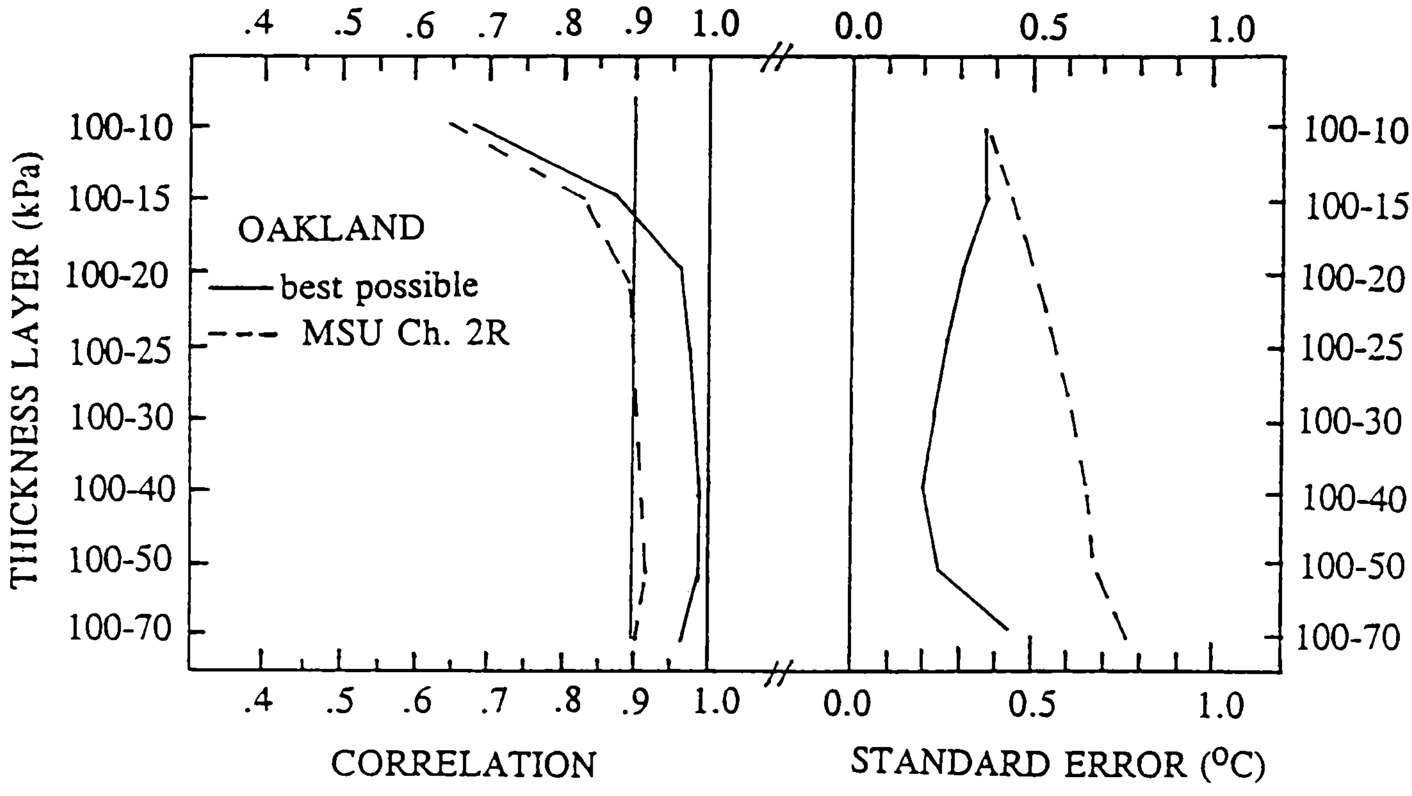
THICKNESS LAYER (kPa)
100-10
100-15
100-20
100-25
100-30
100-40
100-50
100-70
OAKLAND
best possible
MSU Ch. 2R
.4 .5 .6 .7 .8 .9 1.0
0.0 0.5 1.0
CORRELATION
STANDARD ERROR (°C)

Fig. 8

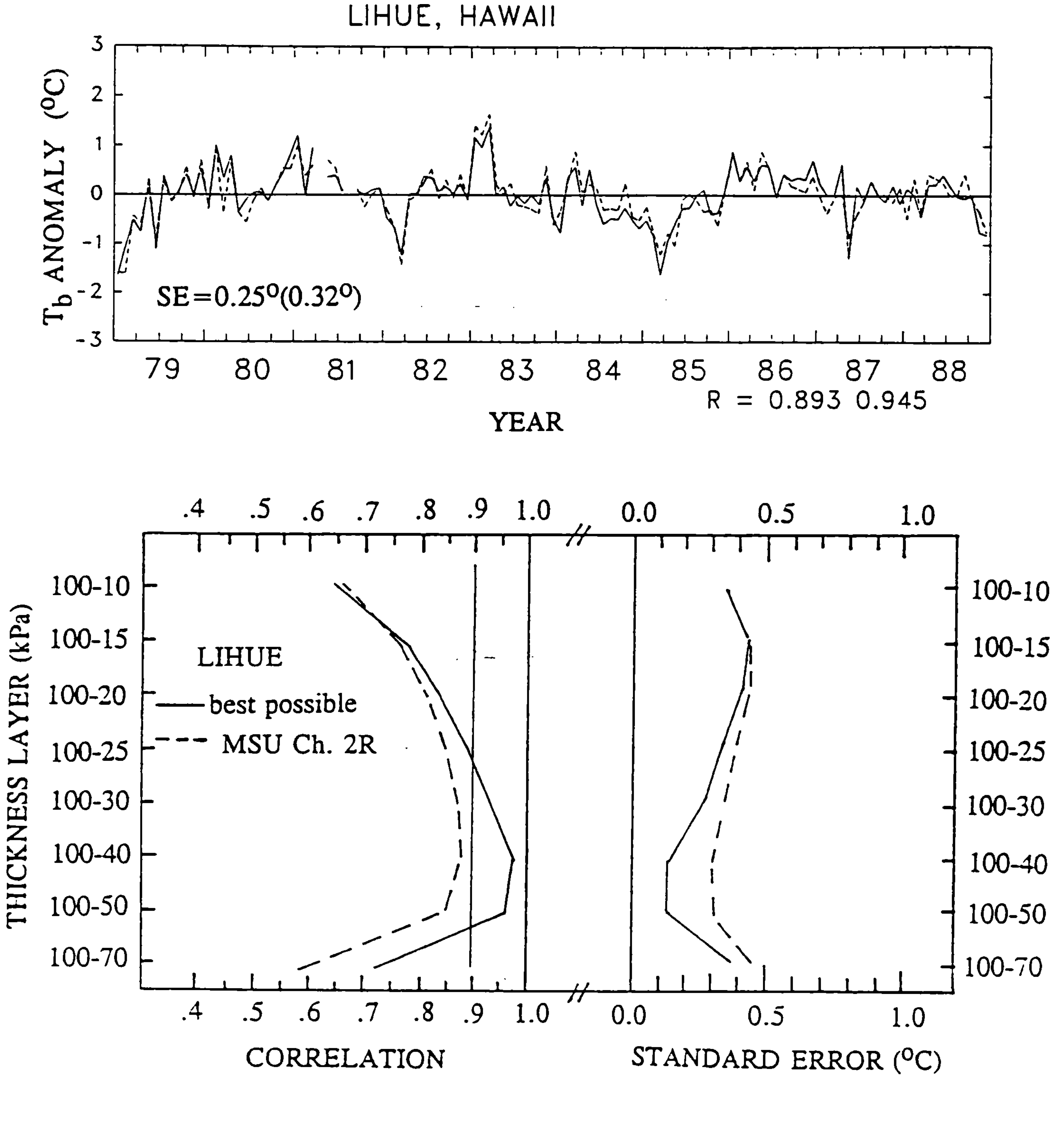

LIHUE, HAWAII
T_b ANOMALY (°C)
3
2
1
0
-1
-2
-3
SE=0.25°(0.32°)
79
80
81
82
83
84
85
86
87
88
R = 0.893 0.945
YEAR
.4
.5
.6
.7
.8
.9
1.0
0.0
0.5
1.0
THICKNESS LAYER (kPa)
100-10
100-15
100-20
100-25
100-30
100-40
100-50
100-70
LIHUE
best possible
MSU Ch. 2R
CORRELATION
STANDARD ERROR (°C)

Fig. 9

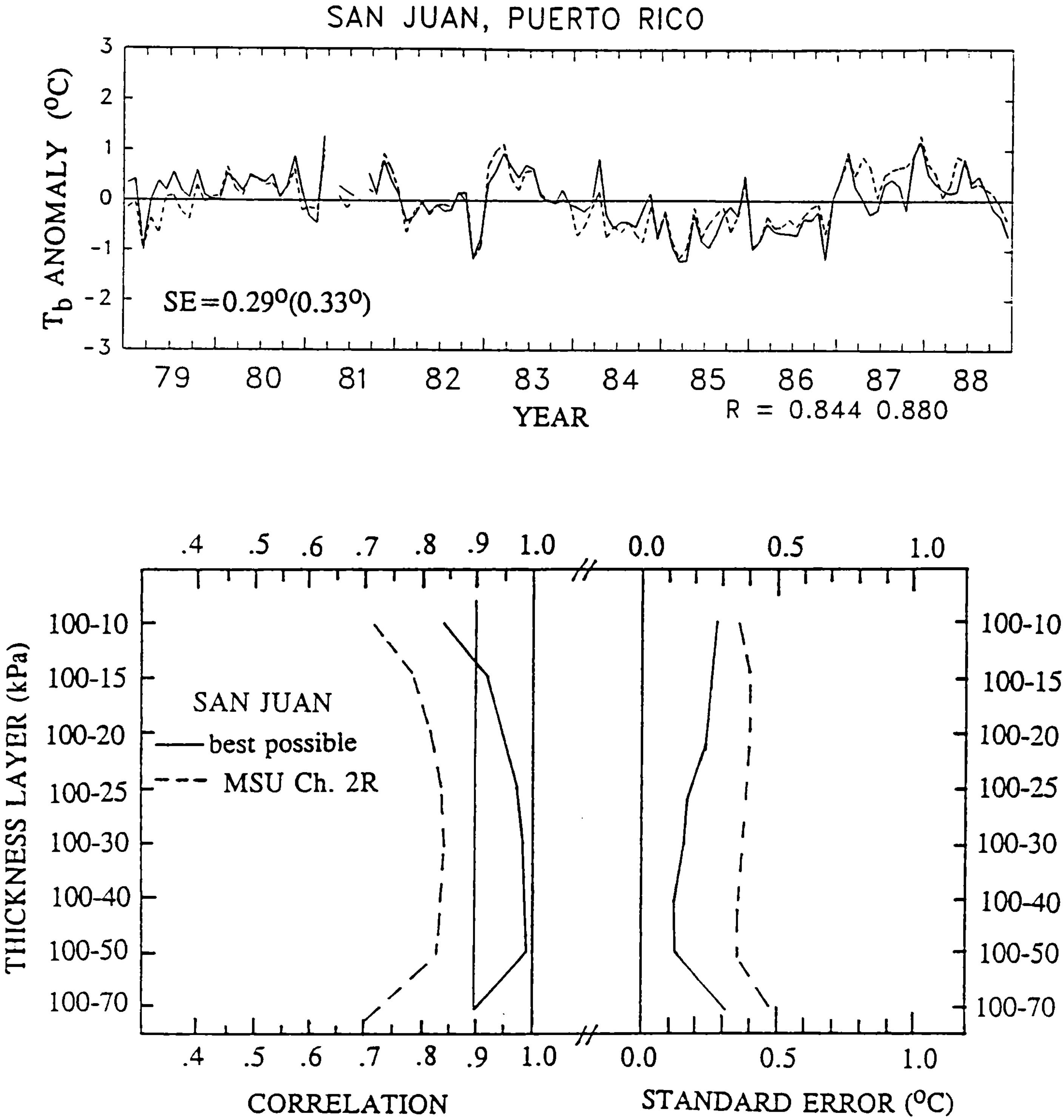
SAN JUAN, PUERTO RICO
T_b ANOMALY (°C)
3
2
1
0
-1
-2
-3
SE=0.29°(0.33°)
79 80 81 82 83 84 85 86 87 88
YEAR
R = 0.844 0.880
.4 .5 .6 .7 .8 .9 1.0
0.0 0.5 1.0
THICKNESS LAYER (kPa)
100-10
100-15
100-20
100-25
100-30
100-40
100-50
100-70
SAN JUAN
best possible
MSU Ch. 2R
CORRELATION
STANDARD ERROR (°C)

Fig. 10

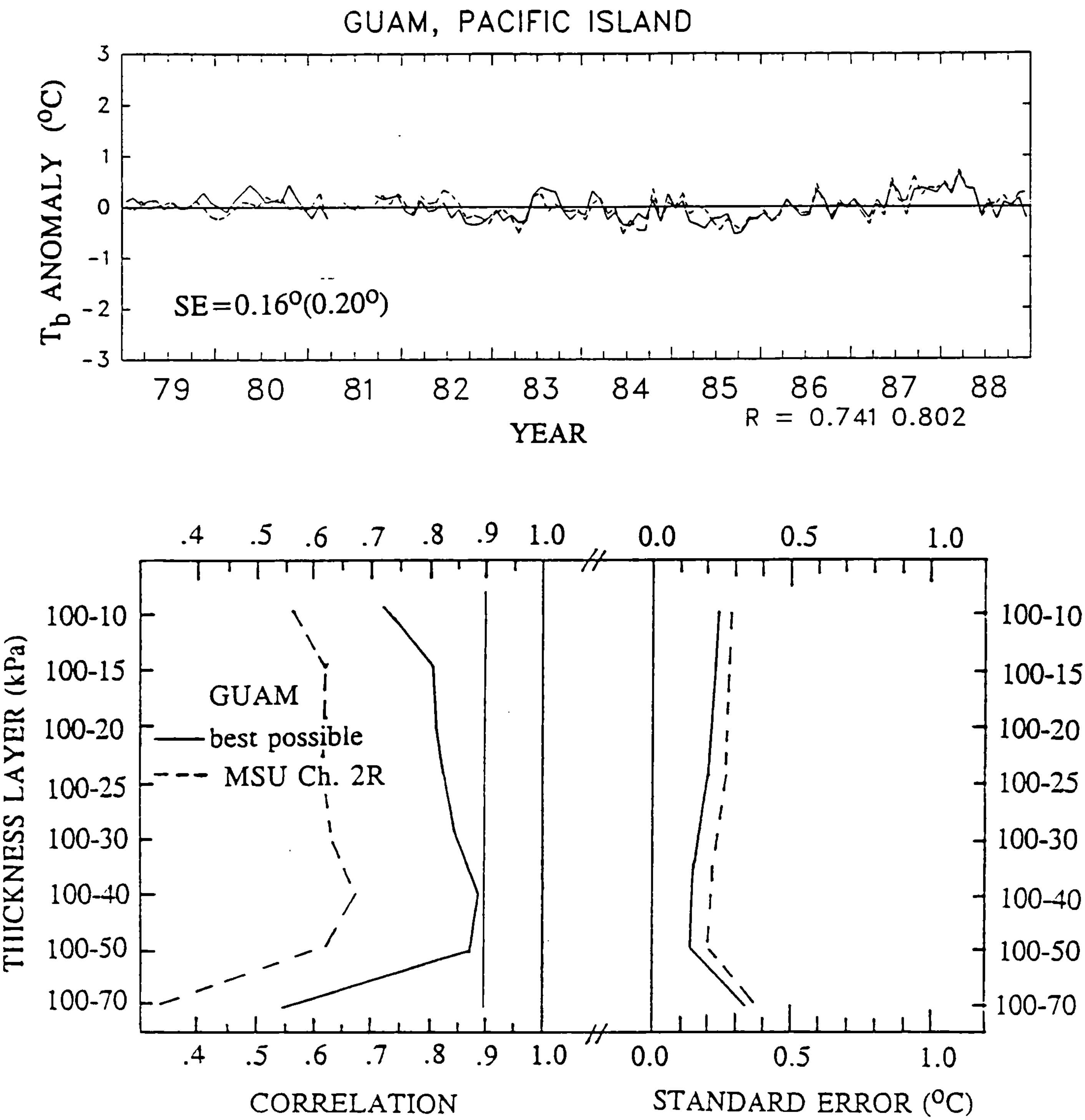

GUAM, PACIFIC ISLAND
T_b ANOMALY (°C)
SE=0.16°(0.20°)
79 80 81 82 83 84 85 86 87 88
YEAR
R = 0.741 0.802
THICKNESS LAYER (kPa)
100-10
100-15
100-20
100-25
100-30
100-40
100-50
100-70
GUAM
best possible
MSU Ch. 2R
.4 .5 .6 .7 .8 .9 1.0
0.0 0.5 1.0
CORRELATION
STANDARD ERROR (°C)

Fig. 11

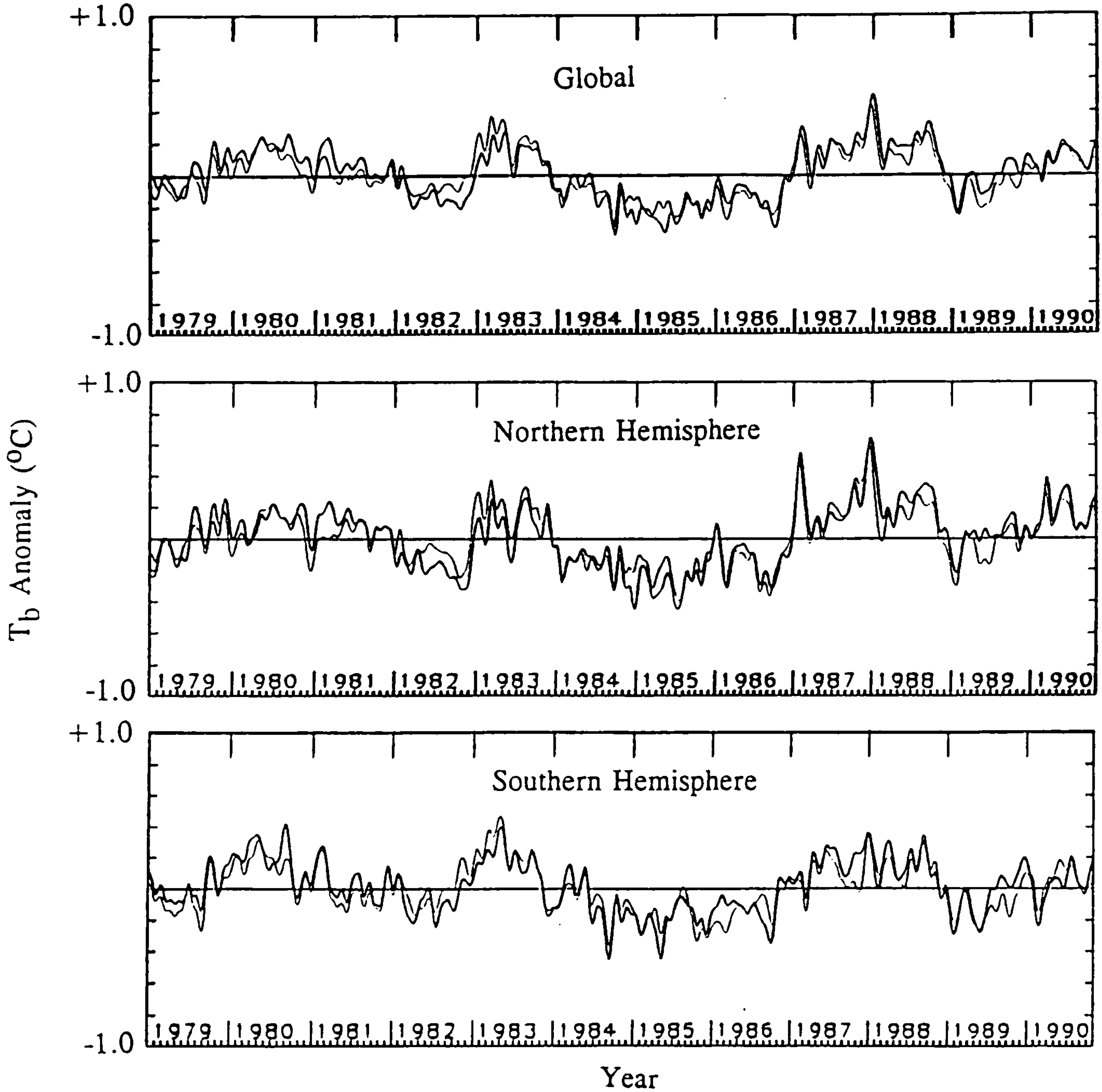

+1.0
-1.0
Global
Northern Hemisphere
Southern Hemisphere
T_b Anomaly (^oC)
1979 1980 1981 1982 1983 1984 1985 1986 1987 1988 1989 1990
Year

Fig. 12

Precision and Radiosonde Validation of Satellite Gridpoint Temperature Anomalies, Part I: MSU Channel 2

by

Roy W. Spencer

ES43 Earth Science and Applications Division

NASA Marshall Space Flight Center

Alabama 35812

John R. Christy

Johnson Research Center

University of Alabama in Huntsville

Huntsville, Alabama 35899

submitted to

Journal of Climate

April 1991

ABSTRACT

In Part I of this study, monthly 2.5^{o} gridpoint anomalies in TIROS-N Microwave Sounding Unit channel 2 brightness temperatures during 1979-88 are evaluated with multiple satellites and radiosonde data for their climate temperature monitoring capability. The monthly gridpoint agreement between concurrently operating satellites is generally better than 0.1^{o}C in the tropics and better than 0.2^{o}C at higher latitudes. Monthly anomalies in radiosonde channel 2 brightness temperatures computed with the radiative transfer equation compare very closely to the MSU measured anomalies in all climate zones, with correlations generally from 0.94 to 0.98 and standard errors of 0.15^{o}C in the tropics to 0.30^{o}C at high latitudes. Simplification of these radiative transfer calculations to a static weighting profile applied to the radiosonde temperature profile leads to an average degradation of only 0.02^{o} in the monthly skill. In terms of a more traditionally measured quantity, the MSU channel 2 anomalies match best with either the 100-20 kPa or 100-15 kPa layer anomalies. No significant spurious trends were found in the ten-year satellite dataset. Thus sequentially launched, overlapping passive microwave radiometers provide a useful system for monitoring intraseasonal to interannual climate anomalies. The Appendix includes previously unpublished details of the MSU gridpoint anomaly data set construction. Part II of this study addresses the removal from channel 2 of the temperature influence above the 30 kPa level, a layer which often experiences considerably different trends than those measured by radiosondes below 30 kPa.

1. Background

The potential of externally calibrated microwave radiometers for precision monitoring of climate change was demonstrated by Spencer and Christy (1990, hereafter SC) and Spencer et al. (1990, hereafter SCG) in the context of deep tropospheric and lower stratospheric brightness temperature (T_b) anomalies. Satellite intercomparisons between simultaneously operating Microwave Sounding Units (MSUs) on morning and afternoon TIROS-N satellites revealed agreement to 0.01°C for monthly, globally averaged T_b anomalies, and instrument stability to better than 0.01°C over a two year overlap period. Whereas these results addressed the precision of the satellite measurements on hemispheric and global scales, we now extend this evaluation to the 2.5° gridpoint scale, and incorporate radiosondes as an independent tool for verifying their quality.

A fundamental question often asked is, what do the channel 2 T_b anomalies represent? First let us address the deep-layer nature of the measurement. The channel 2 weighting function (Fig. 1) is vertically broad and represents the vertical distribution (in $\log_e p$ coordinates) of the satellite-measured radiation over a layer extending from the surface to above 30 kPa. The bulk of this microwave radiation is thermally emitted by molecular oxygen with an intensity directly proportional to temperature. A much smaller contribution is from water vapor thermal emission. Oxygen is an ideal temperature tracer for climate monitoring because it occupies a large fraction of our atmosphere (20.95% by volume), is uniformly mixed, and its concentration is very stable in time. Therefore, MSU channel 2 measurements are dominated by the vertically weighted air temperature through a deep tropospheric layer of air. In typical satellite sounder "retrieval" schemes, this deep layer measurement is combined with other channels having overlapping weighting functions (such as MSU channels 1,3, and 4 in Fig. 1) in order to deconvolve these weighting functions into an "averaging kernel" (see Conrath, 1972, and Grody, 1980) which is considerably sharper than the individual channel weighting functions. However, we rapidly approach a practical limit in our ability to sharpen the averaging kernel because of the finite number of channels, each having a certain amount of measurement noise. Therefore, based upon current theoretical and engineering limits, the satellites simply can not measure the many levels a radiosonde system measures. Thus, even though satellite temperature retrievals often relate the measurements to temperature at a specific level in the atmosphere, this assignment is ultimately based upon certain average statistical relationships which occur in the atmosphere which are, by their assumed time-invariant nature, irrelevant to the climate monitoring issue.

A second issue concerns much of the satellite-measured signal is contaminated by non-oxygen emission. Based upon theory (see SCG) we expect the MSU channel 2 T_b anomalies to have small contaminating influences from interannual variations in precipitation-size ice in deep convection, cloud water, water vapor, and surface emissivity. However, the magnitudes of these contaminants are difficult to quantify without knowledge of interannual variations in these variables. Theoretical evidence was presented by SCG to support interpretation of the T_b anomalies as dominated by thermometric temperature to about $0.01^{o}C$ for globally averaged monthly anomalies, although regional areas might experience contaminating influences exceeding $0.1^{o}C$.

Therefore, at this point we hypothesize that the channel 2 anomalies are dominated by thermometric temperature variations over a layer represented by the channel 2 weighting function. However, theory alone is insufficient for rigorous evaluation of the satellite temperature monitoring technique. Here we will present results of comparisons between ten years of monthly radiosonde thickness anomalies to the MSU channel 2 anomalies, in atmospheric environments ranging from tropical to polar. If it can be demonstrated that individual gridpoint anomalies in MSU channel 2 T_b closely match anomalies in radiosonde measurements, then we will have increased confidence that the full global 2.5^{o} gridpoint dataset can be successfully utilized for intraseasonal to interannual climate studies. Furthermore, if there is little or no ten year trend in the difference between the radiosonde and satellite time series, then the satellite system will be supported for long-term monitoring (e.g. of potential global warming).

2. Some limits of radiosonde precision for gridpoint climate monitoring

Before gridpoint comparisons with radiosonde data are carried out, it is useful to address the capability of a single radiosonde station to measure monthly anomalies in different layers, as well as for long-term trends.

a. monthly radiosonde precision

Individual radiosonde temperature profiles are generally considered to have about a $0.7^{\circ}C$ random error in the absolute calibration of the sonde. If a station makes sixty observations per month, then that station's precision in the measurement of a monthly temperature anomaly is $(0.7/(60)^{1/2})$, or about $0.1^{\circ}C$. The fact that each measured profile might not accurately represent the larger scale environment will produce an additional source of error for climate monitoring which is related to temperature variability on the micro- and mesoscale. Let us assume this error component to be about $0.2^{\circ}C$. Assuming these errors to be uncorrelated, we arrive at an RMS error of somewhat over $0.2^{\circ}C$ for a single station's ability to measure monthly temperature anomalies.

We have chosen two pairs of tropical western Pacific Ocean stations which are closely spaced to see what level of agreement is experienced for monthly temperature anomalies. These are Yap and Koror Islands; and Truk and Ponape Islands. The tropical environments were chosen to avoid significant horizontal gradients in the monthly anomalies. The distances between these station pairs are 450 km and 700 km, respectively. In Figure 2a we have plotted the agreement between these station pairs in terms of correlations and standard errors of estimate for different layers' thicknesses. We see that the agreement between stations is about $0.2^{\circ}C$, which is consistent with our *a priori* estimate.

b. ten year trends

When we plot the ten-year trends of the layer temperatures for these station pairs (Fig. 2b) we see disturbingly large differences of 0.2° to 0.5°C for the period 1979-88. If we also examine two other western Pacific stations, Guam and Majuro, we find somewhat less disagreement and a tendency towards zero trend. Whatever the reasons for such large variability in single station trends, it appears that decadal trends calculated from a single radiosonde station should be viewed with extreme caution. If this station-to-station variability is random in nature, then many-station averages might be more confidently related to real atmospheric temperature trends (as we will see below). In any event, any disagreement we later find in the satellite comparisons to decadal radiosonde trends at the 0.1° or 0.2° level probably falls in the realm of noise.

3. Satellite gridpoint dataset construction and precision

a. limb correction and gridpoint assignment

The MSU measures at eleven scan angles as it scans across the satellite subtrack every 9.5° from 47° left to 47° right of nadir (see SCG for more information regarding the MSU sampling geometry). Each scan position measurement was calibrated as a T_b according to the procedure in SCG. After calibration, regression-derived limb correction equations were applied to all ten non-nadir scan positions data to correct for the off-nadir T_b being an average amount colder than the nadir T_b. This relative coldness is due to the off-nadir weighting functions being slightly higher in the troposphere than the nadir weighting function caused by the increased atmospheric path length of the radiation off-nadir. These limb correction equations have the form

$$T_{bL} = aT_b - b, \quad (1)$$

where T_{bL} is the limb corrected T_b for an individual MSU scan position, and the regression coefficients constants "a" and "b" were derived as a function of satellite, 10^o latitude band, and scan position. Approximately 6,700 scans were chosen from each of twelve calendar months of the separate satellites for certain years, i.e. TIROS-N (1979), NOAA-6 and NOAA-7 (1982); NOAA-9 (1986); NOAA-10 and NOAA-11 (1990). For it to be included, each scan had to exhibit little evidence of horizontal (synoptic scale) temperature gradients, with the difference in the T_b from opposite ends of the scan line not exceeding a few degrees. For each satellite, all twelve months of data (80,000 scan lines) were partitioned according to which 10^o latitude band each occupied (assigned by the nadir scan position). Both northern and southern latitude bands were combined together to avoid averaging biases arising from a single scan position usually being on the warmer (tropical) or colder (polar) side of the nadir footprint. The resulting limb corrected T_{bL} for the first (#1) and last (#11) scan positions were quite noisy, so they were not included in any further processing of the data.

Next, each T_{bL} was binned into the appropriate 2.5^o grid square according to the latitudes and longitudes provided with the raw data by NESDIS. This was done on a daily basis for each satellite separately and for ascending and descending satellite passes separately. At the end of each day, a simple (1/distance) interpolation was performed to empty 2.5^o grid squares for ascending and descending grid fields separately with the nearest non-zero grid data in the east and west directions, out to a maximum distance of fifteen grids. These interpolated ascending and descending T_{bL} fields were then averaged together to provide a single daily T_{bL} field for each satellite. At the end of each month, a time interpolation was performed (+/- 2 days) to any remaining empty grid squares. The daily fields were then averaged together within each month. Further references to the averaged fields will always assume the limb correction procedure was applied to the calibrated data (T_{bL}), so for brevity we will now refer to the data as simply T_b.

b. gridpoint anomaly calculation

Production of monthly gridpoint T_b anomalies would be a simple procedure if a single satellite had been operating for the full period of the satellite record. This would have involved computing, say, a ten-year average for each of the twelve calendar months at every gridpoint and then subtracting this average from individual months within the ten year period. Unfortunately, there are two complications which must be taken into account.

First, the satellite record is made up of seven satellites (six of which we use, see Fig. A1), all of which have calibration biases relative to each other by up to several tenths of a degree. The second complication is the existence of not one, but two separate orbit times alternating throughout the satellite record. Because MSU channel 2 has a small surface sensitivity to diurnal variations in land surface heating, the gridpoint averages are dependent upon the satellite orbit time (2:30 or 7:30) and the local strength of the diurnal heating cycle, which is a function of geography and time of year.

The procedure for the merging of all six satellites' data records into a single time series of anomalies is described in the Appendix. This is the same procedure which led to the global time series reported by SC and SCG, but some details of which have been previously undocumented.

c. gridpoint precision

The precision of the satellite T_b anomaly measurements at the gridpoint level can be readily demonstrated without the satellite merging procedure described in the Appendix. Because the TIROS-N satellite system occasionally had two satellites simultaneously operating in separate orbits (7:30 and 2:30) for more than one year, we can compare their measurements of interannual variability in two successive years. (This, of course, provides an interannual anomaly measurement since any multi-year mean assigned for those two years cancels out in the difference.) Then we can compare the results from the separate satellites to evaluate how well a single satellite can measure monthly gridpoint anomalies in T_b. If this procedure is followed for the month of February from 1982 and 1983, we find remarkable agreement between the NOAA-6 and NOAA-7 satellites (Fig. 3a and 3b, respectively). For this single month, the gridpoint correlation between satellites in each 2.5^{o} latitude band ranges from 0.95 in the tropics to over 0.99 at the higher latitudes, with the standard deviation of the satellite difference ranging from generally less than $0.1^{o}C$ in the tropics to generally less than $0.2^{o}C$ at middle and high latitudes. Note that this level of gridpoint agreement between satellites is as good or better than the accuracy provided by adjacent tropical radiosonde stations, as previously discussed. Further, since these are single-satellite precision, the error is reduced even further (by 0.7) when two satellites are operating.

If we utilize the full gridpoint dataset (assembled according to the procedures in the Appendix) we can evaluate monthly gridpoint precision for many more months when the satellite operating periods overlap. A map of the standard deviation of the monthly inter-satellite differences between NOAA-6 and NOAA-7 (Fig. 4) shows the level of monthly anomaly agreement for an overlap period of twenty months. Note that most areas have gridpoint T_b agreement to better than $0.1^{o}C$, mainly in the tropics, with almost all other non-tropical areas exhibiting better than $0.2^{o}C$ agreement. Degradation of a few hundredths of a degree is seen over land areas, noise which is probably introduced by the diurnal variations in the surface as seen by the morning and afternoon satellites. A few small areas of mountainous terrain (the Andes, Himilayas, Tibetan Plateau, and portions of Greenland and Antarctica) show poorer agreement between satellites due to enhancement of this surface influence as the terrain protrudes up into the channel 2 weighting function.

4. Radiosonde comparisons

While the above results demonstrate there is great precision in the ability of a single MSU to precisely monitor monthly gridpoint anomalies in channel 2 T_b, it still remains to be demonstrated that these anomalies are dominated by a temperature signal. We will address three kinds of radiosonde comparisons to MSU measured anomalies: 1) channel 2 T_b computed from the radiosonde profiles of temperature and humidity with the radiative transfer equation (see Grody, 1983), 2) a much simpler method where an assumed constant weighting function is applied to the radiosonde temperature profile only, and 3) comparisons to traditionally measured thickness anomalies for various standard atmospheric layers.

a. radiosonde data processing

The channel 2 T_b anomalies from the merged multi-satellite dataset at specific 2.5^o gridsquares were compared to radiosonde measurements for individual stations within those grid squares. The radiosonde data utilized for our intercomparisons is a quality controlled dataset provided by NCAR. The stations are United States (U.S.)-controlled and include, in addition to the mainland United States, scattered Pacific, Caribbean basin, and Alaska locations. Of approximately 120 stations which have fairly complete ten year records, here we will present the results from six stations representing various climate regimes (Table 1). Also, comparisons to several stations from each of these six regimes are composited together to provide regionally averaged comparisons.

In the first type of radiosonde comparison, the radiative transfer equation (Grody, 1983) was used to compute a T_b with the temperature and water vapor information provided by the radiosonde. All radiosonde ascents were included which went above 10 kPa, with the most recent radiosonde data above 2 kPa (usually not more than one or two days old) being inserted if the current profile did not go above 2 kPa. Each sounding was capped by an artificial temperature of 250 K at 0.01 kPa level. These T_b computations throughout the 10-year period were averaged on a monthly basis. The ten-year (1979-88) monthly averages were then subtracted from the individual monthly averages to arrive at a 10-year time series of monthly anomalies.

Secondly, a simpler method of computing T_b was used which avoids the computational intensity of the radiative transfer equation. Because the temperature dependence of the oxygen absorption and the water vapor absorption are both small, a static weighting function can be applied to just the temperature profile without risking great error. The channel 2 weighting function for a U.S. Standard Atmosphere (Fig. 1) was applied to the radiosonde temperature profiles to provide a vertically weighted T_b estimate, i.e.

$$\hat{T}_b = \frac{\sum_{i=1}^{N} w_i T_i \log_e(p_1/p_2)}{\sum_{i=1}^{N} w_i \log_e(p_1/p_2)} \qquad (2)$$

where the ith layer of N radiosonde profile layers has an average temperature (T_i), an average weight (w_i) from Fig. 1, and bounding pressures (p_1 and p_2).

Third and lastly, comparisons were made to all combinations of thickness layers having bases at 100 kPa or 85 kPa, and tops at 70, 50, 40, 30, 25, 20, 15, and 10 kPa. Because virtually all of the correlations were somewhat lower for layers having bases at 85 kPa, only the results for the layers having 100 kPa bases are presented here.

b. single station gridpoint correlations

The levels of agreement between the satellite measurements and each of the six stations are presented in Figures 5 through 10 in terms of correlation coefficients (R) and standard error of estimate (SE) of the radiosonde temperature anomalies. The first half of these figures (a) shows the time series of comparisons to radiosonde-computed channel 2 T_b, while the second half (b) shows R and SE for various thickness layer temperature anomalies.

In Cold Bay, Alaska (Fig. 5a) we find a monthly correlation of 0.98 between the satellite-measured and the radiosonde-calculated T_b, with a corresponding SE of 0.24°C. The yearly anomaly correlation is just under 0.99. Use of the simplified T_b computations with Eq. 2 results in R=0.96 and SE=0.28°C, which is only a slight degradation in performance for the monthly anomalies. The best monthly agreement between the satellite and a traditionally measured thickness layer (Fig. 5b) is with the 100-20 kPa layer (R=0.94) which is not quite as good as with the other measures. Most of the stations we examined (of over 100 in number) indicated the 100-20 kPa layer as having the best agreement of all traditionally measured thickness layers. This should not be surprising considering the channel 2 weighting function distribution in Fig. 1.

In St. Cloud, Minnesota (Fig. 6a) we find similar results to those of Cold Bay, with a monthly correlation of 0.98 and SE of 0.24°C. Use of Eq. 2 gives only slightly degraded results with R=0.97 and SE=0.27°C. These figures are slightly better than the correlation with the 100-15 kPa layer (R=0.96) in Fig. 6b.

The comparisons to radiosonde-computed channel 2 for Oakland, California (Fig. 7a) reveal R=0.95 and SE=0.25°C. Interestingly, the results with Eq. 2 are slightly better than those obtained with the radiative transfer equation, with SE=0.23°C. As with the other stations, these are both slightly better than with the thickness layer of best agreement (100-20 kPa) for which R=0.94 (Fig. 7b).

At Lihue, Hawaii (Fig. 8a) the radiative transfer calculations with the radiosonde data show a 0.96 correlation and SE=0.16°. With Eq. 2 these measures become R=0.95 and SE=0.18°C, again revealing the utility of a simple vertically weighted average of the temperature profile with a constant weighting function. Compared to a traditionally measured layer, best agreement is seen in the 100-20 kPa layer, with R=0.95 and SE=0.23°C (Fig. 8b). Note that we are now reaching the limit of agreement (0.20°C) between adjacent tropical radiosonde stations measuring the same layers shown in Fig. 2. In fact, comparison between the Lihue and Hilo, Hawaii radiosonde stations, despite their relatively close proximity to each other, yields *poorer* agreement (the circles in Fig. 8b) than the satellite shows with Lihue. This casts some doubt on the regional representativeness of isolated radiosonde stations when used to construct "global" temperature anomalies. Of some interest are the low correlations between the MSU channel 2 anomalies and the lower tropospheric temperature anomalies at Lihue. This illustrates very little coupling between the lower and middle troposphere in this oceanic region.

The agreement with the satellite anomalies at San Juan, Puerto Rico (Fig. 9a) is about the same as was found in Hawaii, with R=0.95 and SE=0.15°C. Using Eq. 2 for the radiosonde computations, we once again obtain only slightly poorer performance, with R=0.93 and SE=0.20°C. In the comparisons to thickness anomalies (Fig. 9b), for the 100-25 kPa layer R=0.95 and SE=0.21°C. Again, these levels of agreement approach the precision inherent in the sampling provided by a single radiosonde stations.

Guam, in the tropical western Pacific (Fig. 10a) reveals a somewhat lower correlation (R=0.85), but an excellent standard error (SE=0.14°C). This reflects the very weak signal of monthly temperature anomalies in this region of the world. Note that the correlation is no worse than that between the adjacent radiosonde stations in Fig. 2. The constant weighting method (Eq. 2) gives R=0.81 and SE=0.17°C, again only a slight degradation from using the full radiative transfer equation. Considerably worse results are revealed for the 100-15 kPa layer anomalies, where R=0.74 and SE=0.25°C. This degradation is the result of low natural interlayer correlations within the troposphere which makes comparison with the correct vertical weighting profiles very important.

c. composite station correlations

When satellite-radiosonde comparisons are grouped by region, the levels of agreement improve further (Table 2). We see the largest improvement in correlation for the tropical western Pacific, for which Guam was 0.85, and now a six station composite correlation increases to 0.94, with the SE improving to 0.09°C. These station composites thus reveal that the radiosonde (and satellite) noise at individual gridpoints is reduced when several gridpoints are averaged together.

d. trends

Table 3 shows the ten year trends for these station composites as well as the satellite measured trends. Note that the differences are well within the levels of disagreement seen in Fig. 2b between closely spaced tropical Pacific radiosonde stations. Thus the ten year trends in the multi-satellite record of monthly anomalies, when compared to regionally averaged radiosonde station measurements, show no obvious evidence of drift. Unfortunately, these radiosonde station groupings are probably not sufficient to measure drifts to better than 0.1^{o}C.

5. Conclusions

Radiosonde comparisons support the use of satellite passive microwave temperature measurements for precise deep layer temperature monitoring, even at the 2.5^{o} gridpoint scale. Inter-satellite comparisons of monthly TIROS-N MSU channel 2 T_b anomalies at the 2.5^{o} gridpoint level reveal remarkable agreement, generally better than 0.1^{o}C in the tropics and better than 0.2^{o} at high latitudes. Since these are single-satellite precisions, the precision of the gridpoint values with two satellites is improved even further. Comparisons between MSU-observed and radiosonde calculated monthly anomalies in channel 2 T_b reveal correlations generally around 0.95 and standard errors from 0.15^{o}C in the tropics to 0.25^{o}C at high latitudes. This performance degrades by an average of only 0.02^{o}C if a simple vertical weighting is applied to the radiosonde temperature profiles, instead of using radiative transfer calculations. This simple method is recommended for quantitative comparisons to other multiple layer temperature datasets. Compositing of four to fifteen radiosonde stations together in specific regions improves the satellite-radiosonde agreement to 0.10^{o}C in the tropics to about 0.20^{o}C at high latitudes. Thus, the satellite precision approaches that of individual radiosonde stations in their ability to measure monthly temperature anomalies, which we estimate to be 0.2^{o}C from intercomparisons of closely spaced tropical oceanic stations in the Pacific. In terms of traditionally measured layers, the highest satellite correlations exist for the 100-20 kPa layer or the 100-15 kPa layer. These correlations are only slightly poorer than for the channel 2 weighting profile, except over the tropical Pacific where natural inter-layer correlations are low, making the correct weighting of the radiosonde profile very important.

We find no evidence of instrumental drift in the ten years of MSU channel 2 measurements (1979-88) to our ability to measure it with multiple-station radiosonde data.

Acknowledgments

We thank Roy Jenne and Dennis Joseph at NCAR for provision of the raw MSU data sets and radiosonde data. Robbie Hood assisted in the processing of the radiosonde data and radiative transfer modeling. Norm Grody (NOAA/NESDIS) and Shelby Tilford (NASA Headquarters) provided useful advice during the course of this study.

APPENDIX

Merging of Multi-Satellite MSU Data for Climate Monitoring

The TIROS-N series of sun-synchronous polar orbiting satellites have provided a continuous monitoring of the Earth since late 1978. Each satellite has a operational lifetime of one to three years. Nominally two satellites are operated at the same time, one in a morning orbit (7:30) and one in an afternoon orbit (2:30), although a few periods have existed when only a single satellite has been available. Launches of new satellites alternate between morning and afternoon.

If a single satellite had always been operated (and its sensors remained sufficiently stable), then computation of monthly brightness temperature anomalies from this single satellite would have been a simple process of averaging all data into monthly bins for some multi-year period sufficient to observe a representative annual cycle (say 1979-88), and then subtracting this average from the individual single-month averages to arrive at a time series of monthly anomalies. Unfortunately, we must deal with multiple satellites with slightly different sensors in different orbits. As a consequence, merging of the data from these overlapping satellites into a continuous time series requires the removal of two basic sources of differences between satellites. First is the absolute calibration differences between different MSUs, for which we find a very small latitudinal dependence in our two primary channels of interest (2 and 4). The second source arises from the different solar times of the morning and afternoon orbits. MSU channel 2 has some sensitivity to the surface, and so the 2:30 afternoon channel 2 T_b observations over land can be considerably warmer than either the 7:30 a.m. or 7:30 p.m. T_b. This effect becomes stronger as one moves toward the equator and higher elevations, e.g. 5-10^{o}C over the United States, 10-15^{o}C over the Sahara Desert. Therefore, removal of an annual cycle for anomaly computation is not only a function of the different satellite orbits, but also of geographical region.

Following ... ormed in the time

s ... age annual cycle from the monthly ... ion 3 for a single overlap period ... ating satellites. We chose 1982 ... erlap between NOAA-6 (morning) and ... -6 as a base period due to its long

The morning ... n satellite annual cycles were then used as bases from which anomalies for all the other satellites were computed, a simple subtraction of the gridpoint annual cycles ~~the~~ from the monthly averages obtained from the other morning and afternoon satellites. The anomalies at this point are based upon only the 1982 annual cycle of either NOAA-6 or NOAA-7, without any correction for inter-satellite differences.

To make the inter-satellite correction, the anomalies from different satellites were compared during all periods of overlap between satellites (Fig. A1) to find the time- and gridpoint-averaged offsets relative to NOAA-6, which were then individually removed from each satellite's anomalies. At this point, we have anomalies which are intercalibrated between satellites, but are still relative to only a single year's annual cycle (1982).

Finally, the average of 12 years of each month's anomalies was forced to zero by adding an appropriate offset to each anomaly, thus removing the 12-year mean annual cycle.

Table A1 lists statistics of the inter-satellite comparisons and adjustments, including the route of adjustment to a common level (NOAA-6); the dates of overlap between satellites used in the adjustments; the daily standard deviation of the difference (single satellite "error") between the overlapping satellites globally averaged channel 2 T_b anomalies; the daily signal to noise ratio (the sum of the overlapping satellites daily ch. 2 T_b anomaly divided by their daily difference, squared); 30-day statistics; the globally-averaged adjustments necessary to bring that satellite to the NOAA-6 level; and the net trend in the time series of the daily differences between overlapping satellites T_b anomalies. NOAA-8 had many operational problems and was not used in any of our statistics.

References

Grody, N.C., 1980: Analysis of satellite-based microwave retrievals of temperature and thermal winds: Effects of channel selection and a-priori mean on retrieval accuracy. *Remote Sensing of the Atmosphere and Oceans*, A. Deepak, Ed., Academic Press, 381-410.

Grody, N.C., 1983: Severe storm observations with the Microwave Sounding Unit. *J. Climate Appl. Meteor.*, **22**, 609-625.

Spencer, R.W. and J.R. Christy, 1990: Precise monitoring of global temperature trends from satellites. *Science*, **247**, 1558-1562.

Spencer, R.W., J.R. Christy, and N.C. Grody, 1990: Global atmospheric temperature monitoring with satellite microwave measurements: Method and results, 1979-84. *J. Climate.*, **3**, 1111-1128.

List of Figures

Figure 8. As in Fig. 5, except Lihue, Hawaii. Also shown in (b) is the level of agreement between Hilo, Hawaii and Lihue, Hawaii.

Figure 9. As in Fig. 5, except San Juan, Puerto Rico.

Figure 10. As in Fig. 5, except Guam.

Figure A1. Periods of operation and overlap between MSUs during 1979-90. Gaps indicate one or more days of less than 85% global data. The authors do not yet have March 1989 data in their dataset.

Table 1. Radiosonde stations from various climatic regimes chosen for comparison to the satellite gridpoint temperature anomaly dataset.

Station	Climatic Type	Location
Cold Bay, Alaska	Polar	55.2°N 162.7°W
St. Cloud, Minnesota	Continental	45.6°N 94.2°W
Oakland, California	Mid-latitude	37.7°N 122.2°W
Lihue, Hawaii	Sub-tropical	22.0°N 159.3°W
San Juan, Puerto Rico	Sub-tropical	18.4°N 66.0°W
Guam	Tropical	13.6°N 144.8°E

Table 2. Station composite correlations and standard errors of satellite versus radiosonde monthly anomalies in channel 2. Numbers in parentheses are the corresponding single-station values from the stations represented in Figs. 5-10.

Region	R	SE
Alaska(15)	.98(.97)	.17°(.24°)
Great Lakes(6)	.98(.98)	.22°(.24°)
West Coast(4)	.97(.95)	.18°(.25°)
Caribbean(6)	.97(.95)	.10°(.15°)
West Pacific(7)	.94(.85)	.09°(.14°)

Alaska:(15) Anette, Yakutat, Kodiak, King Salmon, Cold Bay, Adak, St. Paul Island, Anchorage, Fairbanks, McGrath, Bethel, Kotzebue, Nome, Barter Island, Barrow. **Great Lakes:**(6) Sault Ste. Marie, MI; International Falls, MN; Green Bay, WI; St. Cloud, MN, Huron, SD. **U.S. West Coast:**(4) Quillayute, WA; Salem, OR; Oakland, CA; San Diego, CA. **Tropical West Pacific:**(7) Koror, Yap, Majuro, Wake, Guam, Truk, Ponape. **Caribbean:**(6) Christ Church, Barbados; Santo Domingo, Dominican Republic; Piarco, Trinidad; San Juan, Puerto Rico; Curacao, Netherland Antilles; Roberts, Cayman Islands

Table 3. Ten year trends (^{o}C, for the decade 1979-1988) in MSU-observed and radiosonde-computed channel 2 T_b anomalies for the regional station composites listed in Table 2. The number of stations is each group is shown in parentheses.

Region	Radiosonde Ch. 2 Trend	MSU Ch. 2 Trend	(Raob-MSU)
Alaska(15)	-0.67^{o}	-0.64^{o}	-0.03^{o}
Great Lakes(6)	+0.33^{o}	+0.43^{o}	-0.10^{o}
U.S. West Coast(4)	-0.03^{o}	+0.18^{o}	-0.21^{o}
Caribbean(6)	-0.01^{o}	+0.10^{o}	-0.11^{o}
West Pacific(7)	+0.14^{o}	+0.08^{o}	+0.06^{o}
Weighted Average			-0.06^{o}

Table A1. Global statistics of all satellite overlaps between MSUs for MSU channel 2 data.

Satellite	Method	Overlap Dates	#days	daily error	daily S/N	30-day error	30-day S/N	Global Adj.	1-yr trend*
TIROS-N	to NOAA-6	7/1/79- 1/19/80	164	.033°	24.4	.013°	48.9	+.068°	+.074°
NOAA-6	BASE								
NOAA-7	to NOAA-6	6/26/81- 4/16/83	596	.028°	36.7	.006°	577.4	-.002°	+.007°
NOAA-9	to NOAA-6	10/30/85- 11/4/86	284	.028°	71.4	.006°	183.0	+.067°	+.015°
NOAA-10	to NOAA-9	11/26/86- 3/7/87	98	.030°	47.4	.006°	361.7	-.281°	-.068°
NOAA-11	to NOAA-10	10/23/88- 10/31/90	641	.030°	29.2	.011°	114.0	+.240°	+.004°

*Due to slightly different crossing times in afternoon satellites, there seems to be a very slight difference in annual cycles between TIROS-N versus NOAA-7. This is also seen in NOAA-7 versus NOAA-11, however, the two year overlap between NOAA-10 and NOAA-11 eliminates any trend due to an annual cycle in the satellite difference time series.

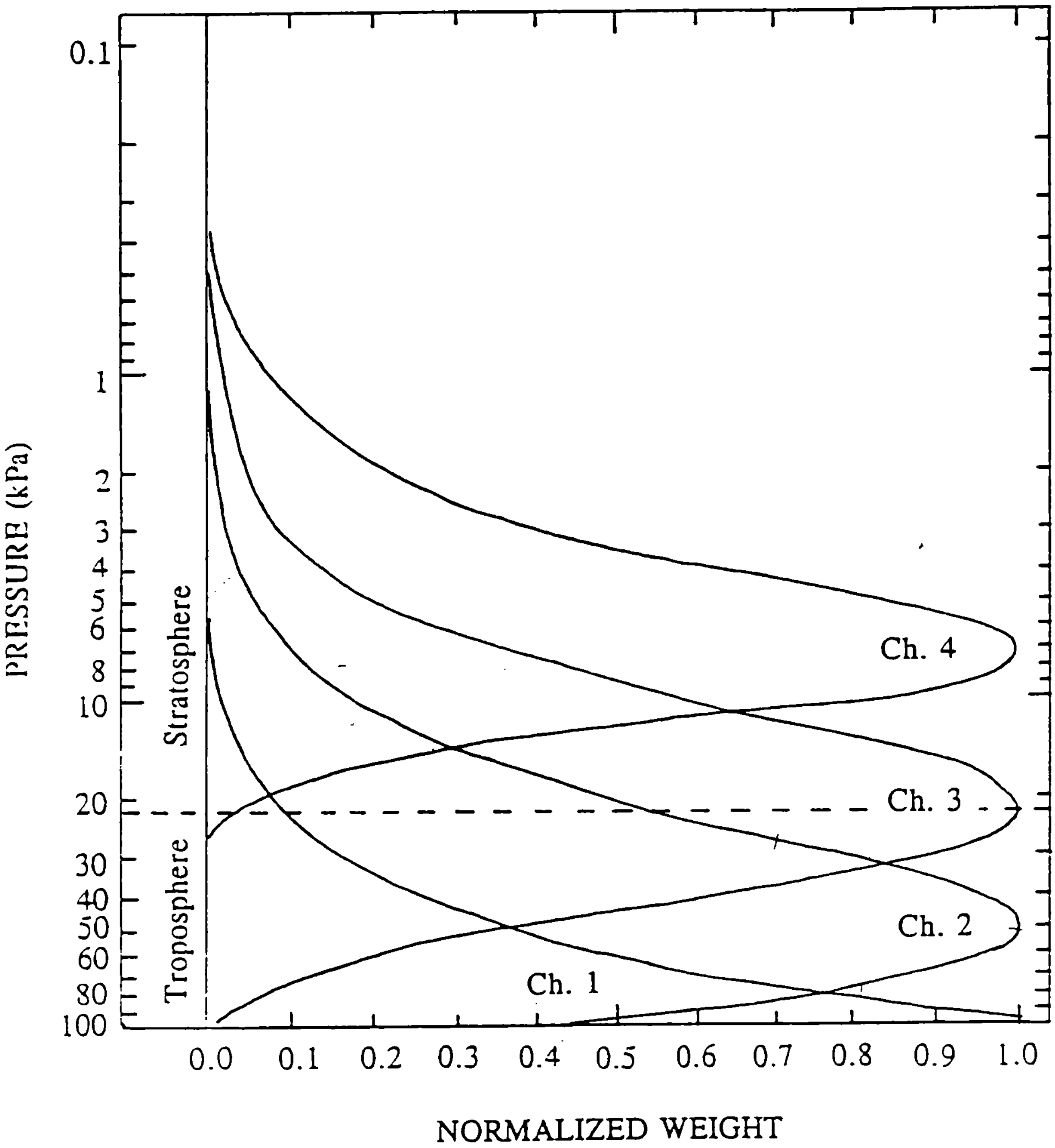

PRESSURE (kPa)
0.1
1
2
3
4
5
6
8
10
20
30
40
50
60
80
100
Stratosphere
Troposphere
Ch. 4
Ch. 3
Ch. 2
Ch. 1
0.0
0.1
0.2
0.3
0.4
0.5
0.6
0.7
0.8
0.9
1.0
NORMALIZED WEIGHT

Fig. 1

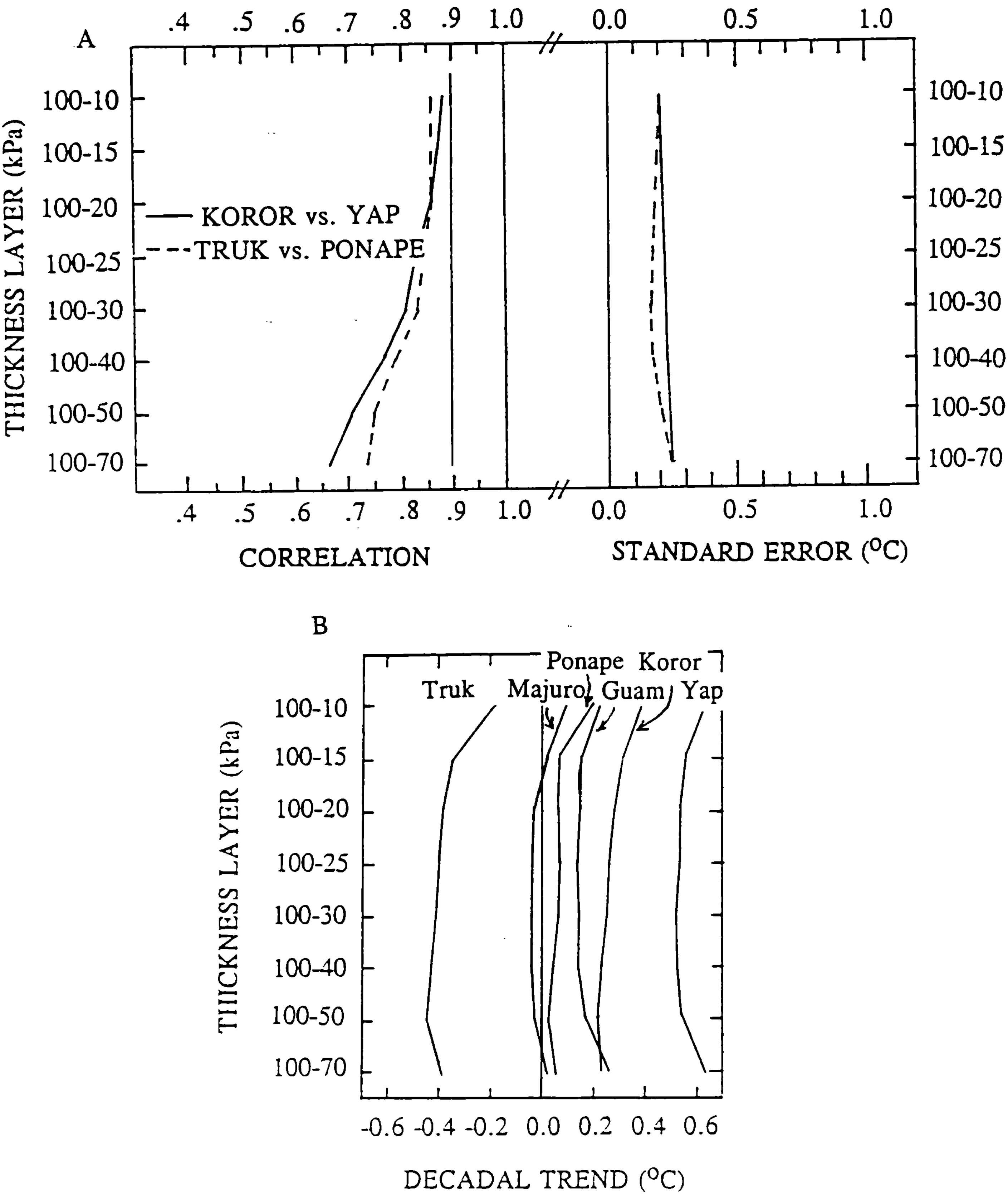
A
.4 .5 .6 .7 .8 .9 1.0
0.0 0.5 1.0
THICKNESS LAYER (kPa)
100-10
100-15
100-20
100-25
100-30
100-40
100-50
100-70
KOROR vs. YAP
TRUK vs. PONAPE
CORRELATION
STANDARD ERROR (°C)
B
Ponape Koror
Truk
Majuro
Guam
Yap
-0.6 -0.4 -0.2 0.0 0.2 0.4 0.6
DECADAL TREND (°C)

Fig. 2a,b

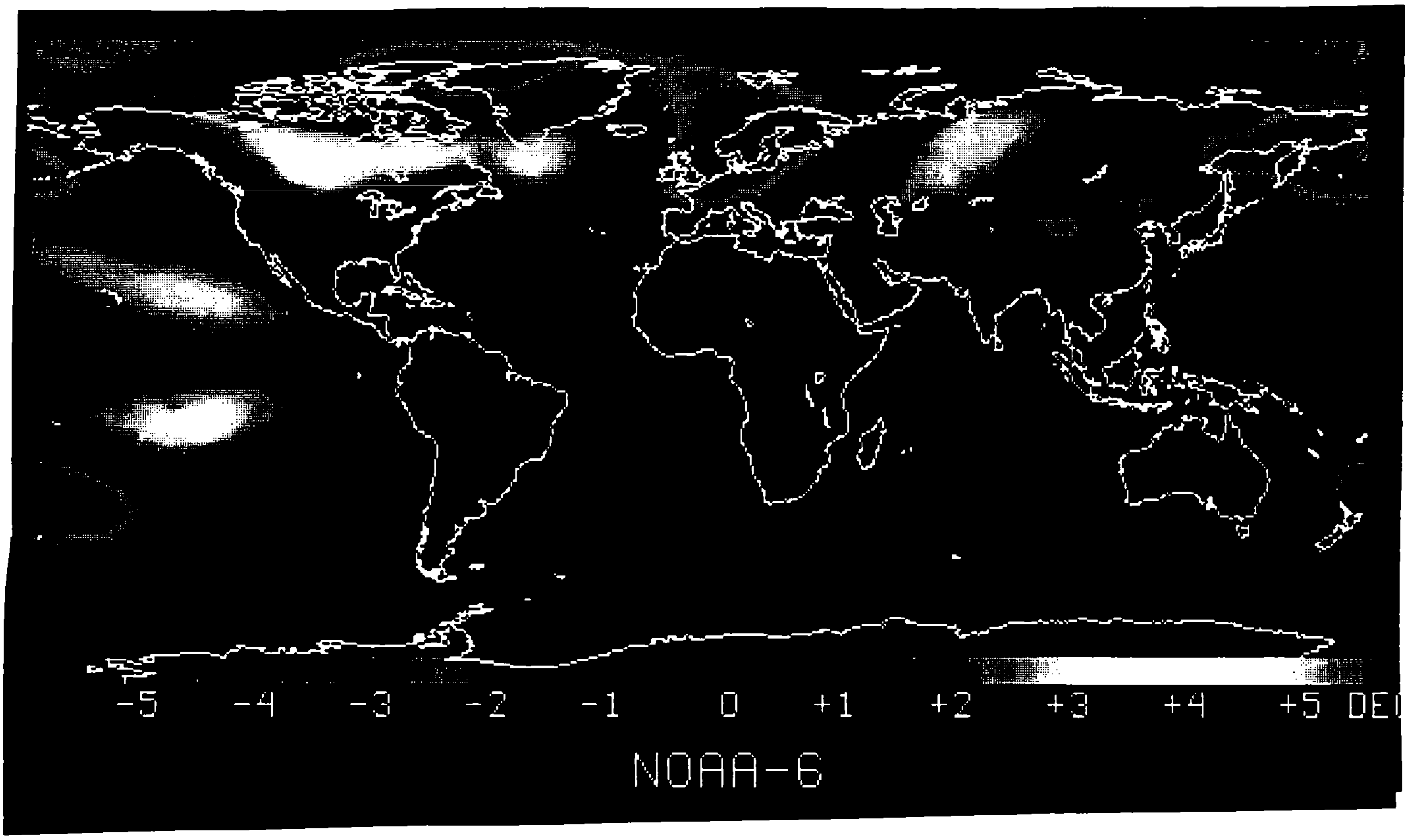

Ch 2
1983 Feb – 1982 Feb

Fig. 3 a,b (overlay)

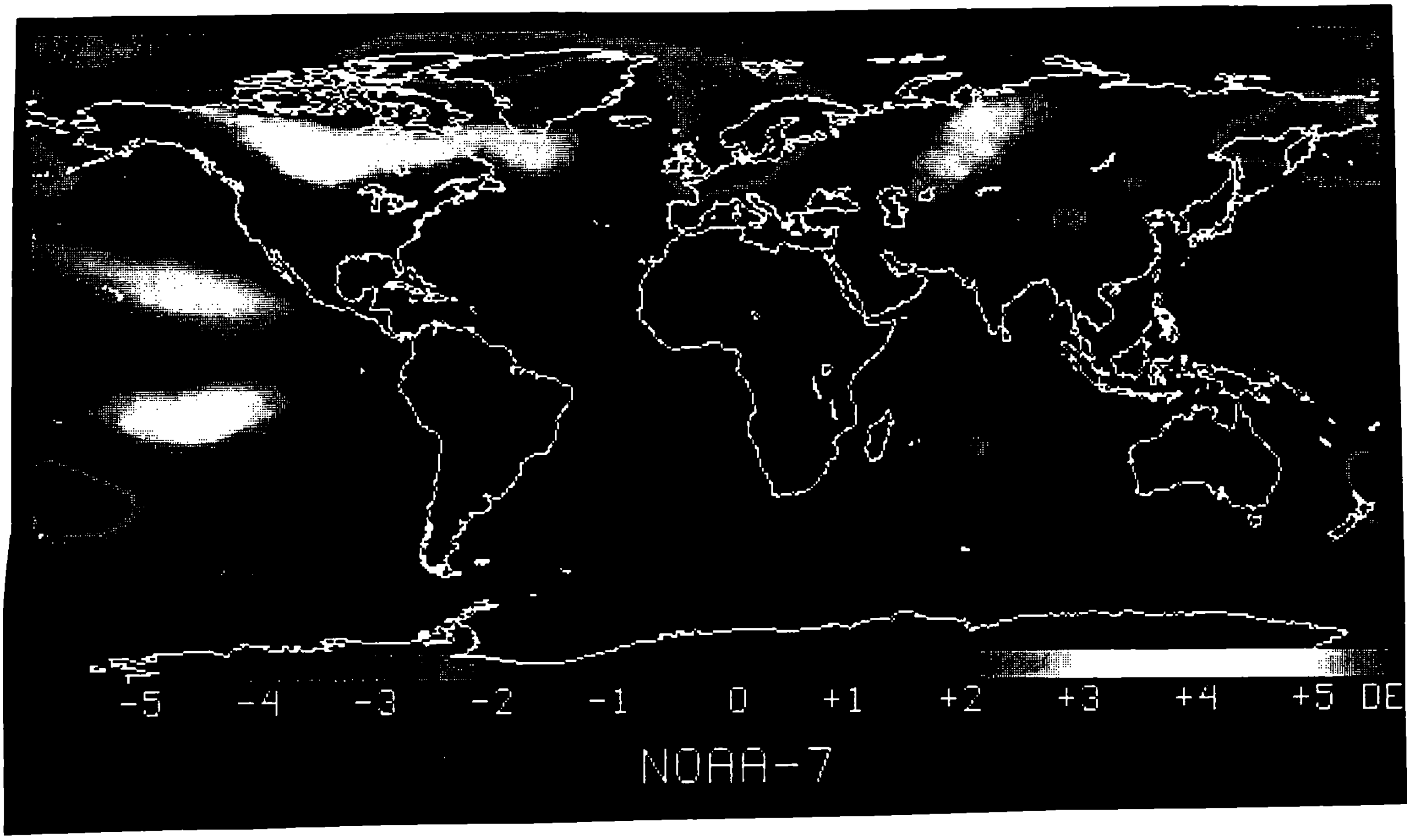

Ch 2
1983 Feb – 1982 Feb

Fig. 3 a,b (overlay)

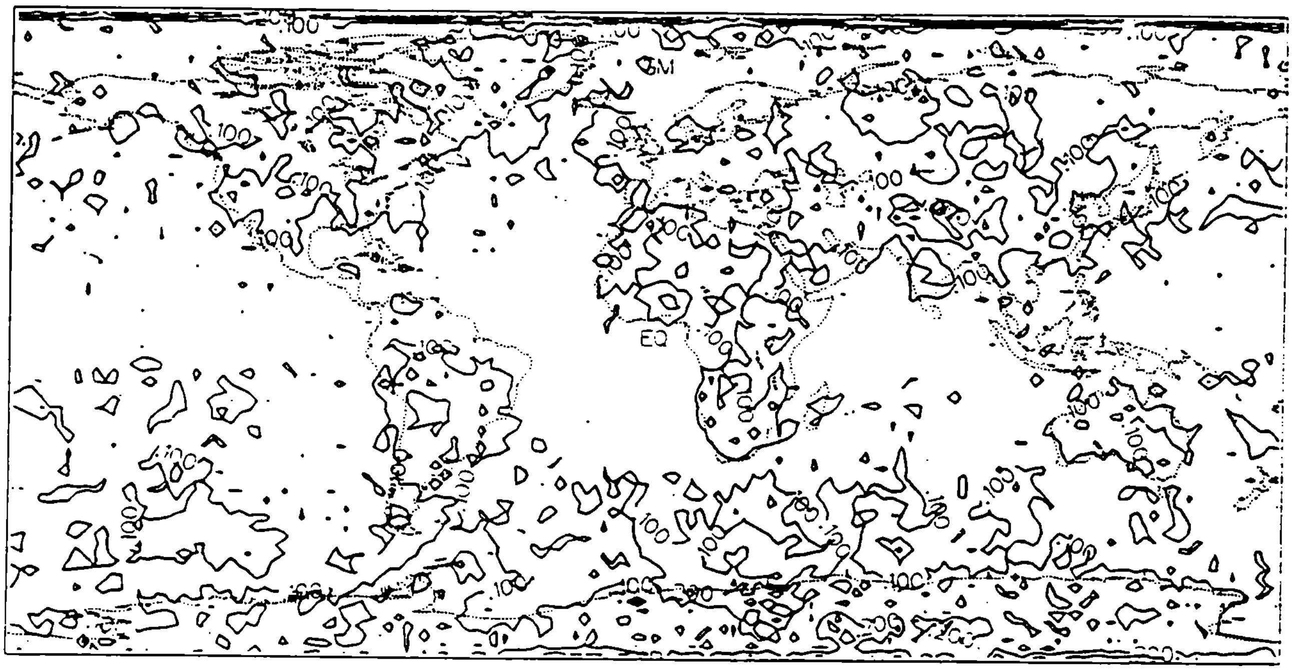

Fig. 4

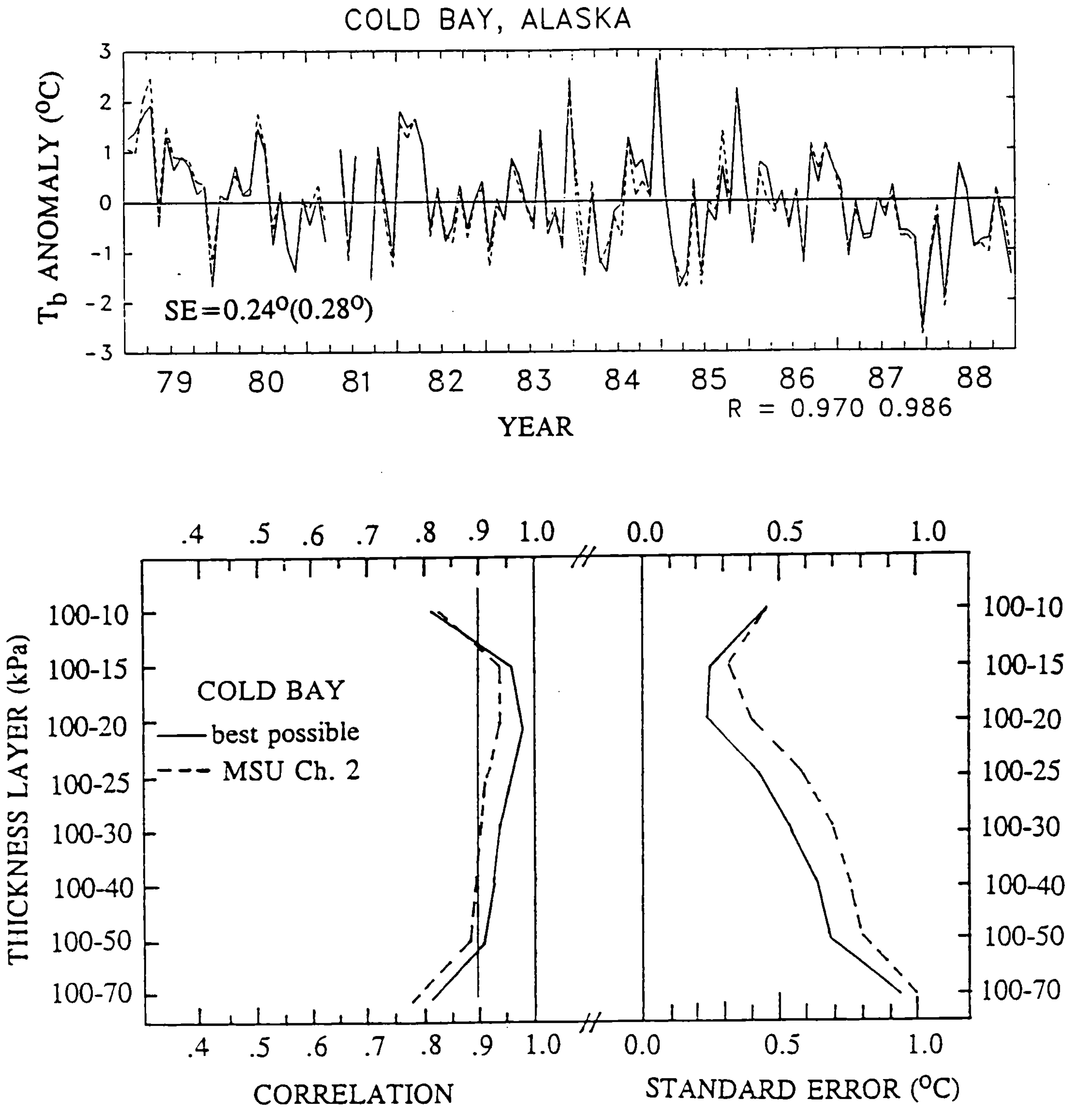

COLD BAY, ALASKA
T_b ANOMALY (°C)
SE=0.24°(0.28°)
79 80 81 82 83 84 85 86 87 88
R = 0.970 0.986
YEAR
THICKNESS LAYER (kPa)
100-10
100-15
100-20
100-25
100-30
100-40
100-50
100-70
COLD BAY
best possible
MSU Ch. 2
.4 .5 .6 .7 .8 .9 1.0
0.0 0.5 1.0
CORRELATION
STANDARD ERROR (°C)

Fig. 5

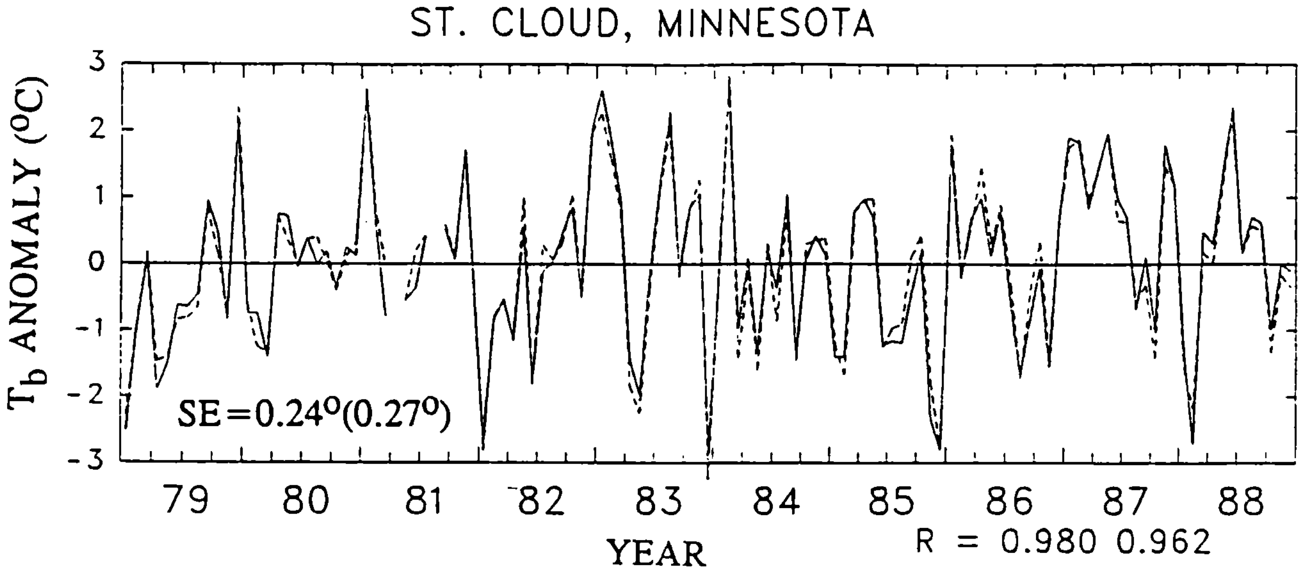
ST. CLOUD, MINNESOTA
T_b ANOMALY (°C)
SE=0.24°(0.27°)
YEAR
R = 0.980 0.962
79
80
81
82
83
84
85
86
87
88

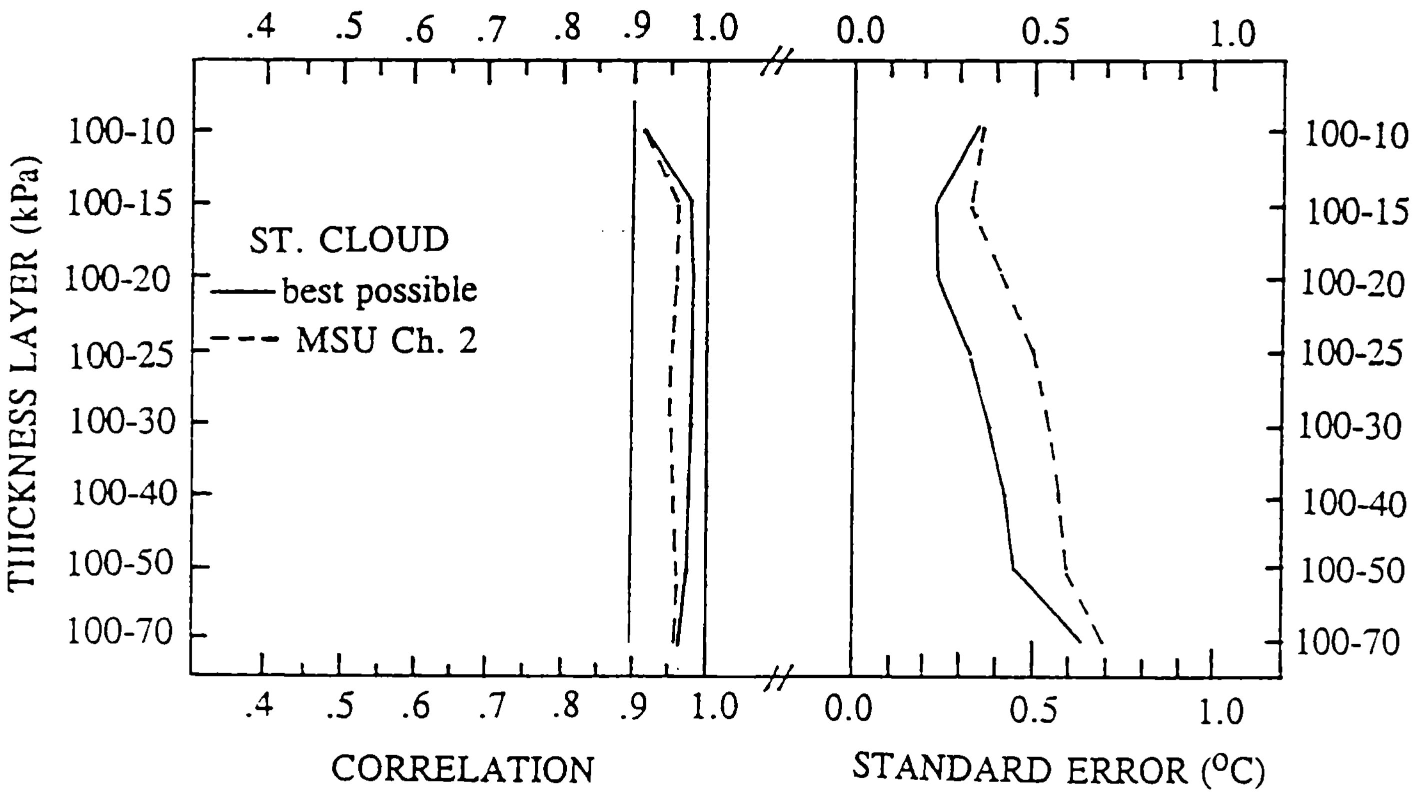
THICKNESS LAYER (kPa)
ST. CLOUD
best possible
MSU Ch. 2
100-10
100-15
100-20
100-25
100-30
100-40
100-50
100-70
CORRELATION
STANDARD ERROR (°C)

Fig. 6

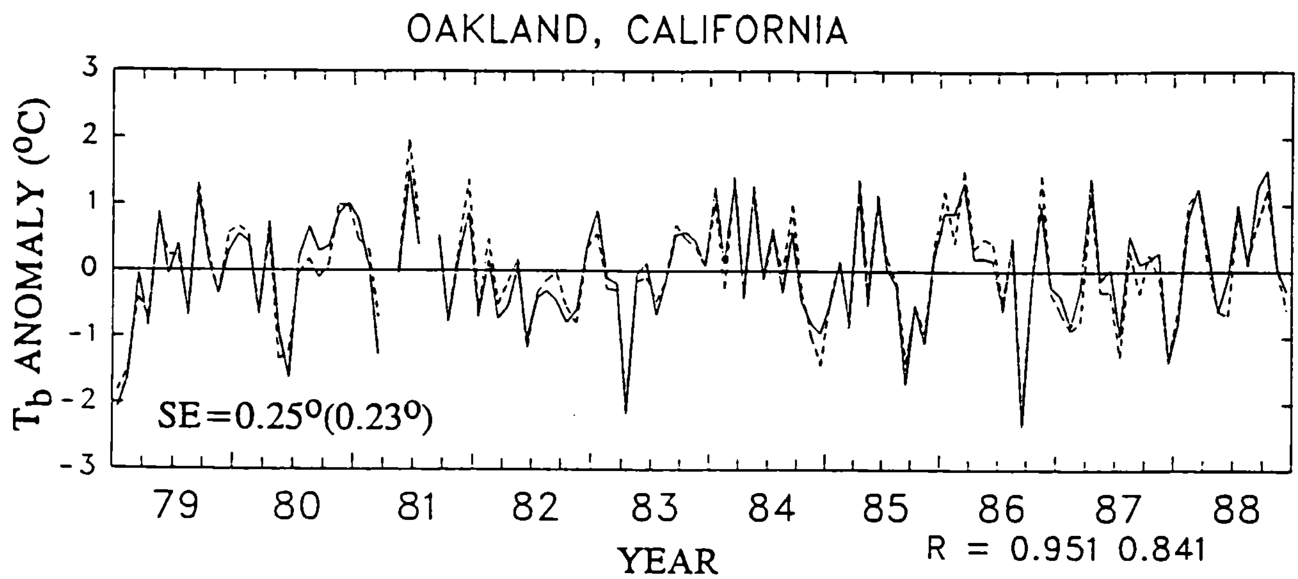
OAKLAND, CALIFORNIA
Tb ANOMALY (°C)
SE=0.25°(0.23°)
YEAR
R = 0.951 0.841

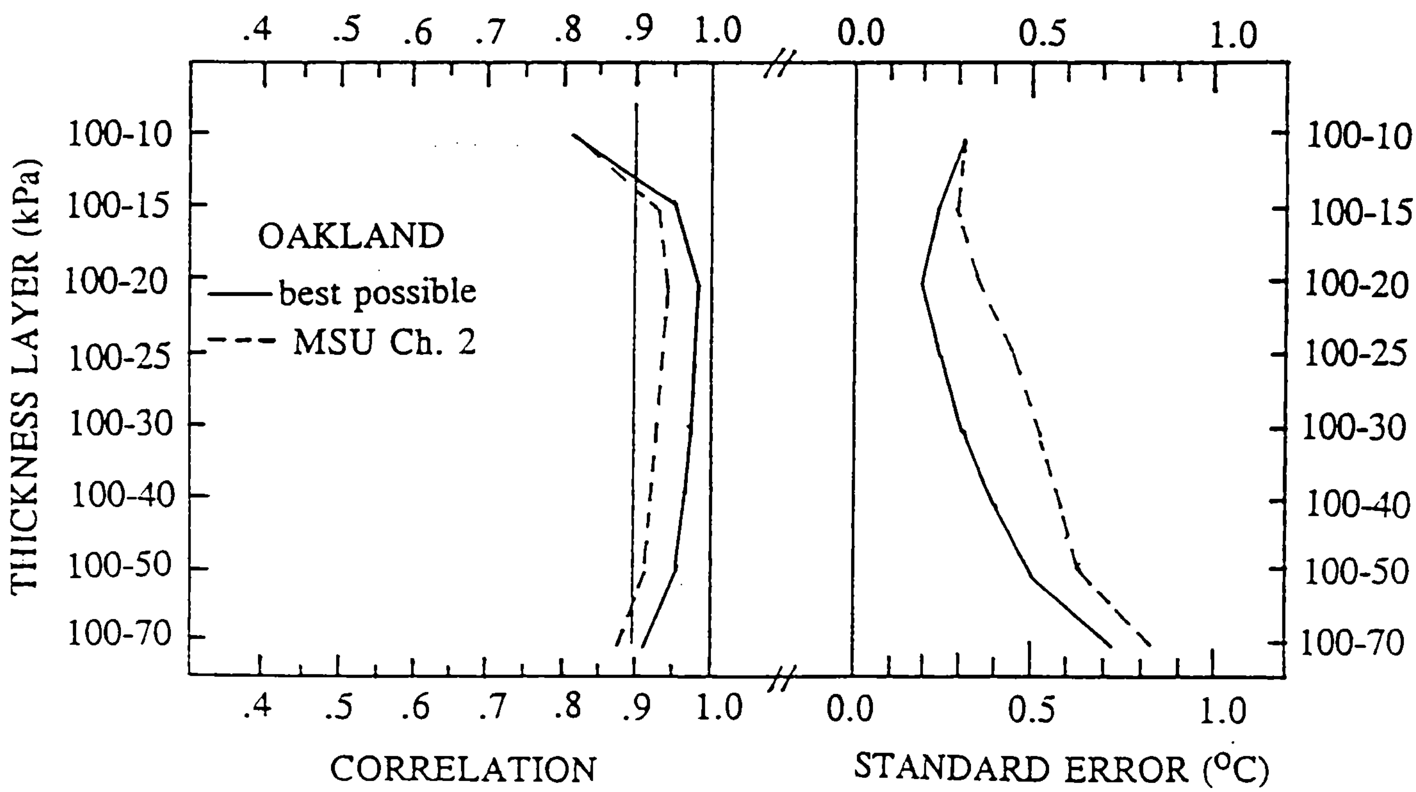
THICKNESS LAYER (kPa)
OAKLAND
best possible
MSU Ch. 2
CORRELATION
STANDARD ERROR (°C)

Fig. 7

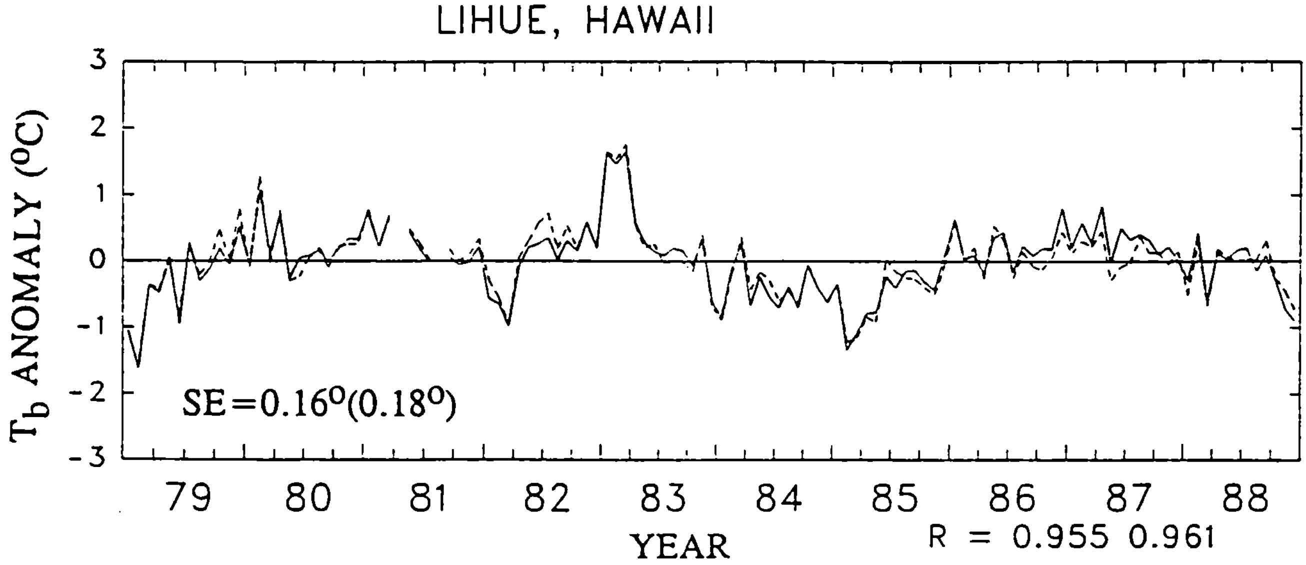
LIHUE, HAWAII
T_b ANOMALY (°C)
SE=0.16°(0.18°)
79 80 81 82 83 84 85 86 87 88
YEAR
R = 0.955 0.961

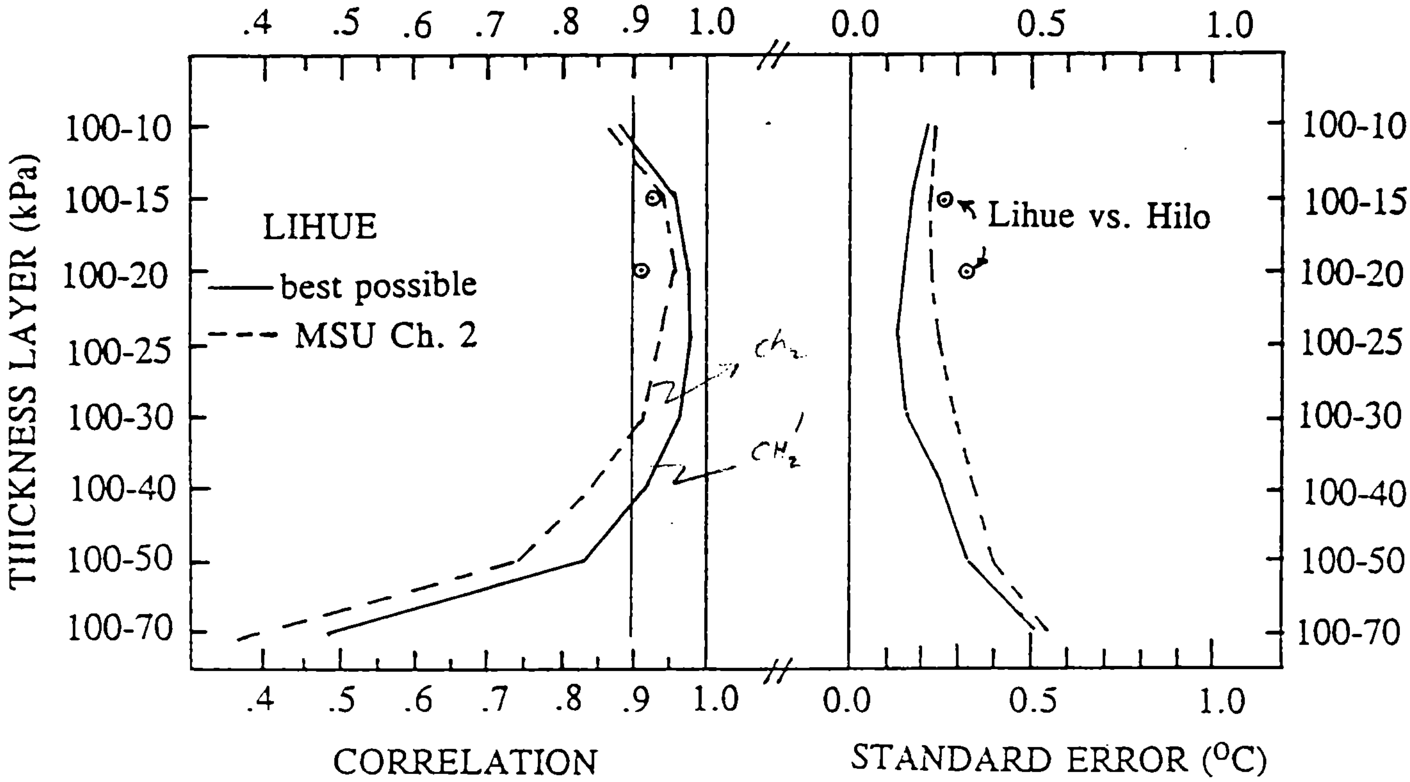
THICKNESS LAYER (kPa)
100-10
100-15
100-20
100-25
100-30
100-40
100-50
100-70
LIHUE
best possible
MSU Ch. 2
Lihue vs. Hilo
.4 .5 .6 .7 .8 .9 1.0
0.0 0.5 1.0
CORRELATION
STANDARD ERROR (°C)

Fig. 8

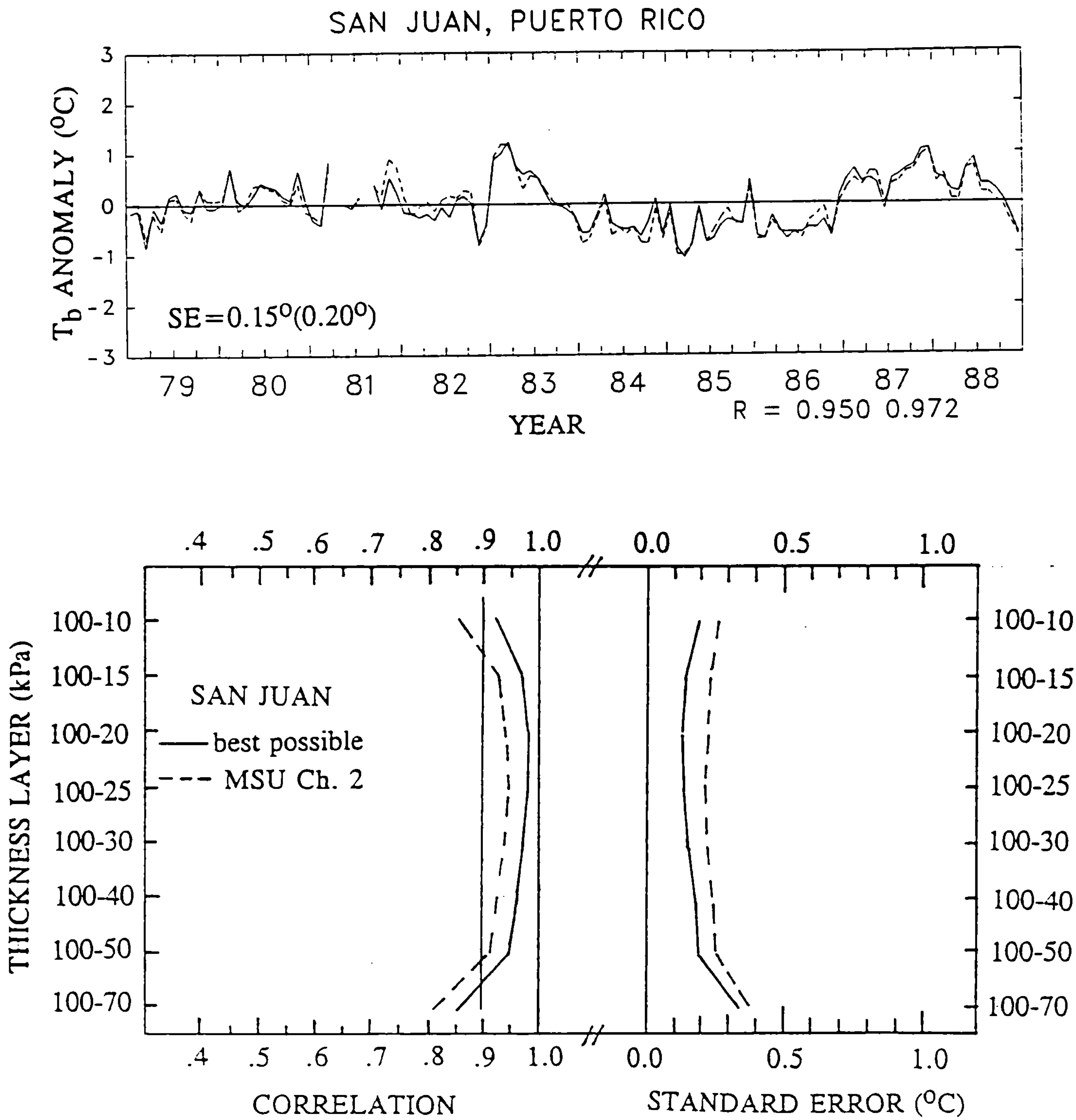
SAN JUAN, PUERTO RICO
T_b ANOMALY (°C)
3
2
1
0
-1
-2
-3
SE=0.15°(0.20°)
79 80 81 82 83 84 85 86 87 88
YEAR
R = 0.950 0.972
.4 .5 .6 .7 .8 .9 1.0
0.0 0.5 1.0
THICKNESS LAYER (kPa)
100-10
100-15
100-20
100-25
100-30
100-40
100-50
100-70
SAN JUAN
best possible
MSU Ch. 2
CORRELATION
STANDARD ERROR (°C)

Fig. 9

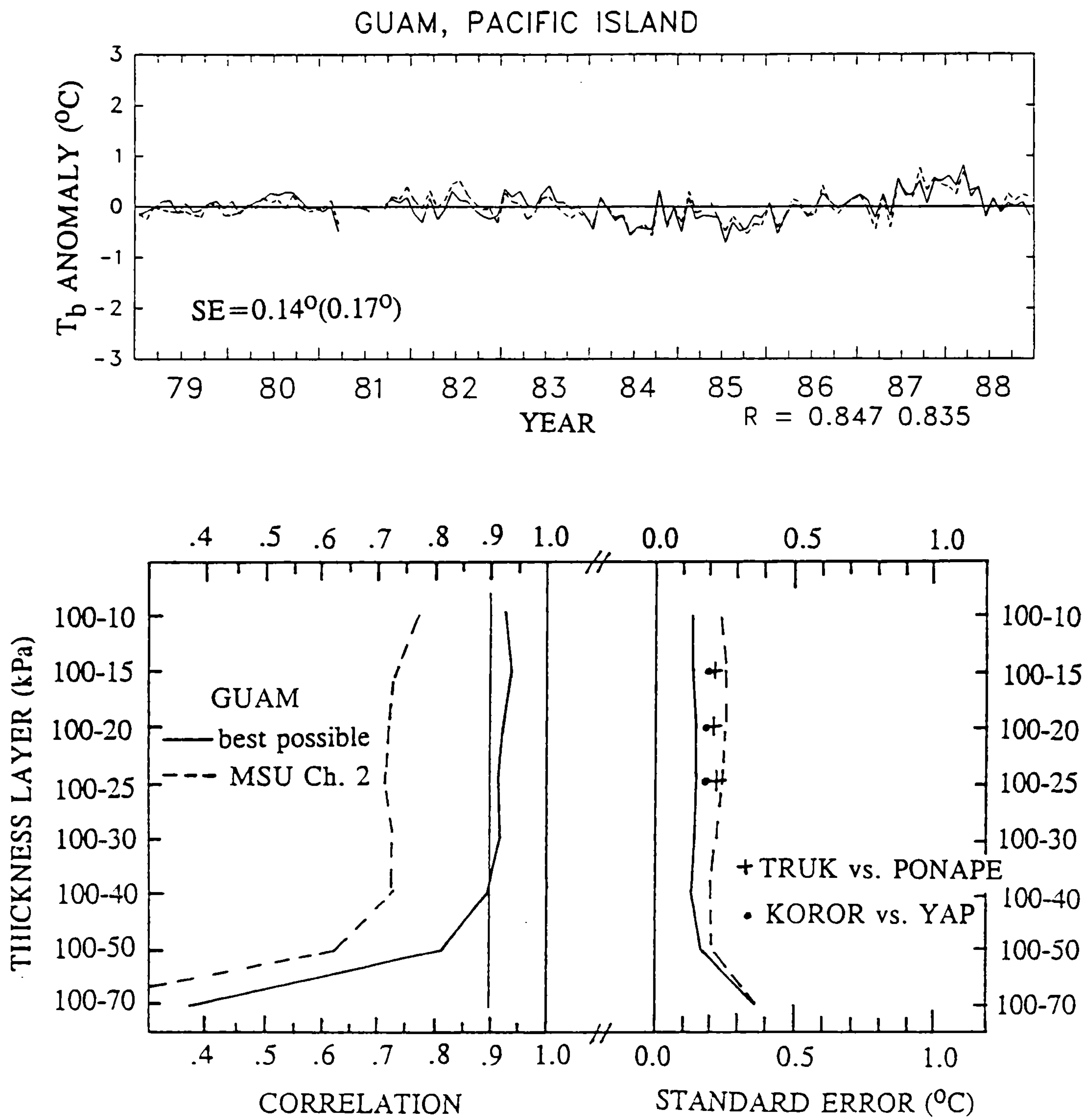
GUAM, PACIFIC ISLAND
T_b ANOMALY (°C)
SE=0.14°(0.17°)
79 80 81 82 83 84 85 86 87 88
YEAR
R = 0.847 0.835
THICKNESS LAYER (kPa)
100-10
100-15
100-20
100-25
100-30
100-40
100-50
100-70
GUAM
best possible
MSU Ch. 2
+ TRUK vs. PONAPE
• KOROR vs. YAP
.4 .5 .6 .7 .8 .9 1.0
0.0 0.5 1.0
CORRELATION
STANDARD ERROR (°C)

Fig. 10

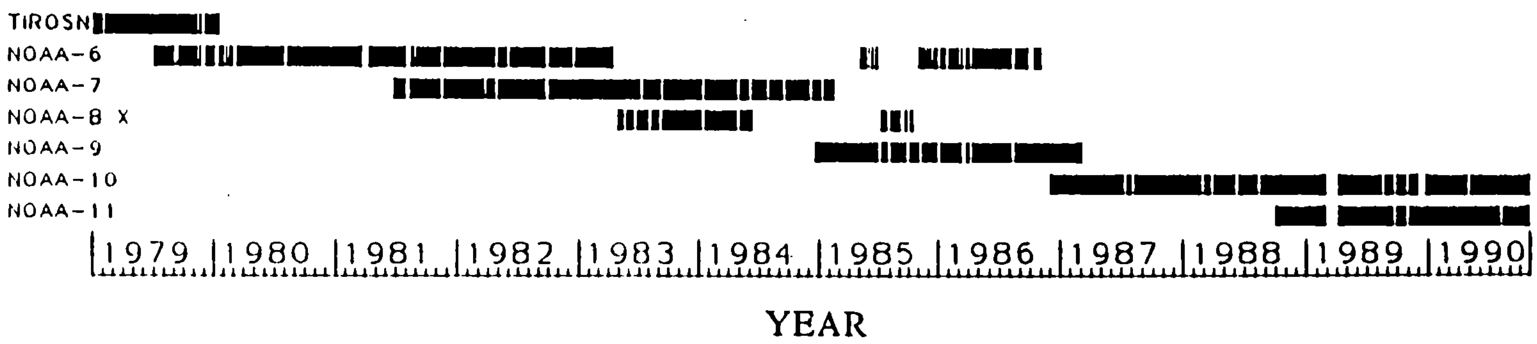

TIROSN
NOAA-6
NOAA-7
NOAA-8 X
NOAA-9
NOAA-10
NOAA-11
1979
1980
1981
1982
1983
1984
1985
1986
1987
1988
1989
1990
YEAR

Fig. A1

LABORATORY FOR ATMOSPHERES

National Aeronautics and Space Administration
Goddard Space Flight Center, Code 910
Greenbelt, Maryland 20771
301-286-3590

CLIMATE AND RADIATION BRANCH

Global Warming: What Do Satellite Microwave Measurements Show?

Prabhakara Cuddapah
GSFC/Code 913

Abstract

In recent studies Spencer and Christy (1990) and Spencer et al. (1990) hypothesized that the microwave brightness temperature observations made by the earth orbiting satellites at 53.74 GHz can help us monitor the global mean temperature over a long period of time. We have examined this hypothesis and find that these microwave measurements are not free from meteorological noise. In particular, clouds and rain can introduce a significant contamination in these data. As a consequence interannual changes in cloudiness and precipitation introduce appreciable interannual anomalies in the brightness temperature. Based on these findings we have reservations on the global index of temperature derived from 53.74 GHz data.

NOTE ROOM CHANGE

WEDNESDAY, June 5, 1991 | 3:00 PM | BUILDING 21, ROOM 183A

WORLD RESOURCES INSTITUTE

1709 New York Avenue, N.W., Washington, D.C. 20006, Telephone: 202-638-6300
Facsimile: 202-638-0036 Telex: 64414 WRIWASH

TRANSMITTAL
Facsimile Telephone Number: 202/638-0036

DATE: 6/4/91 TIME: ____

TO

NAME: Katie McGinty

COMPANY: Sen. Gore

CITY: ____

STATE/COUNTRY: ____

FACSIMILE NUMBER: 224-0580

FROM

NAME: Rafe Pomerance

TOTAL NUMBER OF DOCUMENT PAGES IN TRANSMISSION: 2
(including transmission form)

SUBJECT/REFERENCE: ____

MESSAGE: ____

4/12/91 Dr. Callaghan & Rafe

S&C not startlingly diff from H, etc.

S&C – 10 yrs – don't see a trend.

Sci Vol 25
Jones & Parker → trend from late 70's
data from 1860.

S&C & thermometer → v. good correlat'n over U.S.

Past 15 yrs. – global avg 0.2-0.3° ↑ (Hansen).

Satellite – ~~good~~ uniform data.

* S&C → Channel 2 – satellite does go into strat (20 km)

Over tropical equatorial oceans → v poor correlat'n w/ thermometer. Fr. Chr.

Not v. good corr. over US.

?-why → C's work.

SRC try to underline on this basis.

Ch1 on same cost -- much more sensitive res what happens on surface & NOT sensitive re: Spot.

· result Ch2 → when compare w/ch1 - they track one another.

Ch2 measuring most @ 5Km.

where deep convection & rain

vast convergence of deep convection in tropics - does NOT happen in midlats.

currently can't correct for this.

warmer water more deep convection happens.

Ch2 misses El Niño of 83 due to clouds -- Ch1 picks this up -- shows warmer water though -

poss. magnitude of the "bug" cld be 0.1°C → 25-30%
most of the [illegible] is going into S&C
They aware of error - try to correct but C → most of [illegible] data still in.
then was Negative [illegible].

→ [illegible] in warmer yrs -- prob. El Niño yrs. most
i.e. eq. trop. yrs.

IR channel confirms the bug seen by Ch1.

new S&C papers - incl. Ch4 which looks at [illegible] → will be small correction 'cause of weighting + heat will
we ⊕ [illegible] & key + have ⊕ correlation over trop. land *
→ S&C didn't consider

* 7-8°C →
// WARM pool.
western Eq. Pac.
7-8°C warmer than Earth
potentially due to cirrus clouds
→ coupled system.
Δ [illegible]

LABORATORY FOR ATMOSPHERES

National Aeronautics and Space Administration

Goddard Space Flight Center, Code 910

Greenbelt, Maryland 20771

CLIMATE AND RADIATION BRANCH

Global Warming: What Do Satellite Microwave Measurements Show?

Prabhakara Cuddapah
GSFC/Code 913

Abstract

In recent studies Spencer and Christy (1990) and Spencer et al. (1990) hypothesized that the microwave brightness temperature observations made by the earth orbiting satellites at 53.74 GHz can help us monitor the global mean temperature over a long period of time. We have examined this hypothesis and find that these microwave measurements are not free from meteorological noise. In particular, clouds and rain can introduce a significant contamination in these data. As a consequence interannual changes in cloudiness and precipitation introduce appreciable interannual anomalies in the brightness temperature. Based on these findings we have reservations on the global index of temperature derived from 53.74 GHz data.

WEDNESDAY, June 5, 1991 3:00 PM BUILDING 21, ROOM 183A

ALBERT GORE, JR.
TENNESSEE

393 RUSSELL SENATE OFFICE BUILDING
PHONE: 202-224-4944

United States Senate

WASHINGTON, DC 20510-4202

Date: July 27, 1991

To: Albert Gore Jr. S, Anthony Socci

From: Katie McGinty

spencer and christy--

you may recall that i told you of a conversation that i had with spencer in which he told me that in sept or oct he and christy would be publishing a paper that would discredit hansen's data. he had indicated at that time that hansen's work was bad primarily due to h's sparce data points and that h had taken too many liberties in extrapolating those data points to larger points of the globe.

shortly after that conversation, i learned that 2 scientists at nasa goddard (cuddapah and arking) were working on their own paper that identified inaccuracies in s&c's work that, if when corrected for, would put s&c's results more closely in line with hansen et al.

i met with cuddapah last month here in the office and yesterday rafe pomerance and i went to nasa to talk to arking as well.

upshot: (1) i am now baffled by spencers threatening language re: their upcoming attack on hansen. i have gotten hold of a preprint of the article. hansen is not expressly mentioned or cited in either paper. rather, the point of the paper is to refine their own earlier analysis. their conclusion: "This correction leads to a slightly greater tropospheric warming trend in the twelve year time series (1979-1990) for the tropospheric retrieval (+0.048 C/decade) than for channel 2 alone (+0.015 C/decade)." Now this ain't much, and i am sure that s&c would argue that the point is that -- even when refined -- their data shows no significant trend. I WOULD ARGUE HOWEVER, THAT THE SIGNAL NEVERTHELESS (even for their short data set) IS POSITIVE.

(2) What do cuddapah and arking have to say?? They add still another (and i think very significant) correction to s&c's data -- a correction that enhances still further the POSITIVE signal that s&c's satellite REALLY is detecting. Cuddapah and Arking point out that s&c's data agrees with hansens et al very well over land masses and pretty well over midlatitude oceans. the disagreement seems to inhere in measurements over the tropical oceans. C&A say that the difference highlights a shortcoming in s&c's data (not hansen's). s&c derive their data from the satellite's channel 2. (the correction in their new paper is based on analysis of channel 4 data as well). According to C&A, this channel can't detect a warm signal through hydrometeors (rain and clouds) because this channel is insensitive to the surface. while this would result in accuracies around the globe wherever rain and clouds are encountered, the problem is particularly accute in tropics due to the deep convection that characterizes the tropical ocean-atmospher interaction.

CONT'D...